# Copyright Warning & Restrictions

The copyright law of the United States (Title 17, United States Code) governs the making of photocopies or other reproductions of copyrighted material.

Under certain conditions specified in the law, libraries and archives are authorized to furnish a photocopy or other reproduction. One of these specified conditions is that the photocopy or reproduction is not to be "used for any purpose other than private study, scholarship, or research." If a, user makes a request for, or later uses, a photocopy or reproduction for purposes in excess of "fair use" that user may be liable for copyright infringement,

This institution reserves the right to refuse to accept a copying order if, in its judgment, fulfillment of the order would involve violation of copyright law.

Please Note: The author retains the copyright while the New Jersey Institute of Technology reserves the right to distribute this thesis or dissertation

Printing note: If you do not wish to print this page, then select "Pages from: first page # to: last page #" on the print dialog screen

## INFORMATION TO USERS

This dissertation was produced from a microfilm copy of the original document. While the most advanced technological means to photograph and reproduce this document have been used, the quality is heavily dependent upon the quality of the original submitted.

The following explanation of techniques is provided to help you understand markings or patterns which may appear on this reproduction.

1. The sign or "target" for pages apparently lacking from the document photographed is "Missing Page(s)". If it was possible to obtain the missing page(s) or section, they are spliced into the film along with adjacent pages. This may have necessitated cutting thru an image and duplicating adjacent pages to insure you complete continuity.

2. When an image on the film is obliterated with a large round black mark, it is an indication that the photographer suspected that the copy may have moved during exposure and thus cause a blurred image. You will find a good image of the page in the adjacent frame.

3. When a map, drawing or chart, etc., was part of the material being photographed the photographer followed a definite method in "sectioning" the material. It is customary to begin photoing at the upper left hand corner of a large sheet and to continue photoing from left to right in equal sections with a small overlap. If necessary, sectioning is continued again — beginning below the first row and continuing on until complete.

4. The majority of users indicate that the textual content is of greatest value, however, a somewhat higher quality reproduction could be made from "photographs" if essential to the understanding of the dissertation. Silver prints of "photographs" may be ordered at additional charge by writing the Order Department, giving the catalog number, title, author and specific pages you wish reproduced.

**University Microfilms**

300 North Zeeb Road
Ann Arbor, Michigan 48106

A Xerox Education Company

# AN INVESTIGATION OF THE NEUROMUSCULAR COMMAND IN THE CONTROL OF RESPIRATION

BY

NIRMAL KUMAR MISHRA

A DISSERTATION

PRESENTED IN PARTIAL FULFILLMENT OF

THE REQUIREMENTS FOR THE DEGREE

OF

DOCTOR OF ENGINEERING SCIENCE

AT

NEWARK COLLEGE OF ENGINEERING



Newark, New Jersey
1972

## ABSTRACT

The purpose of the investigation is to study the signals involved in the respiratory system and to obtain a model for the dynamics including the activity of the phrenic nerve as the input and the transpulmonary pressure, air flow and the volume as the response.

Experiments were done on anasthetized dogs under natural breathing, with steady state response to various levels of $CO_2$ in the inspired air, and under electrophrenic stimulation. Bipolar electrodes were used at the phrenic nerve, in the cervical region, either for recording the phrenic neurogram or for supramaximal unilateral (or bilateral) stimulation using pulse frequency modulated sine waves or square waves. Both pulse rate and modulating frequency were kept within the physiological range of breathing. The recorded electromyogram of the diaphragm, picked up by surgical insertion of bipolar electrodes, was amplified, rectified and filtered by a modified third order Paynter filter. The ensemble average of the variables over several breaths of the experimental animal was performed. Spectral analysis of the filtered EMG, under both natural breathing and stimulation, was also carried out.

In the present work, force and tension of the diaphragm were not measured. However, on the basis of physiological evidence, a simple first order model, with a time constant of 0.1 second is proposed to represent the relevant EMG-tension dynamics. The diaphragm, approximated as a segment of a hemispherical dome then yields a ten-

sion-pressure relationship depending on the radius of curvature of the diaphragm. The resting radius of curvature is represented as a non-linear function of the resting lung volume and its variation, in turn, depends on the tidal volume and the resting radius of curvature. Finally, a simple first order transfer function is used to represent the pressure-volume dynamics with estimated respiratory resistance and compliance. An analog computer simulation has been performed using the filtered EMG as the input.

The work reveals a correspondence between phrenic neurogram and electromyogram of the diaphragm supported by both spectral analysis and time-domain measurements. On this basis, the electromyogram is considered to represent the neural command. A special technique facilitates the elimination of the contribution of the cardiac spikes to the spectrum of the EMG. The elimination of the cardiac spike was also facilitated by ensemble averaging. The overall model represents the neuromuscular section of the controller in the respiratory feedback system and its response depends on the recorded EMG under various external conditions. Both the input (EMG) and some of the response variables (transpulmonary pressure, volume and flow) can be measured by non-invasive techniques.

APPROVAL OF DISSERTATION

AN INVESTIGATION OF THE NEUROMUSCULAR

COMMAND IN THE CONTROL OF RESPIRATION

BY

NIRMAL KUMAR MISHRA

FOR

DEPARTMENT OF ELECTRICAL ENGINEERING

NEWARK COLLEGE OF ENGINEERING

BY

FACULTY COMMITTEE

APPROVED: _____ , Co-Chairman

_____

_____

_____

_____ , Co-Chairman

NEWARK, NEW JERSEY

JUNE, 1972

THIS WORK IS DEDICATED IN THE MEMORY OF

MY MOTHER, FATHER, AND TWO BROTHERS.

ACKNOWLEDGEMENTS

The author wishes to express his sincere thanks to numerous people, at various institutions, who made this dissertation possible.

Words are not sufficient to thank Dr. Andrew U. Meyer for suggesting the topic and for his continued interest, excellent advice and sustained encouragement during the entire period of this research. The author is sincerely grateful to Dr. Ruy V. Lourenço of the Abraham Lincoln School of Medicine, University of Illinois, Chicago, for his interest, support and advice; to Dr. Helmi El-Ramli, to Dr. Myron Evanich, and to Mr. Frank Hass of the Hektoen Institute for Medical Research and of the University of Illinois, Medical Center, Chicago, for their technical guidance in experimental surgery; to Dr. Gyan Agarwal of the University of Illinois at the Chicago Circle, to Dr. Arthur Rosen of the University of Illinois, Medical Center, Chicago, and to Mr. Mark Friedman of the Institute of Animal Behaviour, Rutgers University, for stimulating and fruitful discussions during the various stages of development of this research; to Dr. John Sharp and Mr. Walter Druz of the Veteran's Administration Hospital, Hines, Illinois, for their permission and assistance in the use of their EAI-380 Computer; to Dr. William Weissman of the College of Medicine and Dentistry of New Jersey, to Dr. Eugene H. Smithberg, to Dr. Mauro Zambuto and to Dr. Raj P. Misra of Newark

College of Engineering for their careful review of this manuscript; and lastly to Mrs. Peggy Franco for her excellent typing and editorial assistance.

This work was supported by General Research Support Grant number FR0554 of the Hektoen Institute for Medical Research of the Cook County Hospital, Chicago, Illinois, and in part by NIH Grant number HE11805.

TABLE OF CONTENTS

## LIST OF FIGURES

## LIST OF SYMBOLS*

| Quantities Used in Respiratory Mechanics | | Units |
|---|---|---|
| $V$ | Volume | liters or milliliters |
| $V_o$ | Resting lung volume at Functional Residual Capacity | liters, or milliliters |
| $V_t$ | Tital volume | liters, or milliliters |
| $\dot{V}$ | Flow of air | liters per sec or milliliters per sec. |
| $\dot{V}a$ | Alveolar ventilation | liters/minute, or liters/sec. |
| $\dot{V}amt$ | Alveolar minute ventitation as the total volume of air inspired in one minute | liters/minute |
| P | Pressure (This is general symbol and is usually followed by subscripts as shown below) | cm. $H_2O$ or mm. Hg. |
| Patm | Atmospheric pressure | cm. $H_2O$ or mm. Hg. |
| Pbs | Pressure at body surface | cm. $H_2O$ or mm. Hg. |
| Palv | Alveolar pressure | cm. $H_2O$ or mm. Hg. |
| Pao | Pressure in mouth with airways open | cm. $H_2O$ or mm. Hg. |
| Plt | Pressure across lung-tissues | cm. $H_2O$ or mm. Hg. |
| Ppl | Pressure inside pleural cavity | cm. $H_2O$ or mm. Hg. |
| Pes | Esophageal pressures | cm. $H_2O$ or mm. Hg. |
| Prs | Pressure across entire respitatory system | cm. $H_2O$ or mm. Hg. |
| Pmus | Pressure across the muscle (usually contributed by its active state; sometimes divided into two parts, i.e., Pmus rc (rib cage) and Pmus ab (abdominal muscles) | cm. $H_2O$ or mm. Hg. |

*Most symbols follow the glossary of symbols adopted by Mead and Milic-Emili [37]. All variables, unless otherwise stated, are functions of time.

| | | |
|---|---|---|
| Pw | Pressure across chest wall | cm. $H_2O$ or mm. Hg. |
| Ptd | Transdiaphragmatic pressure | cm. $H_2O$ or mm. Hg. |
| Ptp | Transpulmonary pressure | cm. $H_2O$ or mm. Hg. |
| Pab | Abdominal pressure | cm. $H_2O$ or mm. Hg. |
| Pg | Gastric pressure | cm. $H_2O$ or mm. Hg. |
| $PO_2$ | Partial pressure of oxygen in blood | mm. Hg. |
| $PCO_2$ | Partial pressure of carbon dioxide in blood | mm. Hg. |
| $[H^+]$ | Hydrogen ion concentration in blood | milli mol/liter |
| C | Compliance as slope of volume-pressure curve in respiratory mechanics | liters/cm $H_2O$ |
| R | Flow resistance | cm. $H_2O$/liter per sec. |
| I | Inertance | cm. $H_2O$/liter per sec. |
| BR | Breathing rate | breaths per minute |

Variables Used in Electromechanical Dynamics of Muscle

| | | |
|---|---|---|
| F | Force as applied to muscle | $kg/cm^2$ |
| T | Tension, e.g., as developed in a muscle | kg/cm |
| $T_e$ | Elastic tension in the muscle | kg/cm |
| $T_m$ | Total muscle tension (including elastic and electrically generated tensions) | kg/cm |
| L | Length of the muscle | cm |
| $\dot{L}$ | Rate of change of Length | cm/sec |
| r | Radius of curvature of the diaphragm | cm. |
| $r_o$ | Radius of curvature of the diaphragm at rest (FRC) | cm. |

| | | |
|---|---|---|
| EMG | Electromyogram of the muscle as recorded by bipolar electrodes | milli volts † |
| \|EMG\| | Full-wave rectified EMG | milli volts † |
| E | Moving average or filtered \|EMG\| | milli volts † |
| PNG | Phrenic neurogram of whole nerve bundle as recorded by bipolar electrodes | milli volts † |
| \|PNG\| | Full-wave rectified PNG | milli volts † |
| Ep | Moving average or filtered \|PNG\| | milli volts † |

†In most experiments, arbitrary units were used after the signal amplitude had been normalized (with reference to the one under spontaneous breathing, at room air).

# 1. INTRODUCTION

The nature and purpose of respiration - i.e., the external respiration - has been investigated for a long time. The main function of external respiration is to provide oxygen to the cells of the body and to remove excess carbon dioxide from them. Different species may have different ways in which this purpose may be achieved. In large animals, including man, external respiration is also characterized by respiratory regulation whereby a desired level of oxygen, carbon dioxide and hydrogen ion concentration is maintained in the arterial blood. An unbalance of these blood gases will produce respiratory system instability. Several experiments by physiologists, as summarized by Haldane and Priestly [1], throw light on these chemical factors as the principal participants in the 'regulation' or 'control' of respiration. Haldane and Smith had revealed, in 1893, the role of oxygen in the control of respiration by a simple experiment in which re-breathing of oxygen depleted air, from which $CO_2$ is removed, results in an increased respiratory effort [1]. Besides establishing the significance of an optimal range of blood oxygen levels in the regulation of breathing, the result of this experiment also contained the implication of a feedback mechanism, including the existence and location of oxygen-sensitive receptors.

These early experiments led to the development of the first quantitative theory, known as Gray's Multiple Factor Theory in 1945 [2], which represents the first mathematical model of the

'respiratory-chemostat'. Its aim was to relate the steady state ventilation to $CO_2$ inhalation, the lack of $O_2$ in the arterial blood and to the metabolic disturbance in the acid-base balance. Even though Gray did not use feedback control theory, it is implicit in his Multiple Factor Theory. An obvious consequence of Gray's theory has been an increased interest in the study of respiration as a feedback system during the last twenty-five years. While considering the steady state and transient response to $CO_2$ inhalation, Grodins et al. [3] represented Gray's results in terms of a feedback model, adding the effect of $CO_2$ inhalation. This model, shown in Figure 1-1, relates the alveolar minute ventilation, $\dot{V}amt$ (in liters/minute), the partial pressures of oxygen and carbon dioxide, $PO_2$ and $PCO_2$ respectively (in mm. Hg.), and the hydrogen ion concentration, $[H^+]$ (in m M/liter) to a disturbance created by a change of $CO_2$ concentration in the inspired air. As shown in Figure 1-1, the model is broken down to a "controlling system" and a "controlled system", in which $\dot{V}amt$ is considered the controlling variable and $PO_2$, $PCO_2$ and $[H^+]$ are considered the controlled variables. In the first model of Grodins et al. only $PCO_2$ in the venous blood (rather than arterial blood) was considered, whereas $PO_2$ and $[H^+]$ were ignored. In some of the later models to be discussed briefly in the next chapter, all these variables are incorporated. These chemostat models, do not, however, include the internal dynamics of the controlling system.

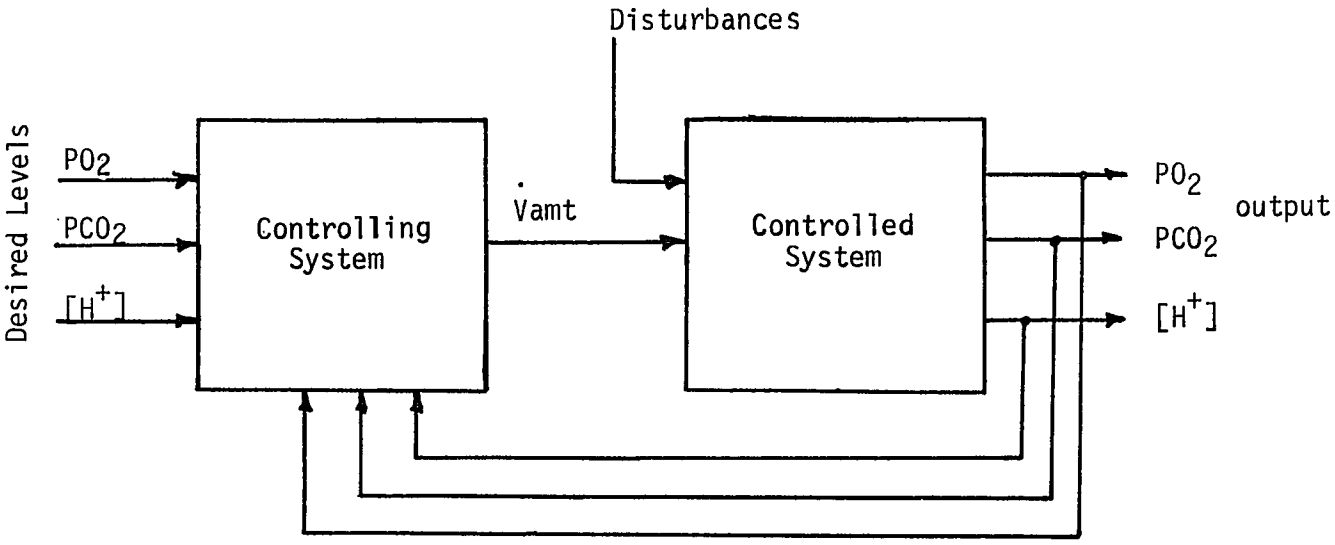


Figure 1-1 Respiratory Chemostat on the Basis of Gray's Multiple Factor Theory (From Grodins et al [41])

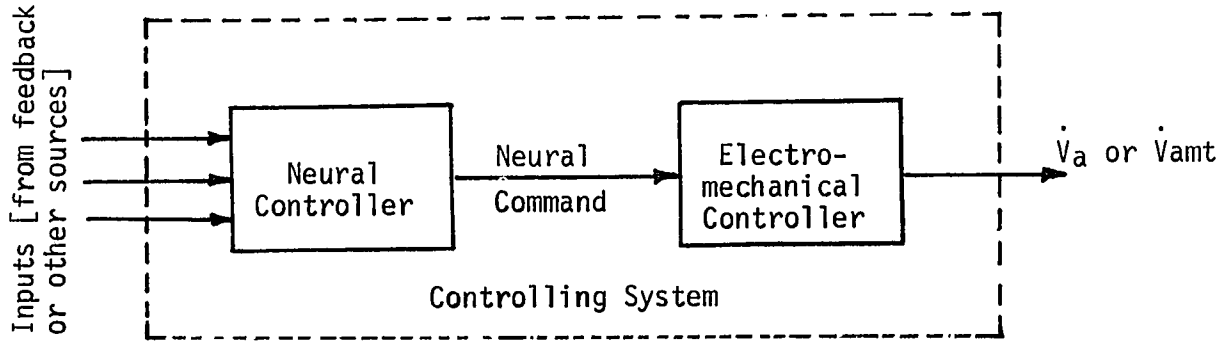


Figure 1-2 Two subsystems within the Controlling System.

There are two major physiological processes involved in the controller dynamics; namely, (1) the transduction of chemical to electrical signals; and (2) the conversion of electrical signals into mechanical work. After the controller has received the feedback input, in terms of $PCO_2$ in the venous blood, the chemoreceptor transforms the chemical signal into electrical signals directed to the respiratory center, which is considered to be located in the medulla in the brainstem. The chemoreceptor thus forms a part of the controller and has a significant physiological role to play. The other important process in the controller is the processing and transmission of neural signal to the respiratory muscles. In addition to being a center where the afferent nerves terminate and from where the efferent nerves originate, the respiratory center is also capable of self-oscillations; this has been referred to as the basic rhythmicity [4], [5]. The chemoreceptors, their afferent nerves to the respiratory center and the respiratory center itself along with its other feedback afferent nerves can be lumped together as the neural controller and can be investigated as a subsystem.

The second physiological process involves the neural command signal to two major muscles; namely, the intercostal muscles in the rib cage and the diaphragm which separates the thoracic cage from the abdominal cavity. The response of these muscles to the inspiratory neural command is contraction of these muscles, resulting in an increase of the thoracic volume. As a consequence,

the lungs expand, producing an inhalation. These factors can be lumped together as the electromechanical controller subsystem. The two major physiological processes, discussed above, are represented in the block diagram of Figure 1-2 and are valid in all models of respiratory control presented here.

It is possible to extend the subdivision of the controller to more than the two levels shown in Figure 1-2. One may, for example, consider a further subdivision of the electromechanical controller into two levels - one which transforms the command signal into the mechanical variables of the respiratory muscles and another which determines the effect of these mechanical variables on the mechanical events in respiration.

Before any modeling is attempted one may consider some of the works of the physiologists whose investigations fall in the 'controller subsystem' of the chemostat. For example, investigations have been made of the rhythmicity of the respiratory center itself [4],[5], on the nature of phrenic neural command [6]-[11], on the discharge pattern of the brainstem respiratory neurons under chemical or neural feedback [12]-[16], and the mechanical events in respiration including the electromechanical dynamics of a skeletal muscle [17]-[33].

If any quantitative approach is to be adopted to extend the model of the respiratory controller, it is important to consider three levels of signal representation. At the first level of

signal representation is the consideration of the activity of the individual neuron as a train of action potentials, characterized by a pulse frequency modulated wave. The second level is the consideration of the envelope of the pulse trains as superposed in a bundle of nerve fibers or at the muscle fibers as seen in an electromyogram. It is this envelope which contains the relevant information on the temporal variations in respiratory mechanics as produced in a single breath. Subsequent breaths are repetition of the same process and present a periodic signal. At the third level of signal representation,long-time rectified average signals are considered,such as the 'minute ventilation' as included in most chemostat models. These three levels of signal representation describe the modeling 'hierarchies' from the point of signal processing. In addition to separating the levels of signal representation, these hierarchies require their own experimental verification and possess their particular limitations. The neural activity quantification, for example, requires microelectrodes and special recording systems. The third level, on the other hand, is experimentally obtained easily, but since it represents long-time averaged signals, it cannot be used in a model of the (short-time) dynamics of the system.

The present investigation concentrates on the dynamic input-output relationship between the neural command and some selected mechanical events in respiration. It begins with a review of present models and their limitations. Since the major interest lies

in the dynamics of the electromechanical sub-block of the controller, an attempt is made to formulate a method of quantification of the electrical activity of the nerve bundle and the muscle. Assuming a one-to-one correspondence between the action potentials of the nerve fiber and the muscle fiber, which it innervates, the major emphasis is placed on the electromyogram (EMG). The EMG itself is measured at the diaphragm because the diaphragm is considered a major muscle in respiration and the EMG can be recorded in human subjects without any surgical technique. The variables chosen for the respiratory mechanics are transpulmonary pressure, airflow and volume. By selecting a moving average of the rectified EMG, all variables are functions of time and emphasize breath-by-breath events. All experimental work is obtained from anasthetized dogs. The choice of the quantification techniques, places this investigation in the second level of modeling hierarchies discussed above. The system modeling is guided by physiological evidence and by experimental studies both under natural breathing and under electrophrenic stimulation. It is verified by an analog simulation using the recorded electromyogram as the input to the proposed model.

# 2. MODELS OF RESPIRATORY SYSTEM

In treating respiration as a feedback control system several models have evolved during the last twenty-five years. Even though the major effort has been to explain the chemical control of respiration, attempts have also been made for the study of the model of ventilation and for system identification of a feedback model. Furthermore, some models have included the neuromuscular dynamics in respiration. These represent a progressive refinement of the modeling approach not only to understand the respiratory physiology but also to produce a workable diagnostic tool in respiratory abnormalities - especially with the aid of analog or digital computers. Before these models are reviewed, a brief description of the physiology of respiration is relevant.

## 2.1 Review of Physiology of Respiration

Respiration is the process of utilization and supply of oxygen to the body tissues. The cellular metabolic processes by which oxygen is utilized are called internal respiration whereas the processes which are responsible for the supply of oxygen to the cells and the removal of carbon dioxide from them is called the external respiration. This review is restricted to those processes which form the external respiration - especially as they appear as elements in a feedback system. This feedback is negative; its purpose is to maintain the appropriate partial pressures of oxygen and carbon dioxide and the pH in the arterial blood (and thereby in the tissues). The system stability is affected by alveolar ventilation

rate. As shown in Figure 1-1, such a system has two basic subsystems called the controlling system and the controlled system.

The controlling system has one major generator of neural command. It is believed to be located in the medulla and is often referred to as the respiratory center, RC. In the model the respiratory center acts as an error detector whose function is to compare the desired levels of the body $PCO_2$, $PO_2$ and the hydrogen ion concentration $[H^+]$ with the output of the controlled system and to transmit the necessary neural command to the respiratory muscles. Anatomically the respiratory center consists of groups of inspiratory and expiratory neurons located bilaterally in the medulla of the brainstem. It is this center which generates an inherent rhythmicity though the physiological nature of this rhythmic activity is not clearly understood. By using microelectrode techniques and by surgical sectioning of the brainstem containing pons and medulla, Salmoiraghi and his associates [4],[5] have localized the basic respiratory neural oscillator in the medulla. Burns [34] postulated an interconnected group of inspiratory and expiratory neurons with the process of reciprocal innervation. The interconnections are such that the neural signals thus generated exhibit the typical pattern of neural signals for respiration. A simple example of such an interconnection of two inspiratory and two expiratory neurons is illustrated in Figure 2-1.

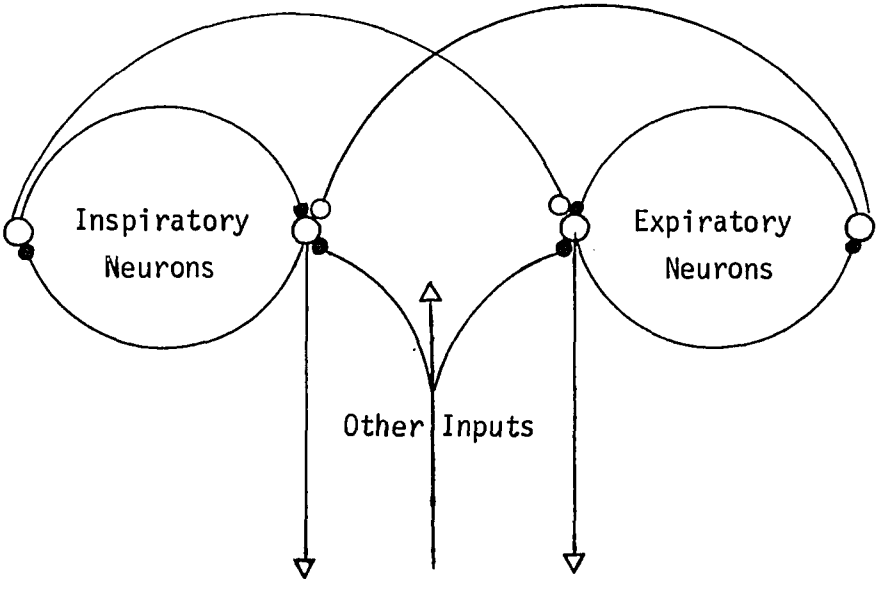


● Excitatory Synaptic Junctions

o Inhibitory Synaptic Junction

Figure 2-1 Simplified schematic of a self-oscillating respiratory center (From [35]).

This schema postulates the existence of an oscillator,the frequency of which corresponds to the frequency of respiration containing an inspiratory and an expiratory period. Although the medulla contains this basic respiratory oscillator, the frequency of oscillation is also affected by the inputs from several afferent fibers terminating at the center. These inputs are in response to several chemical, mechanical, or psycho-physiological (such as excitement or pain) factors, which may originate in the higher brain centers, to induce a voluntary change in respiration. A comprehensive study of all such feedbacks to the respiratory center is not available. However, in most models, emphasis is justifiably placed on chemo- and mechano- receptors since they are considered to play a major role in the control of respiration. The known peripheral chemoreceptors (or chemical sensors) are located in the bifurcation of the common carotid arteries and also at the arch of the aorta. These receptors are activated only when the arterial $PO_2$ level falls below a certain threshold value, however, their sensitivity to changes in $PCO_2$ and pH is not so significant. The central chemoreceptors, on the other hand, are considered to be sensitive to the increase of $PCO_2$ in the arterial blood. These are also sensitive to $[H^+]$ and are located in the medulla, though they are anatomically distinct from the respiratory center. Due to their location in the medulla, they are not only perfused with blood but also bathed in cerebrospinal fluid. This suggests their response is controlled not only by the chemical changes in the blood but also by those in the cerebrospinal fluid.

There are several other afferent pathways through which feedback signals, in response to mechanical changes, can reach the respiratory center. The major pathways are for proprioceptive feedback from the intercostal muscles (and to a very small extent from the diaphragm) transmitted via the nerve fibers along the vagus nerve and, in the case of the diaphragm, via the phrenic nerves. Lungs also contain mechanoreceptors sensitive to lungs' stretch or collapse. The afferent discharge from these receptors participates in what is known as the Hering-Breur reflex. Near the upper respiratory passages are receptors producing afferent discharge stimulated by chemical or mechanical irritants. These are responsible for the cough reflex.

The only predominant output of the respiratory center is the neural command to the respiratory muscles. These are trains of action potentials along the motor fibers running downwards from the respiratory center into the spinal cord. With synaptic junctions on the anterior horn cells, these fibers activate the motor neurons at different segments of the spinal cord. The major muscle responsible for ventilation is the diaphragm. This is a dome-shaped (concave downwards) sheet of striated muscle separating the abdominal and the thoracic cavities. In quiet breathing, this may be the only muscle active in respiration. The diaphragm is innervated by phrenic motor nerves whose fibers have their origin in the spinal cord at the 3rd to 5th cervical segments in man. External intercostal muscles are located between the ribs and the contraction of these

muscles pulls the ribs upwards and outwards during inspiration to increase the volume of the thoracic cavity. Their innervation is provided by the intercostal nerves which leave the spinal cord between the 1st and 11th thoracic segments. The contraction of intercostal muscles is not essential for breathing if the diaphragm is able to function normally. The scalene and sternomastoid are other muscles which may be active in inspiration. Again, they are not considered necessary for normal quiet breathing.

The diaphragm is the major muscle of inspiration, its relaxation is a passive process upon the cessation of inspiratory motor impulses along the phrenic nerves. The muscles, which are active in expiration, are the internal intercostal muscles. In abnormal situations, the abdominal muscles can act to support expiration.

As striated muscle, both the diaphragm and the intercostal muscles contain receptors which are responsible to length change and rate of length change of the muscle fibers. These are called proprioceptors. Their location, function, and significance so far as the diaphragm is concerned, is not clearly understood.

The purpose of the neural command is to activate the muscle fibers by depolarizing them for muscle contraction. There is a one-to-one relationship between a nerve impulse and its muscle fiber action potential due to the release of acetylcholine and the production of end-plate potential at the neuromuscular junction. An individual motor nerve fiber usually spreads out at

muscle and is connected to several muscle fibers in parallel. The bundle of such muscle fibers activated by a single neural input is called a motor unit. If the discharge of the motor unit is picked up by electrodes, the recorded signal is the electromyogram. The fundamental property of the muscle's response to an action potential in its fibers is to contract. This is measurable either as physical shortening of the muscle or as changes in the tension of the muscle. The nature of the mechanical properties of the muscle - especially one relating EMG-tension dynamics is an important aspect of this dissertation and shall be explored later. Considering the two major respiratory muscles, the diaphragm and the intercostal muscles, contraction leads to volume and pressure changes within the thoracic cage. If the inspiratory effort is considered as the only active effort, the diaphragm's contraction causes it to flatten or descend whereas the rib cage is expanded due to contraction of the inspiratory intercostal muscles.

The ventilatory process is completed by expansion or contraction of the lungs. Air is conducted from the external environment to the lungs by a series of dichotomously branching tubes. Beginning at the trachea, this undergoes 23 generations of the bracheo-bronchial tree. The first 17 generations function as conducting passages; the remaining ones ending in alveolar ducts, provide the access for gas diffusion across the alveolar membranes which separate the air space within the lungs from the circulating pulmonary blood. Each lung lies within a double layered sac forming the parietal and

visceral pleura. During quiet expiration, the volume of the lungs decreases due to the elastic recoil of the lungs. The dynamics of the lungs and the respiratory mechanics can be briefly summarized in Figure 2-2.

Figure 2-2 illustrates several pressures that are involved in respiratory mechanics. All pressures are relative to an arbitrary reference pressure, usually atmospheric pressure, Patm. In a normal environment, the body pressure, Pbs, can be assumed to be the same as Patm. Flow of air takes place when a pressure difference exists between the alveolar pressure, Palv, and the mouth pressure, Pao, with airways open. The expansion or contraction of the alveoli of the lungs depends not only on the pressure difference across the lung tissues but also on the visco-elastic properties of the lungs. The pressure difference across the lungs, Plt, represents the difference between the pleural pressure, Ppl, and the alveolar pressure. The direct measurement of pleural pressure is very difficult. However, since this pressure is approximately equal to the esophageal pressure, Pes, the measurement of Pes by balloon technique is considered an acceptable procedure to measure Ppl. Under static conditions the pressure in the total respiratory system, Prs, equals Palv assuming the reference pressure to be zero. Stated otherwise, this Palv is the sum of Plt and the chest wall pressure, Pw. Under dynamic conditions, muscular pressure, Pmus, must be added to this to yield Palv, as shown in Figure 2-3. Here the muscular pressure, Pmus, represents the increase in Pw due to active state of the respiratory muscles.

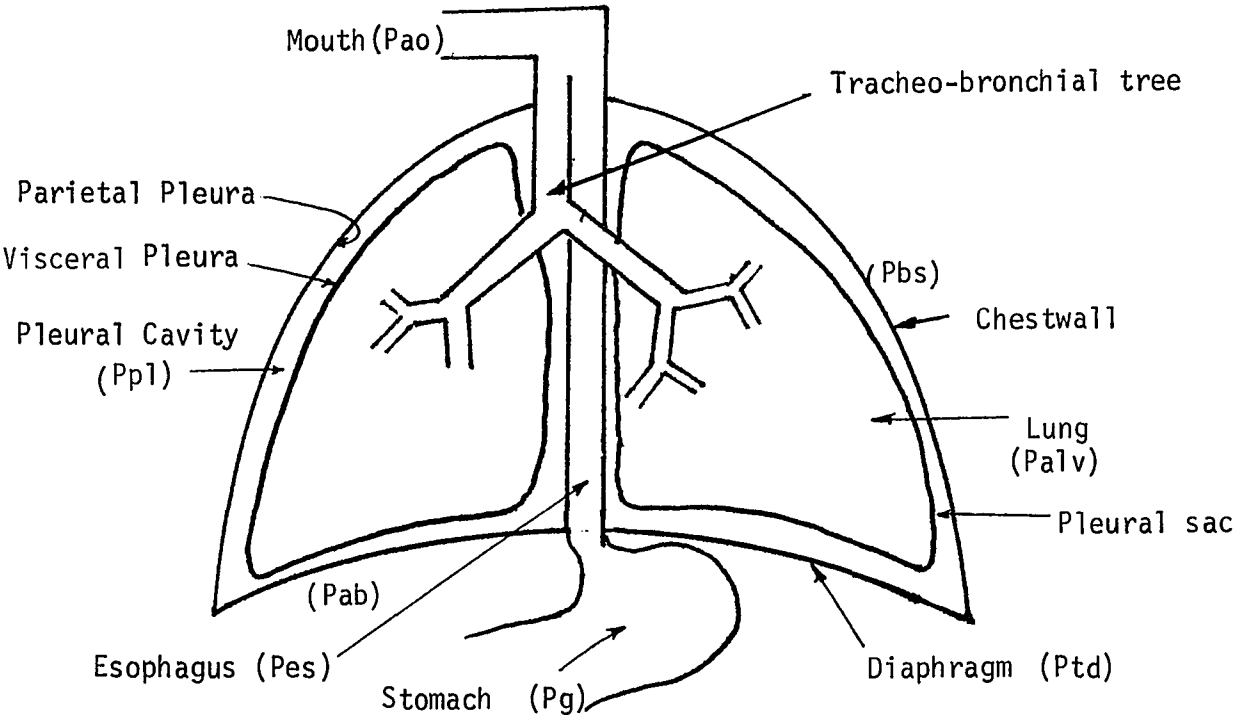


Figure 2-2 Some pressures involved in respiratory mechanics. For details see text (From Hidebrandt and Young [36]).

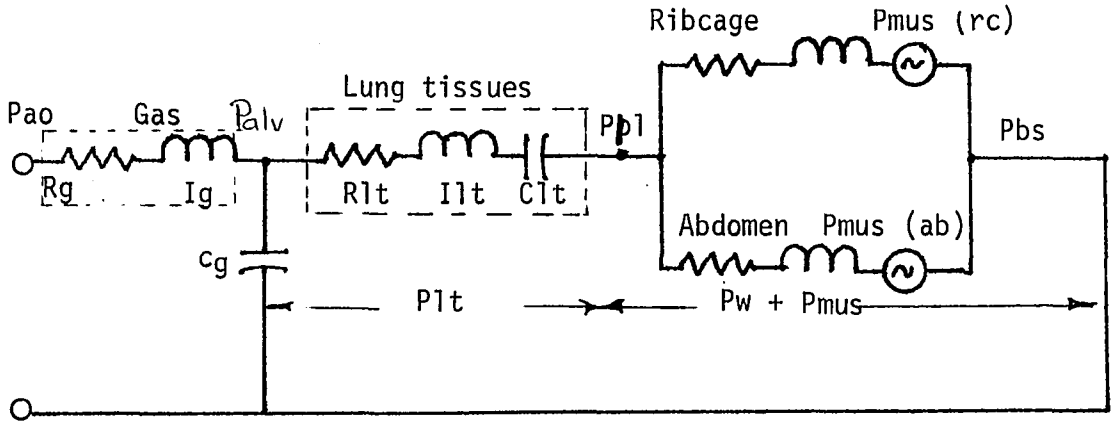


Figure 2-3 A simplified electrical analog of the total respiratory system (From Mead and Milic-Emili [37]).

The dynamics of the respiratory mechanics are rather complex since they involve many driving forces and distributed parameters including airway resistance, compliance of various anatomical parts and inertia. A simplified electrical analog has been described by Mead and Milic-Emili [37] in which it is assumed that distributed parameters can be lumped and that the entire system has only one degree of freedom. Such an analog is shown in Figure 2-3.

The pulmonary ventilation along with the cardiac output results in the pulmonary gas exchange. This takes place at the alveolar membranes which separate the gas region of the lungs from the surrounding blood perfusion. The membranes permit the diffusion of $CO_2$ from the liquid phase to gas phase and also allow the diffusion of $O_2$ from the inspired alveolar air into the arterial blood. These diffusion processes depend on concentration gradients and the membrane's resistive property to ionic diffusion. The path of fluid input is the pulmonary 'artery' containing higher percentage of carbon dioxide which is accumulated in the venous blood due to metabolic production of $CO_2$ by the body tissues. The fluid output path is the pulmonary 'vein' which has the gas composition of arterial blood. An important factor which determines the rate of gas exchange is the pressure gradient between alveolar gas and the mixed venous blood in the pulmonary 'artery'. This gradient in turn depends on the alveolar ventilation rate, metabolic rate of production of $CO_2$ and the cardiac output. The arterial blood, after diffusion, must maintain the desired level of $PCO_2$ and $PO_2$. The peripheral and central chemoreceptors are

the chemical sensors which determine these levels in the arterial blood. Finally, the afferent nerves from the chemoreceptors 'close the loop' in the respiratory chemostat.

The physiology of respiration, as reviewed above, is a gross simplification but adequate for modeling. It does, however, reveal that the controlling system as shown in Figure 1-1 is over-simplified. This controlling system includes several features between the chemical feedback as its input and the alveolar ventilation as its output. Some essential physiological features are the central and peripheral chemoreceptors, the respiratory center, its output as neural command to the respiratory muscles, the respiratory muscles and their electro-mechanical dynamics yielding pressure variables in the thoracic cage and the viscoelastic lungs. Certain minor loops in the controlling system are shown as subsystems of the total respiratory system in Figure 2-4. These inner loops are due to neural feedback from the stretch receptors in the lung and the proprioceptors in the muscles. Furthermore, the medullary respiratory center itself has been investigated as a self-oscillating subsystem. The controlled system also has several hidden physiological features, such as the diffusion process, transport delays due to blood circulation system, metabolic process producing $CO_2$ in venous blood, the transport of arterial blood to body and brain tissues, and similar transport delays in venous blood flow. The recent modeling approach utilizes most of these physiological factors to produce a workable model. Yet still larger areas remain unexplored.

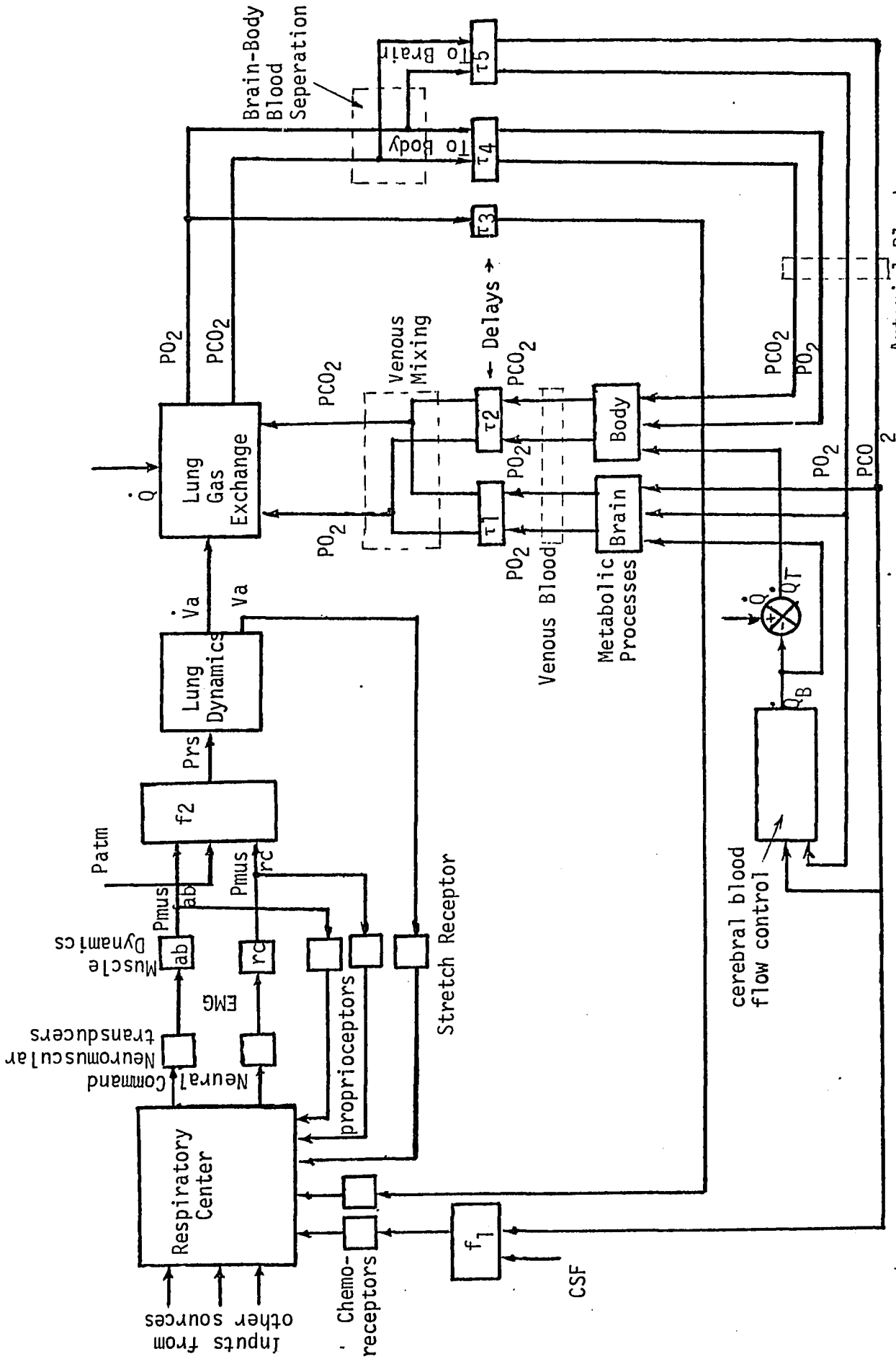


Figure 2-4 A simple schematic of the overall respiratory control system. The figure represents anatomical parts, physiological functions, and basic signal-flow paths.

The regulation of respiration, thus, involves a complex biological system. Its analysis is feasible upon simplifying assumptions which are adaptable to changing data. The major aspects of respiratory physiology can be summarized in a simple diagram of the entire respiratory system. This is shown in Figure 2-4.

## 2.2 Models of Respiratory System

2.2 (a) Respiratory Chemostat. Gray [2], in 1945 had proposed the 'Multiple Factor Theory' of ventilatory control by chemical stimuli. His hypothesis suggest that three stimuli, $PCO_2$, $PO_2$ and $[H^+]$ act individually and the ventilatory response is additive. Gray supported this hypothesis by empirical evidence and attempted the first quantitative description of respiratory regulator. He was also able to investigate the separate effects of $PCO_2$, $[H^+]$ and $PO_2$ by simple experiments [38]. For example, the effect of $PCO_2$ and $[H^+]$ can be separated by data of $CO_2$ response under two different conditions; one in which $PCO_2$ and $[H^+]$ both increase and another in which $PCO_2$ decreases but $[H^+]$ increases due to metabolic acidosis. The equation suggested by Gray is:

$$\dot{V}amt = 1.1(H^+) + 1.81\ PCO_2 + (2.38\times10^{-8})(104-PO_2)^{4.9} \qquad (2.1)$$

where $\dot{V}amt$ = alveolar minute ventilation in liters/min., $[H^+]$ is arterial hydrogen ion concentration in m M/liter, and $PCO_2$ and $PO_2$ represent arterial gas tensions (as partial pressures) in mm Hg. Thus an increase in arterial $PCO_2$ will increase the minute ventilation. This is what Gray described as 'compensatory adjustment'

because the increase in $\dot{V}amt$ will tend to reduce the arterial $PCO_2$. This way, Gray had implicitly suggested the negative feedback effect in the chemical control of ventilation. The 'compensatory effect' was mathematically formulated as:

$$PCO_2 = PCO_2' + \frac{k(MR)}{Vamt} \tag{2.2}$$

and

$$PO_2 = PO_2' - \frac{k(MR)}{Vamt} \tag{2.3}$$

where the primed variables represent tracheal pressures, MR is the metabolic gas exchange rate and k is a constant to equalize the units on both sides of equations (2.2) and (2.3). The problem of obtaining the dependence of $[H^+]$ on ventilation was solved by linearizing Henderson-Hasselbalch's blood buffer equation yielding:

$$[H^+] = a\ PCO_2 + b \tag{2.4}$$

where a and b are constants depending on oxygen capacity, oxygen saturation and the bicarbonate contents of the blood.

Grodins et al. [3] used this quantitative approach to propose the first mathematical model of respiratory regulator with the specific purpose of predicting the respiratory response to breathing of air mixed with $CO_2$ as a disturbance variable (as shown in Figure 1-1). Their simplified model was the result of theoretical analysis of the respiratory system. There were several assumptions made. It

is necessary to mention these assumptions since later models were developed partly after modifying these assumptions. Furthermore, on the basis of these assumptions certain models can be compared. These assumptions were: (1) that lungs can be regarded as a rigid box of constant volume, zero dead space, and homogeneous content ventilated by a continuous unidirectional stream of gas; (2) the respiratory quotient, (RQ = volume of $CO_2$ expired/volume of $O_2$ absorbed), is 1 at every instant; (3) blood transport delays are negligible; (4) the respiratory center can be lumped with all other body tissues in a homogeneous reservoir having constant blood flow; (5) the arterial blood, venous blood, and the body tissues have the same linearized $CO_2$ absorption curve; (6) expired air and the arterial blood are in continuous $CO_2$ equilibrium as are the tissues and the venous blood; and (7) the controlling system gives a linear relation between $CO_2$ concentration, $\theta_T$, and alveolar minute ventilation $\dot{V}amt$ namely:

$$\dot{V}amt = a\ \theta_T - b \tag{2.5}$$

where the constant a represents controller gain and b represents controller bias. To establish the equation for the controlled system, the chemical continuity equations were established for the lung reservoir and the body tissue reservoir. The controlled system dynamics were represented by a second order differential equation of the type:

$$a_1\ \ddot{\theta}_T + (a_2 + b\ \dot{V}amt)\ \dot{\theta}_T + \dot{V}amt + \theta_T = a_3 + (a_4 + a_5\ FCO_2)\ \dot{V}amt \tag{2.6}$$

In equation (2.6) $\theta_T$ represents the output of the controlled system and the forcing function is represented by $FCO_2$, the fraction of $CO_2$ in inspired air. This forcing function enables the model to predict transient response of the respiratory chemostat to sudden change in the $CO_2$ contained in the inspired air. Equations (2.5) and (2.6) together represent a nonlinear closed loop system. The constants in (2.5) and (2.6) depend on certain physiological constants. Grodins and his associates had simulated this system on an analog computer to compare experimental results for the step changes in $CO_2$ in the inspired air, $FCO_2$. Significantly, the response to a step input of $FCO_2$ in inhalation was in agreement with the model prediction, though the off-transient, due to cessation of $CO_2$ content in the inspired air, showed some discrepancy. This discrepancy represents the failure of experimental off-transient undershoot as expected from the theoretical model.

The attempt to modify the model began by removing the various assumptions which Grodins had made in his first model. Defares et al. [39] presented the first modified model where two important changes had been made in the earlier assumptions. First, they divided the single body-tissue compartment into two tissue compartments - one called the brain compartment and the other the non-brain (i.e., the remaining body tissue) compartment. Second, while recognizing the experimental evidence that cardiac output is unaffected by $CO_2$ inhalation, there was experimental evidence to support the view that cerebral blood flow depends on blood $PCO_2$. The two

modifications in the earlier assumptions are interrelated in the model of Defares and his associates. Except for adding a brain blood-flow controller equation by which brain blood flow $\dot{Q}_B$ is a nonlinear function of arterial $PCO_2$, the modeling approach is similar to one adopted by Grodins et al. The resulting effect is a nonlinear open loop equation. The overall behaviour of the model, however, does not provide any significant change in that earlier model.

Before these models could be extended or modified, Yamamoto [40] had made a theoretical analysis of the temporal variations of the alveolar $CO_2$. The general form of the dilution equation for determining the concentration of gas is:

$$C(T) = \frac{\int_0^T Q \, dt}{\int_0^T \dot{V} \, dt} \qquad (2.7)$$

where C(T) is the volume concentration at time T and Q represents quantity flow of concentrate. The numerator and the denominator integrals in (2.7) are short form versions of summated integrals using continuity equations during inspiration and expiration. The arterial $PCO_2$, as a function of time is oscillating about a mean. If the metabolic load is increased, as in exercise, the mean remains the same, though the amplitude of oscillations increases. On the other hand, under $CO_2$ inhalation, the mean may increase though the amplitude of oscillations decreases. Yamamoto also questioned the

validity of venous $PCO_2$ as the input to the controller in Grodins' model. Another implicit suggestion was to propose a model where respiratory variables shall be considered as continuous functions of time.

Grodins and James [41] used the above hypothesis to make some major modifications in their earlier chemostat model. This was done by considering flow signals, $\dot{V}$, in the form of a sinusoidal signal within the respiratory frequency range as the input to the controlled system. This replaced the concept of minute ventilation, $\dot{V}amt$, as used in their first model, as the input to the controlled system. Sinusoidal input to lung compartment needed two continuity equations - one valid during inspiration and the other one for expiration. Likewise, the alveolar arterial $CO_2$ equilibrium equation included a volume dependent parameter. The arterial $PCO_2$ was considered as the input to the controller. The controlling system was also modified by adding integral control to the proportional control. Also included in the model were the metabolic rate in exercise, arterial blood into brain and non-brain paths and the use of blood flow changes as another variable. By doing this, the model could predict the response both under $CO_2$ inhalation and under exercise. The important factor was the time course of arterial $PCO_2$ as suggested by Yamamoto.

The models developed so far have emphasized the control of ventilation by changing the $CO_2$ content in the inspired air. As shown in Equation (2.1), Gray's Multiple Factor Theory suggests the

dependence of ventilation on three independent variables. By using this multi-input significance and by using modified Henderson-Hasselbalch's equation, Milhorn and his associates [42] proposed another modification by considering $\dot{V}amt$ dependent on $PCO_2$ and $PO_2$, i.e.,

$$\dot{V}amt = f(PCO_2, PO_2) \tag{2.8}$$

With this equation, a linear relationship was proposed between minute ventilation and the two inputs, $PCO_2$ and $PO_2$, in the cerebral arterial blood. Inclusion of $O_2$ as a new variable necessitated the use of the $O_2$ dissociation curve which was assumed to be the same for arterial and venous blood. In addition, the major modification by Milhorn et al. in the earlier assumptions is the inclusion of transport delays due to blood circulation. Since the controlled system includes the three compartment scheme (i.e., lungs, brain tissues and body tissues) and since the peripheral chemoreceptors were localized to generate the $PO_2$ response, there were five time delays involved, two for arterial paths (lungs-to-brain and brain-to-lungs), two for venous paths (body-to-lungs and brain-to-lungs) and one for lungs-to-peripheral receptor, all due to blood circulation time. The physiological significance of this approach is clearly evident from Figure 2-4. Thus, the modeling approach of Milhorn and his associates includes certain known physiological facts which were likely to affect the system dynamics. Again, its basic purpose was to improve the model so that the results would be closer to experimental observation. This also implied modification of the earlier

assumptions underlying the first model by Grodins. The place of Grodins' first model in the chemostat system is illustrated in Figure 2-5.

Among the various model modifications, the one by Horgan and Lange [43] have proposed a model which represents not only for the normal breathing patterns, but also a type of abnormal breathing known as Cheyne-Stokes breathing. This breathing abnormality is exhibited by an oscillatory pattern in the changing minute-ventilation and can be explained, theoretically, by an increase of blood transport delays. There exists experimental evidence to support this hypothesis [43]. Horgan and Lange also incorporated a nonlinear chemoreceptor response. Except for these two changes, the model follows the same approach as that of Grodins' first model. Further modification of this model was proposed by Horgan and Lange [44] by inclusion of oxygen control loop, representing the effect of $O_2$ receptors to ventilation. This model did not simulate the $CO_2$ inhalation response successfully since the time constants used were not within realistic range. Horgan and Lange [45], therefore, presented yet another modification in their model by incorporation of the effect of $CO_2$ in the cerebrospinal fluid and the brain tissues. This needed additional compartments like brain tissue, blood-brain barriers and the cerebrospinal fluid in the controlled system. It may be pointed out that Milhorn and Guyton [46] also modified Grodins' earlier model, by including transport delays, to explain periodic breathing (Cheyne-Stokes breathing).

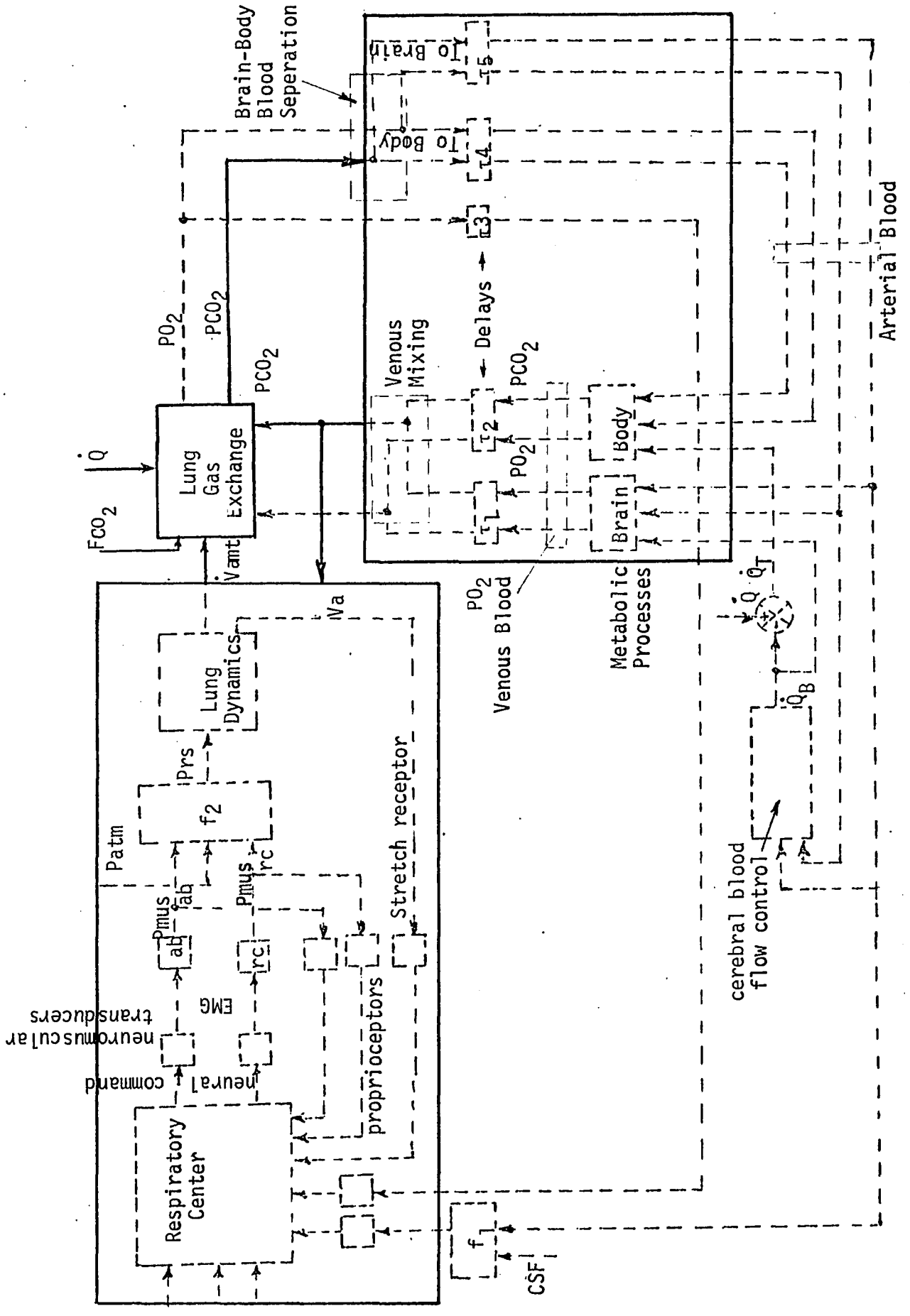


Figure 2-5 Simplest scheme for chemostat study. Grodins' Model I is shown by solid lines and the broken lines represent the factors not included in that model.

The model to explain Cheyne-Stokes breathing was continued by Longobardo and his associates [47] and was tested by Cherniack et al. [48] on periodic breathing in dogs. Basically the model included a first modification of Gray's Multiple Factor Theory, namely a multiplicative rather than additive effect of chemical stimuli on ventilation. Furthermore, the new approach was adopted to describe the dynamics of the controlled system. This was done by consideration of $CO_2$ and $O_2$ storage in the body and lung tissue since the arterial and venous $CO_2$ and $O_2$ tensions are related to this storage. Longobardo et al. concluded that Cheyne-Stokes breathing could result not only by increasing circulation time but also changing $CO_2$ sensitivity. Cherniack and Longobardo [49], [50] and their associates further substantiated the dynamics of $CO_2$ and $O_2$ stores when ventilation was altered under conditions like apnea, hyperventilation, or asphyxia.

Models discussed so far are all related to overall chemical control of respiration. The dynamics of the controller and of the controlled system have been studied under various assumptions. The changes in the assumptions have resulted in closeness to reality and refinement in modeling. Basic alteration has been outside the controller block, thus eliminating any discussion on the internal dynamics of the controller. Figure 2-6 shows the extension of controlled system study by various investigators. The exclusion of the dynamics of the controlling system in all these models is clearly evident in Figure 2-6. This dissertation is an attempt to explore the nature of a subsystem within this controlling system.

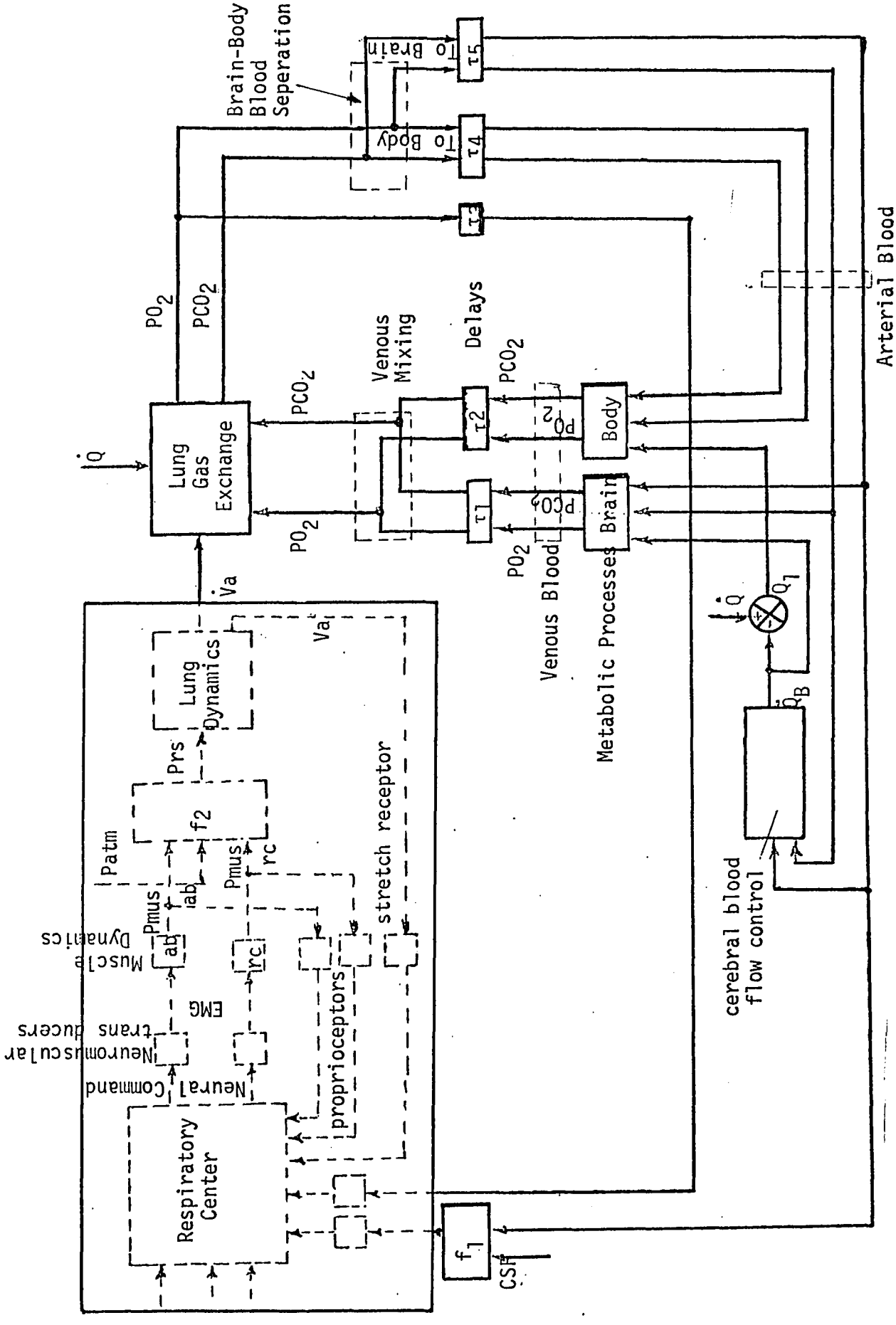


Figure 2-6 Factors considered in later chemostat models [39]-[54] shown by solid lines. The dotted lines represent areas that remain unexplored in these models.

Edwards and Yamamoto [51], Yamamoto [52], and Horgan and Lange [53] have provided an excellent review of the physiological approach to modeling as well as the development of various models. Certain possible theoretical alterations in the modeling procedure have also been suggested. On the basis of available physiological information, Grodins et al. [54] have produced a completely modified model which initiates a new mathematical technique in modeling. The significant features are the use of differential-difference equations with delays and use of temporal variations of all parameters. It does provide a comprehensive and synthetic study of pulmonary ventilation. Also the generality of this model makes it possible to simulate the response to several forcing functions such as $CO_2$ inhalation, hypoxia at sea-level, altitude hypoxia, and metabolic disturbances.

2.2 (b) Other Models and Subsystem Analysis. Having discussed the various models of overall chemical control of respiration, it is possible to review some features of other models and the investigation of subsystems which form the controlling system and the controlled system as discussed above. This group is rather scattered and is a collection of diverse approaches from theoretical investigators to the practical approach of respiratory analysis as a diagnostic tool. If any practical overall model has to emerge, a discussion of other models and analytical techniques may be useful.

While reviewing the chemostat models, it was pointed out that Yamamoto [40] had doubted the significance of 'minute ventilation' as a measurable variable in all models with the exception of the latest one by Grodins and his associates [54]. Yamamoto has presented a theoretical approach to substantiate his earlier hypothesis. Consideration of 'minute volume' as a respiratory response rests on the assumption of continuity in a unidirectional air flow in the lungs. This overshadows the dynamic response where breath-by-breath analysis is required or where a short interval of time during a respiratory period is to be considered. It is, therefore, suggested that air flow be considered as the basic variable. Both the 'minute-ventilation' and the rate of breathing can be obtained from the plot of air flow as a stochastic time function sometimes referred to as time-series. Yamamoto describes the air flow in the form:

$$\dot{V}(t) = P(t) \cos \theta(t)$$

where, $P(t)$ and $\theta(t)$ are random variables. He suggested autocorrelation and power density analysis on the basis of which he measured the various variables.

As mentioned earlier, the signal representation determines the hierarchies of modeling (Chapter 1). By using 'minute-ventilation' as a controller response, the analysis uses a full wave rectified and averaged flow signal $\dot{V}$ (sometimes referred to as envelope). Even with 'minute ventilation' as a signal, the stochastic process has been investigated. By examining the oscillations in ventilation over a long interval of time (running into hours), Goodman [55] pro-

ceeded with analysis of cumulative volumes of inspired air over regular intervals of time. By spectral analysis, he identified the ventilation as a superposition of denumerable sets of almost periodic oscillations under steady-state breathing pattern. Goodman and his associates [56] extended this approach to get similar analysis of several other variables, e.g., carbon dioxide release, endtidal $CO_2$ concentration and respiratory quotient.

The other end of the hierarchy of modeling poses serious experimental limitations since it involves microelectrode techniques to select neural pulse trains. While physiological data have been gathered concerning the electrical activity of neural and muscular fibers involved in respiration, little is known about its association with a feedback model of respiration. Rubio [57] has proposed a mathematical model of the respiratory center as an important subsystem of the controller. He extends the hypothesis of Salmoiraghi et al. [4], [5] by a mathematical investigation of the firing pattern of two interconnected neuron groups at the respiratory center. The phenomenon of temporal summation and reciprocal innervation leads to a nonlinear integral equation of the self-oscillating autonomous system. This oscillation has a limit cycle which is responsible for the basic respiratory drive. How this drive depends on chemical input and how it affects the resultant ventilation is not clearly answered. The hypothesis of self-oscillating respiratory center has recently been found to be inadequate by Merrill [58]. His experimental observations reveal the effect of vagal feedback to the respiratory center as well as the independence

of the inspiratory and expiratory neuronal populations in the respiratory center.

Going 'down the line', in the controller, one faces the problem of studying the neuromuscular dynamics which represents an important subsystem forming the link between the neural output of the respiratory center and the mechanical action of the respiratory pump. Significant work in this direction has been reported by Aizerman and Andrejeva [59]. They presented a hypothesis of muscle response wherein the 'muscle' represents the total muscle including the neuronal organization of the spinal segment directly connected to it, i.e., it includes $\alpha$ -and $\gamma$ - motoneurons and the adjacent interneuronal pool. The response of the muscle is measured in the form of a rectified and filtered EMG. It is assumed that this response is related to the number of $\alpha$ motoneurons firing, $N\alpha$ which itself is proportional to the number of excited neurons, $N_r$, in the random interneuron pool, RIN. Both $N\alpha$ and $N_r$ are random numbers and their temporal variation depends on the command volley received from the higher center. It is assumed that the arrival of this command volley, in the form of a short duration train of pulses, would increase $N_r$ and thus $N\alpha$ and therefore produce the muscle response as a 'splash' whose amplitude may be considered to be a random variable. It is assumed that the only significant feature, in so far as the response of the muscle is concerned, is the time when this command volley arrives. Since the muscular output can be considered to be either tension, angular motion, or the velocity of contraction,

the goal of such a muscle is to search for such an output and maintain it at the desired level by minimizing any possible changes about this level.

This process is described as a simple search mechanism, SSM, illustrated in Figure 2-7. A key element in this model is the "U-function" between the variables y and u. The relation between muscle output y, the U-function, and the command volley is shown in Figure 2-7(a). This command volley is generated only when the variable U, while increasing, exceeds the threshold value A. When the value y drops below the desired tension level by an amount $\Delta$ then U reaches the threshold point A, causing onset of command volley at time $t_1$. The muscle dynamics are such that a "volley" will cause y to go up to a maximum and then decrease again. This "splash" may be large enough to bring y up to the value $y_a$ (shown in Figure 2-7(a) at time $t_2$) in which case the U-function will rise again above the threshold value A initiating another command volley. As shown in Figure 2-7(a) for $t = t_2$, this new volley will increase the existing "splash". Finally, y will come down again until it reaches the value $y_b$ (at time $t_3$ illustrated in Figure 2-7(a)) at which time U rises above the threshold value A again and a new command volley is initiated. From the control system point of view, this process can be shown by a simple diagram as shown in Figure 2-7(b).

Zakharova and Litvintsev [60] had earlier tested this SSM hypothesis for the muscle response in animal experiments with arti-

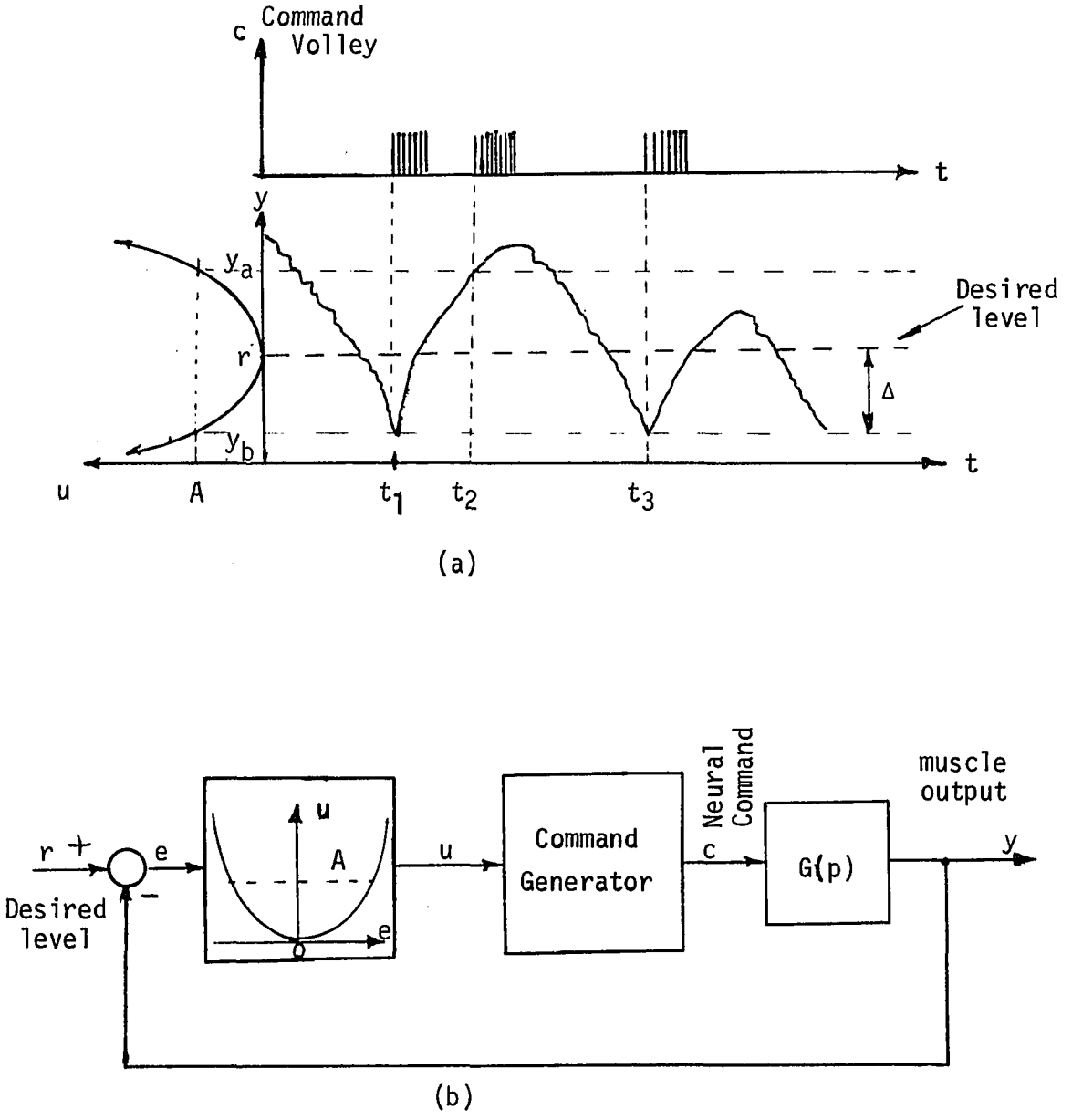


Figure 2-7 Simple Search Mechanism [59] and the related control system. The principle of SSM is shown in (a). A simple control system model is shown in (b) in which the command generator initiates command "volley" whenever u increases above the threshold value A.

ficial feedback. The purpose of the artificial feedback was to generate a pain stimulus to the animal as soon as the recorded EMG in the animal's skeletal muscle, crosses a threshold level (as shown in Figure 2-7(a)). The ultimate goal of the muscle response is to maintain small oscillations about some point (point r in Figure 2-7(a)) in order to avoid the pain stimulus. Furthermore, if this point is shifted, the animal response would also follow this shift.

Tenenbaum [59], [60] extended the SSM hypothesis to the neuromuscular command in respiration. If the 'U' curve (Figure 2-7(a)) is shifted vertically with a constant velocity during inspiration and is suddenly brought back at the end of inspiration, then the recorded EMG will exhibit the typical ramp-like periodic signal as shown in Figure 2-8. If the shape or size of the motion of the threshold point is changed, the muscular response will also change. Tenenbaum [62] postulates a second level of control to determine this motion of the threshold point. This control level involves another function S which, as shown in Figure 2-8(a), depends on a function F representing the EMG (in a modified form) and a function G , representing lung volume. There is a threshold level at which the rising S function will terminate inspiration. Tenenbaum supports this hypothesis by experimental results of breathing with increased airway resistance, which would cause reduction in the slope of the G function (with respect to time) thus increasing the inspiratory period. Tenenbaum also postulated a third level of control which slowly changes the function F and the threshold level under changing external conditions like $PO_2$, $PCO_2$, or work of breathing.

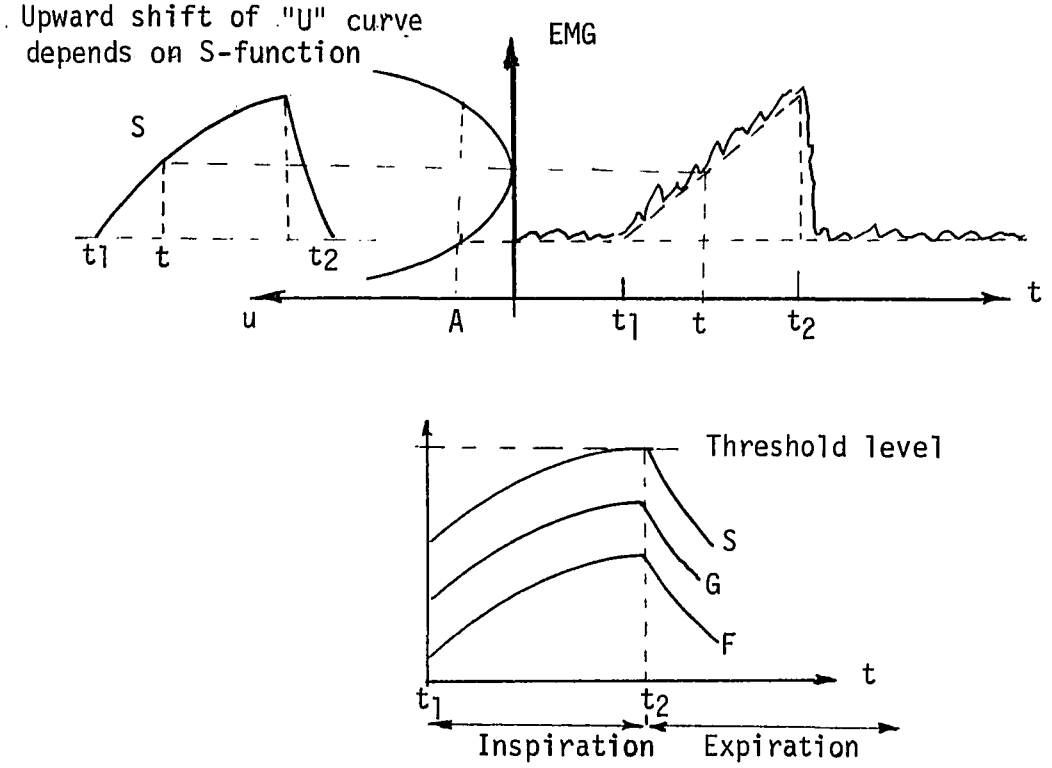


(a) SSM as applied to neuromuscular dynamics of the diaphragm in respiration [59].

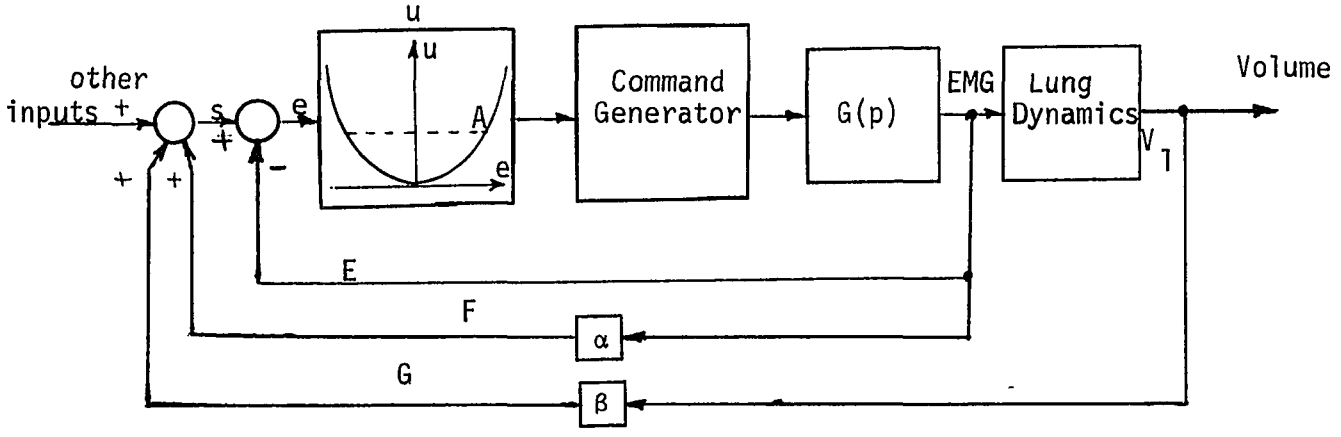


(b) Possible model to explain the neuromuscular dynamics in respiration.

Figure 2-8 SSM and its application to a control system model of respiration.

The SSM hypothesis and its use to explain neuromuscular dynamics of respiration rests on several assumptions which are either explicit or implicit. One such major assumption is that the rate of discharge of $\alpha$-motoneurons or the number of action potentials is not significant. Physiological observation of impulse discharge in afferent nerves does not support this argument. Again, the process of recruitment of neuromuscular fibers and the temporal variations in pulse rate as shown in respiratory system seem to be ignored by the authors of SSM. The model has an implicit assumption of a feedback from the muscle to the higher center which is responsible for the control of the command volley. If the second and third levels of control, as suggested by Tenenbaum, are included in the control system, it can be illustrated as a simple multiloop feedback system as shown in Figure 2-8. This figure includes an element $G(p)$ , whose response will depend on system states at the time of a command volley as well as on the volley itself, giving rise to total response signal that appears to consist of random "splash". A clear explanation of second and third levels of control, as described by Tenenbaum, does not seem possible in neurophysiological terms, at least at the present time.

Another important subsystem of the controller is the one which includes the dynamics of the respiratory pump. Physiological investigations have provided substantial background with which Mead and Milic-Emili [37] lay the framework of respiratory mechanics. The variables involved in respiratory mechanics are the pressures due to muscle efforts and their influence on lung mechanics. Jodat et al.

[63] have proposed a system model including these factors. They develop their model by selecting pleural pressure as the intermediate variable through which the muscle force is transformed into the volume changes in the lung. The model is developed by following the analog model shown in Figure 2-3, in which abdominal and chest wall volume-pressure dynamics are included. By ignoring mass, the authors consider first order differential equations for lung, chest wall and abdominal muscle structure. Pleural space is considered stiffly coupled, i.e., without any mass or resistance factors. Available physiological results are used for the parameters of the model. For model simulation, transdiaphragmatic pressure is used as the total muscle pressure which can be separated into chest wall and abdominal components. As interesting feature of the model is the inclusion of the interaction between rib cage and diaphragm forces during initial phases of inspiration and expiration. The model has significant value in abnormal breathing since under normal breathing the diaphragm's actions can be considered as the major muscle force. The model does not include the pressure-force relationship of the active diaphragm.

Considering the entire respiratory pump as a simple R-C circuit involving external pressure, alveolar pressure and flow, theoretical studies have been made by Wald et al. [64] from the point of its utility in respiratory failure which needs positive pressure breathing. Since the use of a positive pressure respirator may lead to alveolar pressure changes which may cause cardio-pulmonary damages,

the authors have studied optimally controlled positive pressure respiration by selecting various forms of external pressure signals. The criteria for optimality are the peak of alveolar pressure, the time of its occurrence, the time-average alveolar pressure and the work of breathing during passive expiration. Out of five waveforms of applied pressure with similar results, the authors consider the rectangular waveform the best since it gives absolute lowest value of alveolar pressure. This model uses an external pressure waveform with fixed structure of the respiratory system. Jain and Guha [65] have extended the positive pressure respiration with variant respiratory parameters. The alveolar pressure is considered as an important index of optimal respiratory performance and the 'respirator system' has been assigned to minimize the effects of positive pressure when lung parameters change.

The chemostat model has also been studied from the system identification point of view. Stoll [66] has approached the problem by sinusoidal response, assuming a linear transfer function in the overall chemostat model. Sinusoidal response is experimentally obtained by an ingenious device which controls the inspiratory $CO_2$ mixture in a sinusoidal fashion (frequency range 0.108 to 4.38 cycles/min.) at different amplitudes. Stoll considers the sinusoidal response test preferable to earlier step-response tests specially when steady-state, internally generated outputs and random noise are to be separated from the response to known sinusoidal inputs. Linearity was tested by verifying the small influence of second and third

harmonics of output data. The absence of large second and third harmonic components was further verified by power spectrum analysis. The subsystem outputs were tidal volume, minute volume, and alveolar $CO_2$ concentration. By gain and phase plots of these variables, the overall transfer function was found to be the type:

$$G(s) = \sum_{i=1}^{n} \frac{k_i \exp(-T_i s)}{\tau_i s + 1} \qquad (2.9)$$

The problem then reduced to estimation of various parameters and transport delays involved in Equation (2.9) which was accomplished by use of least square estimation techniques [67]. In a subsystem, like the one involving lung dynamics alone, parameter estimation has been used as a clinical tool for the diagnosis of respiratory disease [68].

## 2.3 Summary

The above literature review was divided into two parts. The first part was related to a survey of chemostat models presenting an essential part of the entire respiratory system as a feedback control system. Evolution of the modeling is related to modifications of basic assumptions so that physiological facts could be included step by step. The state-of-the-art leads to a multi-compartment, multi-input, multi-output model of the chemical control of respiration. With the exception of Grodins' model, all others have practically ignored breathing as a function of time; in other words as Yamamoto points out [52], these models 'don't breathe'.

Another important factor, which has been ignored in the chemostat models, is the internal dynamics of the controller.

The second part of the review deals with some of these subsystems as well as with various aspects of modeling and application of engineering approaches in the study of respiratory physiology. Discussed are several aspects of respiratory control from the neural and chemical points of view considering several theoretical and experimental techniques. This review also points out the hierarchy of modeling and specifies the relation between subsystem study and the overall control system. This dissertation is limited to study of the subsystem involving the neuromuscular aspects of the controller.

# 3. ANALYSIS OF THE NEURAL COMMAND AND THE ELECTROMYOGRAM

The present investigation considers the neural command from the respiratory center as the input to the neuromuscular subsystem. This neural command is transmitted to the respiratory muscles via various neural paths. Two bundles of efferent nerves, known as phrenic nerves lead to the diaphragm. At the neuromuscular junctions the neural command initiates bioelectrical signals in the muscle fibers. Except for the transmission delays involved at the neuromuscular junction and the increase in the number of parallel paths at the muscular level, the bioelectrical signals both at the nerve and muscle fibers can be considered to be essentially of the same nature. It is, therefore, conceivable to study the electromyogram as a signal which contains the basic information in the neural command. This is an important assumption in this dissertation. A discussion on the physiological nature of the neural activity further clarifies this assumption.

## 3.1 Physiological Nature of Neural Activity

The phrenic nerves consist of nerve fibers leaving the spinal cord at the segments in the neck. There is a slight difference, among species, about the segmental exit of the phrenic nerve fibers. In man, for example, the phrenic nerves come out of cervical segments $C_3$, $C_4$ and $C_5$, whereas in the dog they leave at $C_5$, $C_6$ and $C_7$. The phrenic nerves then reach the diaphragm in two bundles, the left phrenic nerve and the right phrenic nerve. Landau and her associates [69] have reported that each phrenic nerve in dog

has about 1500 myelinated fibers and that the number of efferent fibers is approximately 60% of the total number of fibers. The distribution of diameters of the efferent fibers is predominantly unimodal with a peak between 9 and 11 microns. Most of the efferent fibers are motoneurons and the number of $\gamma$-motoneurons seems insignificant. The afferent fibers in the phrenic nerve constitute feedback pathways. The presence of proprioceptive pathways from the diaphragm has not been explored. The afferent innervation of the diaphragm is supplied by the phrenic nerve, though it is believed that a small amount of innervation of the diaphragm may be provided by afferent nerves from the intercostal region. Ogawa, [70] from his studies, has discarded this hypothesis. The fibers of the phrenic nerve are usually divided into three groups for innervation of ventral, lateral and dorsal regions of each half of the diaphragm hemisphere. In addition to this branching, each efferent fiber is branched further for connection to several muscle fibers. The innervation ratio, i.e., ratio of muscle fibers to nerve fibers for dogs is not available. The innervation ratio in the rat diaphragm is about 25, about 115 in rabbit and about 83 in cat. As compared with the innervation ratio in gastrocnemious muscle (about 2000), the diaphragm has a small innervation which provides a better precision for motor control by the neural command.

The signal transmission along the phrenic nerve is in the form of the propagation of train of action potentials along a number of nerve fibers. Two phenomena exist - change in pulse rate and

recruitment of nerve fibers. Adrian and Bronk [6], in 1928, investigated the nature of neuromuscular command by studying small groups of fibers of the phrenic nerve. They observed that in rabbits under normal breathing, inspiration is due to action potentials with frequency about 20-30 pps. This frequency increases under load and the higher the frequency the greater is the asynchronicity of discharge in phrenic nerve fibers. They also considered the possibility of recruitment of fibers under forced inspiration. Further studies on the phrenic nerve by Gessell et al. [7] and by Gill and Kuno [9], [10] clarify the recruitment as well as the fact that a progressive increase of pulse frequency begins from the onset of inspiration and terminates at the end of inspiration. In dog, under normal quiet breathing, the pulse frequency rises from 10 pps to 40 pps during the entire period of inspiration. Even if the pulse frequency was maintained at some fixed average value, due to external stimulus, the interpulse interval in a single nerve fiber can be a random variable and various statistical analyses may be useful for the interpretation of such a signal [71]. If the stimulus is time-varying, then the pulse frequency would also be time-varying.

The cause of time-varying pulse frequency in neural command in respiration has not been studied in detail and is outside the domain of this dissertation. It is tempting to hypothesize a pulse frequency modulator as proposed by Jones, et al. [72], [73] in their study of the photoreceptor response. In respiration, the source of neural command, as observed in the phrenic nerves, lies in the respir-

atory centers. As pointed out earlier, the discharge pattern of respiratory center is a rather complex process. There are several feedback paths which affect the observable neural command in the phrenic nerve. They are either of chemical or of mechanical nature. Several attempts have been made to study their effect on phrenic nerves [8], [11]-[15]. Since this investigation is related to the input-output relationship between neural command and time-varying mechanical events, the analysis of the source of neural command is excluded. However, since the pulse frequency variations in neural fibers are known, an alternate approach is attempted, namely the stimulation of the nerve trunk by pulse trains from a pulse frequency modulater with given modulating signals.

The resting membrane potential of the phrenic motoneuron is in the range of 40-70 mv and the action potential of 40-90 mv with the duration of about 1.1 m sec [9]. Such an action potential can best be measured or recorded by using microelectrode techniques on a single axon. The recording of the entire nerve trunk is done by external metal electrodes touching the trunk. The electrodes are usually 0.5 cm apart and a small section of the nerve trunk, with the applied electrodes, is surrounded by a pool of mineral oil. The extracellular electrodes are away from the potential source, i.e., from the fibers in the nerve trunk, the interstitial fluid acting as a conducting medium. The potential difference between the recording electrodes, with respect to a 'ground' electrode connected to another region of the body, can then be studied using the property of a dipole layer.

A theoretical analysis of the action potential has been presented by Brown [74]. Bipolar electrodes record bidirectional (or biphasic or polyphasic) action potentials. The recorded signal has zero mean and the peak-to-peak amplitude is much smaller (usually less than 1 mV) than that of the actual action potential. If there is a train of action potentials, where a random phase difference exists between an action potential in one nerve and the corresponding action potential in the adjacent fiber, the compound action potential, due to superposition of such trains in active fibers, exhibits the typical biphasic (or polyphasic) 'noisy' phrenic neurogram PNG.

If the action potential is detected at the diaphragm, the electromyogram, EMG, is essentially similar to the PNG. There are several factors which may indicate differences in shapes and sizes of an EMG and the PNG. First, there is a transmission time involved which depends on the diameter of the nerve fiber. It is generally accepted that the conduction velocity, in meters/sec, is about six times the diameter in $\mu$ of the nerve fibers. Thus, the mean diameter of 10 micron would have the conduction velocity of 60 meters per second. Considering the length of 24 cms of the phrenic nerve in a dog, the mean transport delay would be 4 msec. Since the nerve fibers are not of the same diameter, the randomness in the phase differences at the nerve bundle will be altered at the motor unit 'bundle'. The second important factor is the distribution of the nerve fibers to motor units in various anatomical regions of the diaphragm. The location of electrodes in the diaphragm constitutes the third factor

which determines the difference between an EMG and a PNG. These differences are visible if the entire phrenic nerve is stimulated supramaximally by a pulse generator with constant frequency. Such a stimulation removes the randomness of pulse frequency in the nerve fibers, however, mainly due to the random distribution of transport delays of nerve fibers, there will be a random distribution of the phase-angles of the pulse trains. An experiment relevant to this phenomenon was conducted by stimulating the right phrenic trunk in the neck of the dog at a distance of about 25 cms from the diaphragm. The results are shown in Figure 3-1. The phrenic activity was picked up by bipolar platinum electrodes in the thoracic region and the EMG by sewing wire electrodes in the diaphragm. All electrodes were 0.5 cm apart. The complexity in the waveshape of an electromyogram, as also illustrated in Figure 3-1, may be due to the polyphasic nature of the superposed potentials at random phase angles. Such complexity is noticed even in the PNG. Thus, with the exception of delays at the neuromuscular junction as well as other transport delays, the essential complex nature of the EMG and the PNG remain unchanged. It is, therefore, reasonable to assume that the electromyogram contains the essential information carried by the neural command signal. In this dissertation, this assumption has been used to focus the attention on the electromyogram as a representative signal of the neural command.

Significant features of the EMG may be represented in terms of two signal parameters, namely the amplitude and the interval between

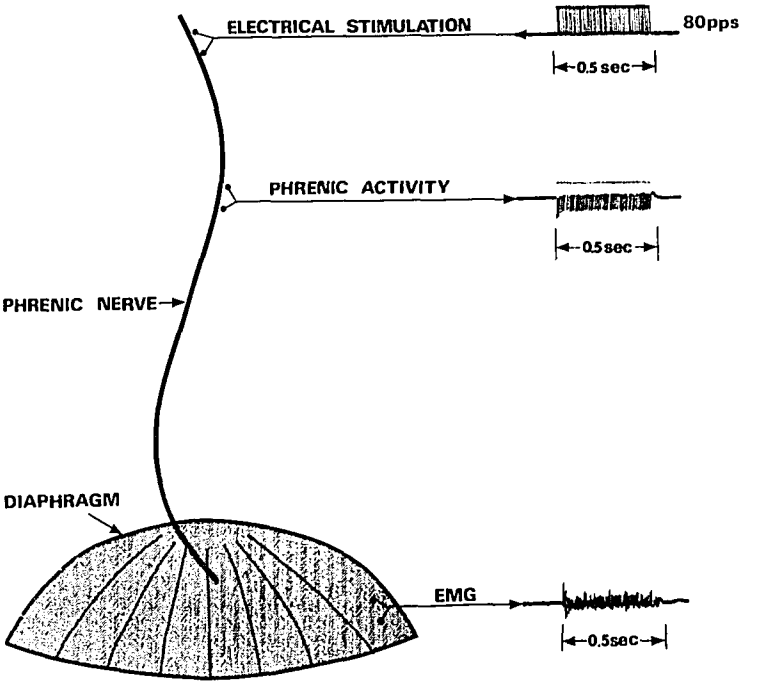


Figure 3-1 Electrical stimulation of the phrenic nerve. Stimulating pulses 80 pps, 2 msec width and 0.4 volts amplitude for supramaximal stimulation. PNG and EMG amplitudes are adjusted arbitrarily.

two successive zero-axis crossing points. Both may be considered random variables. If the EMG is to be studied as a continuous random variable, then the recording equipment must have enough bandwidth (0 - 500 Hz at least) in order to avoid any loss of significant information. Several attempts have been made to study the EMG. Kendell et al. [75] discuss the interpretation of an EMG in statistical terms. They obtained peak distribution histograms by taking the number of peaks falling within a set voltage range, and made comparative study between normal and myopathic subjects both under isotonic and isometric contraction of the muscle. The basic hypothesis in such a study is that the peak amplitude is a measure of electrical discharge and the number of active motor units. Using this hypothesis, Gatev [76] proposed to obtain mean amplitude of all peaks over a fixed interval of time. Dowling et al. [77] also used histogram studies on a programmed computer. All these results have significant clinical value and are empirical approaches to interpret the electromyogram. From such observations it is not possible to have a quantitative evaluation of an EMG especially one which would lead to an understanding of the relationship between the EMG and the muscle dynamics. It has been shown that the amplitudes of peaks do not have a linear relationship with the muscle tension [78]. A significant quantitative evaluation was provided by Lippold [79] by demonstrating a linear relationship between the tension of the muscle, under isometric contraction, and the integrated EMG. This has led to several approaches to quantify the electromyogram and to relate it to

the summation of firing motor units due to recruitment. These methods are discussed below; they provide the basis for selecting a suitable filtering technique for the experimental work on neuromuscular activity.

## 3.2 Quantification of Electromyogram

### 3.2 (a) Integration Procedure

The simplest form of an integrating circuit is a R.C. low pass filter with transfer function $\frac{1}{1 + RCp}$. Since the EMG is bidirectional, with zero mean, the integration is preceded by full wave rectification of the electromyogram. The response of such a filter depends on the choice of the time constant, RC. A large time constant, for example, would reduce the bandwidth and the EMG with high frequency contents would produce a slow time response in filtering.

Bigland and Lippold [17] used a modified Miller circuit. The Miller circuit [80] is basically an operational integrating amplifier with feedback through a capacitor. The voltage across the capacitor was used by Bigland and Lippold as an ideal integration of the rectified EMG. The capacitor is discharged at each preset peak value by a switching mechanism which was controlled by the muscle force. The total amount of integrated EMG was obtained by counting the pulses produced at each moment of the automatic zeroing of the capacitor. With operational amplifiers, the construction of such an integrator is fairly simple and has been accepted as a suitable mode of quantifying the electromyogram [81], [82].

Fink and Scheiner [83] used a combination of R-C filter with a low gain amplifier and a resistive feedback. A simple scheme is shown in Figure 3-2(c). Such an integrator is normally used with a balanced amplifier. It makes it possible to adjust the decay time to a very large amount. Furthermore, the balance control also facilitates selection of any arbitrary base line to cancel out background noise such as those which may be present between successive bursts of EMG in the respiratory muscle.

If any of these integration techniques are to be used in recording the EMG of a respiratory muscle, the almost-periodic burst of electrical activity is an important feature. It has been pointed out earlier that there exists a one-to-one correspondence between phrenic nerve discharge and the discharge of the diaphragm. Under quiet breathing, the phase of the EMG burst coincides with the inspiratory phase. Some activity may persist during expiration also and the general nature may be altered during forced efforts [31]. In order to have a quantitative evaluation of the EMG with known variables in respiration, the choice of quantification of the EMG depends on the quantification procedure accepted for a selected variable. If, for example, minute ventilation is considered to be the variable under study, the total electrical activity, by integration procedure, over a period of one minute will be a desirable quantification procedure. In order to have a comparitive study with tidal volume in each breath, the height of the integrated EMG during one breath becomes a measurable parameter. Lourenço et al. [84] in

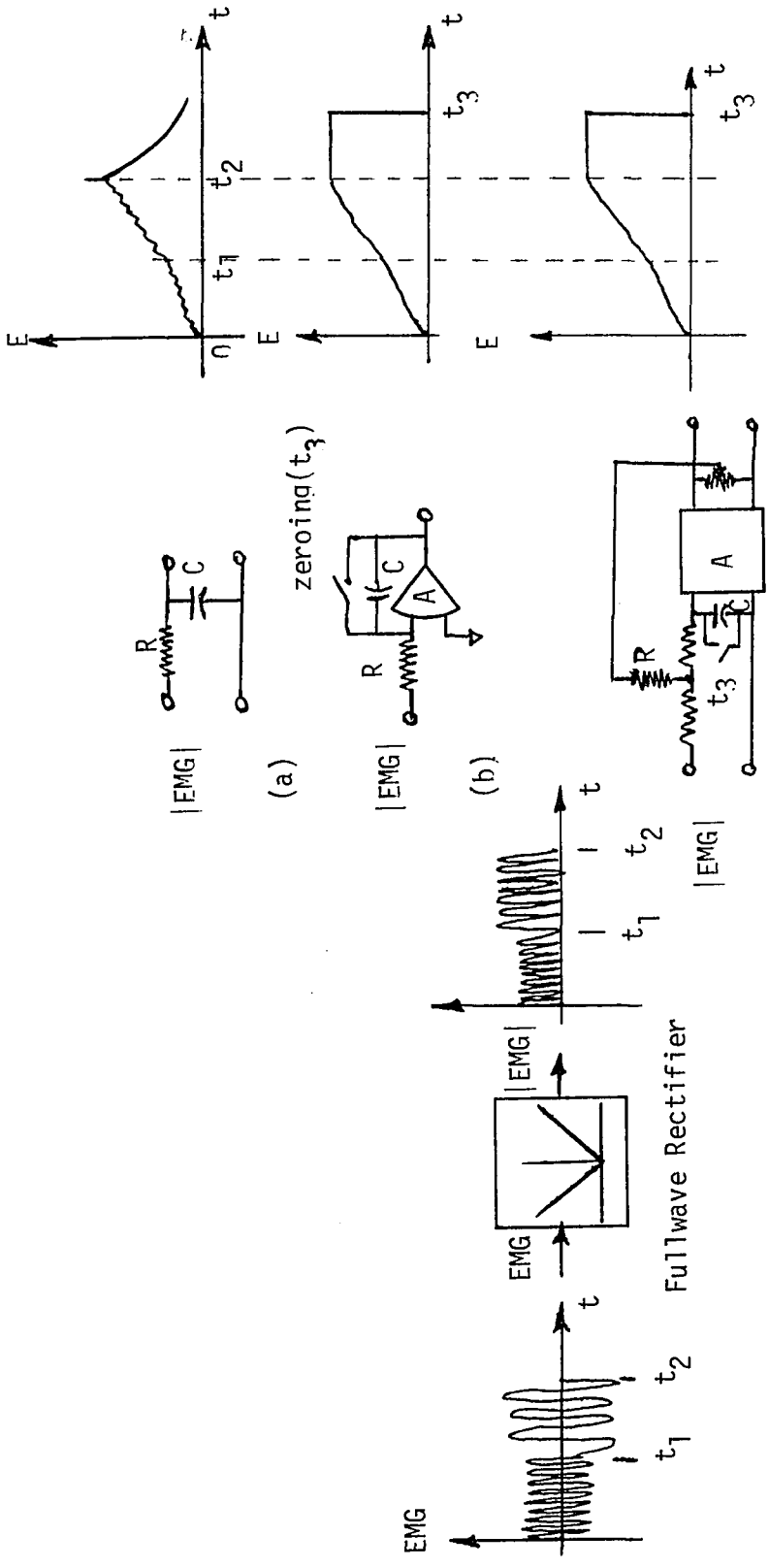


Figure 3.2 Three possible methods of integrating a rectified EMG
(a) Low Pass Filtering
(b) Integration with operational amplifier (similar to the 'averager' used in [79])
(c) Integration with low gain amplifier (based on balanced integrater in [83])

their observations confirm the linear relationship between the integrated PNG and the integrated EMG which is not affected by the location of the recording electrodes in the diaphragm. During obstructed breathing, while the tidal volume falls, the EMG shows an increase, thus emphasizing the study of neural command as an important output variable - and not the tidal volume or the minute ventilation. This observation further clarifies the role of the internal dynamics of the controller and leads to the study of neuromuscular subblock.

In human subjects, the best way to record the electromyogram of the diaphragm is by locating bipolar electrodes (on a polyethylene tube) in the esophagus in the section where it crosses the diaphragm. Even though the balancing can reduce the net effect of noise while recording an EMG in this region, the presence of high amplitude cardiac spikes can be rather disturbing. Lourenço and Mueller [85] used a diode-voltage clamping circuit to reduce the height of the cardiac spikes; thus reducing the contribution of such spikes to the integrated EMG. The system was improved [86] for further reduction of the cardiac pulses which coincide with the EMG. The technique involves filtering the EMG, via a parallel path, and then using the subtraction of the clipped cardiac spikes from the signal containing the EMG and similar cardiac pulses.

The significance of electronic integration of an EMG, in a comparative study with selected variables in respiration is thus clear. Both as an empirical tool and as a variable involved in the dynamics of the neuromuscular system, several other quantification procedures

have been tried. Their selection depends on the hierarchi of modeling and level of signal analysis accepted for that model. Some of these methods have been attempted in the present study and are discussed below.

3.2 (b) Stochastic Process. The electromyogram, as well as the electroencephalograms, have been studied as stochastic processes. The investigations include techniques such as autocorrelation and cross-correlation analysis and ensemble averaging. The randomness has been explained in terms of superposition of several pulse trains [71]. In the study of bioelectrical process, emphasis on such an analysis was placed on records of electroencephalogram [87]-[91]. This approach has also been extended to the study of an electromyogram [92], [93].

Many bioelectric signals, including the EMG in respiratory muscles, fall into the category of non-stationary data. The auto- and cross-correlation studies in non-stationary data are possible in neural signals [94], [95]. Ensemble averaging is usually considered more appropriate in analyzing non-stationary data [96]. Several special purpose computers, like Enhencetron, are available for such study. Ensemble averaging was also used in the analysis of an EEG [87], and resulted in the average evoked response. Several traces of the EEG resulting (evoked) from some applied stimulus such as an auditory click or light flash were studied. The application of a stimulus served as the synchronizing time-signal from which the response would be averaged. The basic assumption in such an

averaging is the additive mixture of signal component $S_i(t)$ and independent noise component $n_i(t)$ producing the non-stationary signal, i.e., $f_i(t) = S_i(t) + N_i(t)$ where $f_i(t)$ represents the ith functions in an ensemble of non-stationary signals. Furthermore, if the noise component has an ensemble average of zero, then the ensemble average obtained as

$$Z(t) = \frac{1}{N} \sum_{i=1}^{N} f_i(t)$$

tends to eliminate the noise and recover the signal.

In the present work, the ensemble average of the EMG of the diaphragm is studied to distinguish the presence of noise in various measured variables such as the flow, pressure and a filtered version of rectified EMG. In natural breathing some criterian for the time-reference has to be established. On the basis of physiological evidence [31],[84], it is reasonable to assume that the onset of the EMG has a fixed phase relationship with mechanical events in respiration. It is, therefore, possible to generate a pulse which as a fixed phase difference with the variables such as flow, pressure, and EMG and then proceed with the ensemble averaging over number of breaths under steady state conditions. For this purpose, the flow signal was considered ideal for generating the required synchronizing pulse at the onset of inspiration.

A simple schematic for such a pulse generator is shown in Figure 3-3(a). The circuit contains a saturating operational amplifier, a differentiator and a diode suppressor (for eliminating negative output

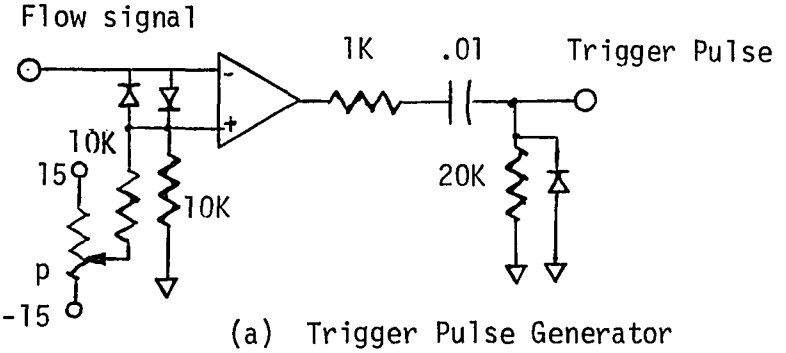


(a) Trigger Pulse Generator

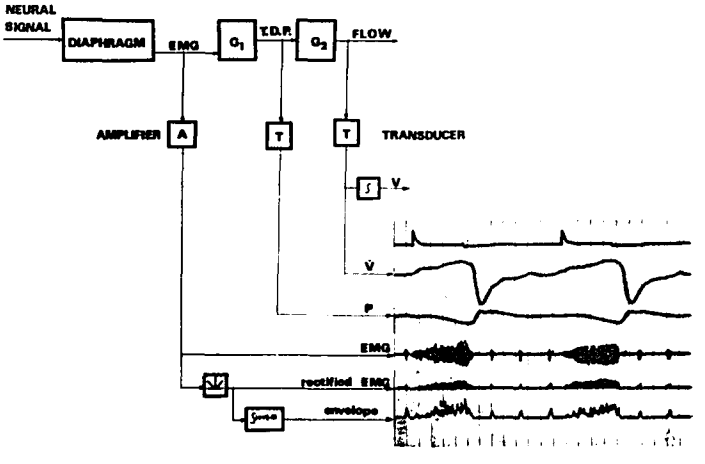


(b)

Figure 3.3 Schematic for signal transfer and recording procedure.
(a) Shows the circuit used for generation of trigger pulse from flow signals
(b) Shows experimental setup with typical records under natural respiration of a dog

pulses and d.c. restoration), all connected in cascade. The flow signal, as recorded by a phemotechograph and trausducer and amplified by a balanced amplifier* is the input to the trigger pulse generator. The potentiometer p, (Figure 3-3(a)), is used for adjusting a d.c. shift to select the location of generated pulse with respect to the onset of inspiration. This is sometimes necessary in order to avoid the generation of a pulse due to zero-axis crossing of noise components in the flow signal. Such a scheme causes a lag in the trigger pulse and if this pulse were to be used as a trigger for the averaging computer, the section of EMG occuring slightly before the pulse is ignored. Since all data are recorded on an eight-channel FM-tape recorder, the pulse can be recorded in 'advance' by interchanging the record and playback heads of the channel selected during recording mode. Since the record and playback heads have a fixed separation of 10cm (in Sanborn Tape Recorder), the advance of recorded pulse depends on the tape speed.

The electromyogram was averaged by rectifying and filtering. This filtering technique is discussed later in Section 3-2(d). It is assumed that this filtered version of the EMG contains noise and the true signal which could have significant relation to pressure and flow variables. All data were first recorded, under steady state condition with inspired air containing 5%, $CO_2$, 3% $CO_2$, and room air. More than 500 breaths were recorded and the total time for 500 breaths was recorded by stopwatch. The average time per breath varies from 1.5 seconds in room air to 1 second in 5% $CO_2$ breathing.

---

*A summary of the experimental procedure appears in Appendix A.

This time period helps the selection of dwell time (sweep time) for the Enhencetron averaging computer. Since the electrical activity occurs mainly during inspiration, a dwell time of 1 second was chosen for averaging. The input to the Enhencetron are the trigger pulse, to initiate the sweep, and the selected channel output to be averaged.

Figure 3-4 shows the average of 50 breaths under three different conditions. The results reveal a significant noise reduction in the EMG. The 'noise' content in the flow and the transdiaphregmatic pressures do not seem to be present in the data of individual breath. Without going into details, one more visual observation should be mentioned. This is the relative change in amplitude in all signals when external disturbance (changes in $CO_2$ breathing) levels are altered. This observation is not sufficient to conclude a linear relationship between the EMG, pressure and the flow. A better understanding of the linearity (or nonlinearity) could be obtained by stimulating the phrenic nerve by pulse frequency modulated signals with step or sinusoidal envelope.

The pulse trains were generated by an integral pulse frequency modulator similar to one described by Meyer [97]. A simple circuit for this is shown in Figure 3-5(a). The bias level adjusts the rate of pulse generated by square wave or sinusoidal modulation. Figure 3-5(b) shows the response of the animal when the cervical phrenic nerve was stimulated by square wave modulating signal (0.5 cycles/sec) with pulse frequency of 30 pps and 50 pps. For sinewave stimulation with modulating frequency of 1Hz the bias adjustment was

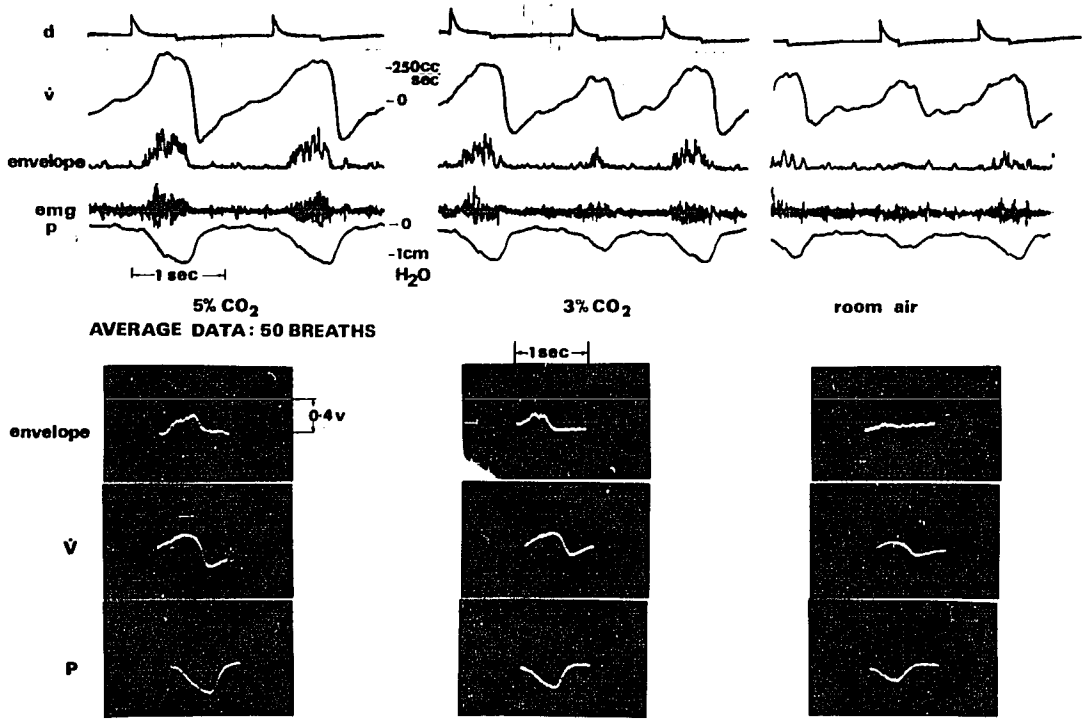


Figure 3.4 Respiratory data and their ensemble average. Upper records under three different conditions (steady state $CO_2$ response). Lower displays represent ensemble average of 50 breaths recorded on storage scope.

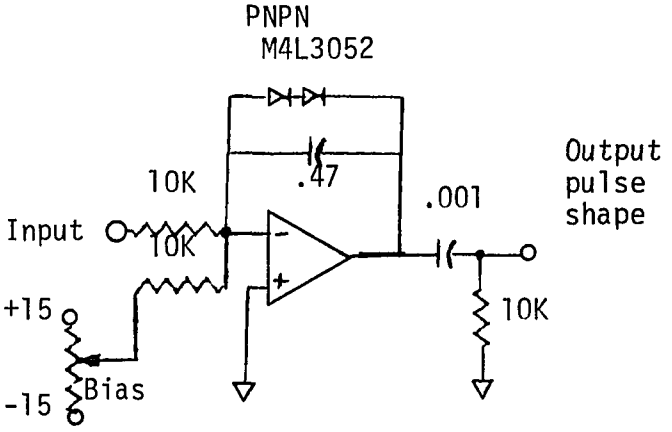


(a) Pulse Frequency Modulator

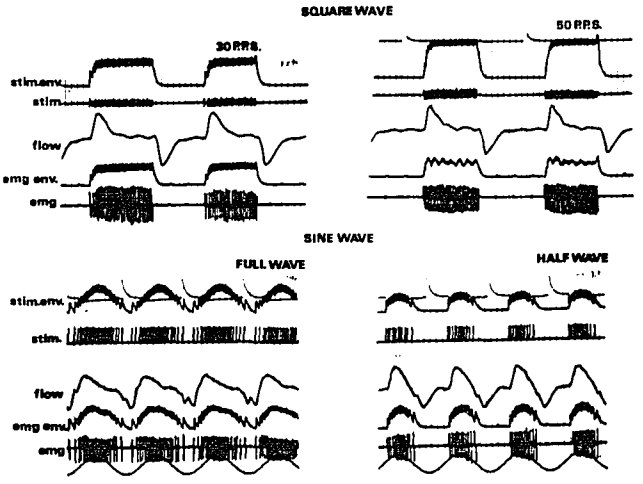


(b) Response to Stimulation

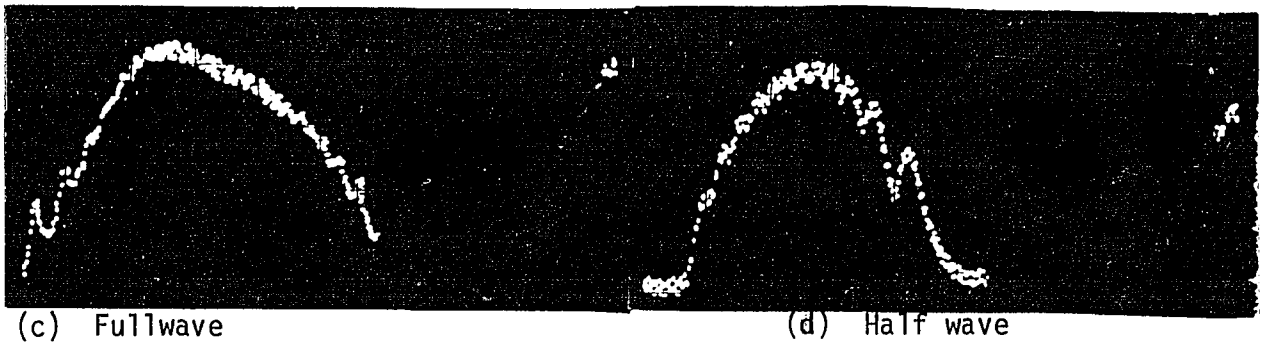

(c) Fullwave (d) Half wave

(Amplitude Scale)
1 mV

(Time Scale)
0.5 sec.

Figure 3.5 Ensemble of the EMG as a response to artificial stimulation of the phrenic nerve with PFM. (a) Shows pulse frequency modulator used. (b) Represents typical responses with square wave and sinusoidal modulating signals. (c) Average over 50 periods of full sine wave, and (d) Over 50 periods with half wave modulation.

used to produce fullwave and halfwave pulse frequency modulation ($10 < pps < 50$). Figure 3-5(c) shows the ensemble average of EMGs during 50 breaths due to stimulation of the phrenic nerve by sinusoidally modulated pulse trains. These results shall be discussed when the model of the subsystem under consideration is proposed.

A significant feature of ensemble averaging is the elimination of cardiac spikes due to the asynchronicity of cardiac spikes with respect to the breathing cycle. This has been possible because of the fixed phase relationship between the onset of each event in each respiratory cycle. The method alone is not enough to lead to any model proposal. The experimental result obtained when the phrenic nerve was supramaximally stimulated by square-wave modulated pulse trains does not show significant changes in the pressure and flow variable when pulse rate was changed from 30 pps to 50 pps thus confirming the hypothesis that muscle dynamics depend on other factors such as recruitment of fibers in the inspiratory phase. Moore [98] has investigated the nonlinear relation between the rms value of the EMG and the number of fibers recruited with random distribution of phase angles of pulse trains. Person and Libkind [99]-[101] also investigated a stochastic model by adding randomness in interspike intervals and formulated a nonlinear relation, depending on a synchronicity of superposed pulse trains, between integrated EMG and the number of recruited fibers. The major difficulty is due to temporal variations in pulse frequency and the temporal variation in the recruitment of fibers.

3.2 (c) Spectral Analysis. The investigation of spectral analysis of the EMG is another possible approach to be used. Its clinical value lies in the fact that pathalogical conditions can alter the spectrum of an EMG [102]-[105]. Analytically, the autocorrelation and power spectrum density for a stationary random process can be obtained with no difficulty. Kwatny et al. [106] used this approach by first confirming the stationarity of an EMG of the flexor pollicis brevis and the extensor digitorum with sustained contraction and with fatigue. No such study has been reported for the EMG of the diaphragm. Inspite of the difficulty of relating the spectrum to the output variables of a muscle, the spectrum analysis of the EMG may still provide empirical data for clinical use.

The limitation is due to the fundamental property of the muscle dynamics which essentially acts like a low-pass filtering signal recovery device. The information transmitted to the muscle is a superposition of several neural pulse trains. The spectrum analysis of the EMG could then be limited to the basic concept of superposition (or recruitment) of several parallel information channels each of which exhibits a pulse frequency modulated signal. Bayly [107] investigated the spectral analysis of neural pulse trains with this basic concept. He used the model of IPFM with sinusoidal modulating signal and a constant d.c. level. The constant level determines the carrier frequency of pulse trains and the sinusoidal modulating signal establishes the frequency modulated pulse trains. The spectrum then is related to the carrier frequency,modulating frequency and

modulation depth. The modulation frequency appears in the spectrum without any harmonics. If the modulation frequency is the primary signal to be recovered, then a simple low pass filter should be sufficient for this recovery. The skeletal muscle is assumed to possess such a property and perform its function like a simple demodulation. Bayly points out how the recruitment process improves the signal-to-noise ratio. Spectral analysis, such as this, has serious limitations when applied to the respiratory system which are related to the physiological nature of phrenic nerve activity and about which several points have been made previously. The modulating signal is not a sinusoidal signal and the number of parallel channels involved, known as recruitment, is also time-variant. The experimentally observed pulses in a single nerve fiber are also not ideal rectangular pulses (as assumed in Bayly's model). Moreover, the presence of cardiac spikes introduces an error in the spectral analysis. In the phrenic nerve and the diaphragm EMG signals there are silent periods during expiration; therefore, the concept of carrier frequency operating at all times cannot be extended to this case. Even if sinusoidal modulation were accepted, one would have to consider 'over-modulation' to account for the silent zone representing expiration. These limitations, then, leave the spectral analysis of an EMG of the diaphragm in the zone of empirical study with which some clinical correlation could be established in pathalogical cases. It is for this purpose that the spectral analysis of the EMG was investigated.

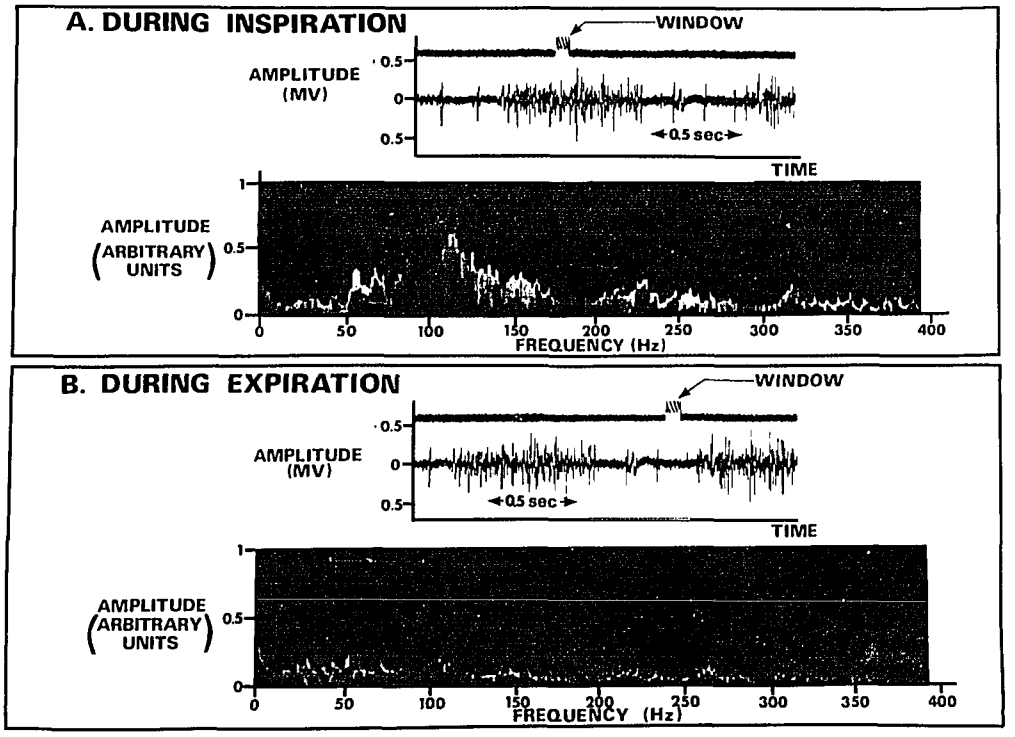


Figure 3.6. Spectral analysis of the EMG of the diaphragm of a natural breathing dog. Section A represents spectrum due to the EMG corresponding to the window shown in top trace. Section B shows spectral contribution due to noise section related to window. [The purpose of window is explained in Appendix B].

Experiments were done in which the EMG of the diaphragm was recorded on an F-M tape. Since the EMG burst, under steady state conditions is almost periodic, a portion of the tape of a length corresponding to the respiratory period, was selected and made into a loop. The loop replays a periodic EMG waveform whose spectrum was then analyzed on a Tektronix Tape 3L5 spectrum analyzer plugged into Type 564B Storage Scope. A special technique was used to avoid the contribution of the spectrum due to cardiac spikes which are superposed with the recorded EMG. This technique and other experimental procedures appear in Appendix B.

A typical result of the EMG spectrum obtained from an anasthetesized dog breathing room air, appears in Figure 3-6. The major contribution to spectral lines is due to the EMG alone. This is clear by comparing the results shown in Figure 3-6(A) and (B), where the lower trace shows the contribution due to noise alone. The peak of the upper trace, due to EMG, is at about 110Hz. This finding is representative of the observations obtained on seven dogs. It should be noted that the spectrum analyzer used in this experiment displays the amplitude of the various frequency contents of the input signal while ignoring the phase angles with each frequency. At this stage, therefore, the presence of a dominant peak at about 110Hz, cannot be interpreted analytically.

3.2 (d) Method of Filtering. The three methods of quantification of the EMG, as discussed above, have their limitations. The major decision to select a quantification technique should depend on

the purpose of such a quantification.

With respect to the objectives of the present investigation, the EMG of the diaphragm as well as the neural command in the phrenic nerve can be considered only as a complex signals containing some information which the muscle has to recover. The recovery of the signal generates the mechanical response of the muscle. This response is a function of time and in respiratory response, this may be measured either as tension or as transdiaphragmatic pressures. Both these variables are functions of time and are almost periodic in steady-state conditions. The muscular response of activation and relaxation is related temporally to the onset and termination of electrical activity respectively. It is, therefore, necessary to select a mode of quantification of the EMG which allows study of the temporal correspondence between the EMG and the mechanical events in respiration. Since the muscle, acting like a low-pass filter, ignores the high frequency contents of the EMG,a possible method of quantifying the EMG is by a process of low-pass filtering and averaging. The integration of the rectified EMG, as discussed in Section 3-2(a) falls in this category. The choice of integration-time is a significant parameter. If this time is made large, by having a large RC-time constant, as well as an infinite decay time, the dynamics of the EMG signals are also lost. Gottlieb and Agarwal [108] have used a filtering technique which has lower time constant and provides a running average of the rectified EMG.

It was felt that such a filter should be the satisfactory technique of quantifying the EMG. The chief advantages are the maintenance of signal dynamics as well as the time of activation and relaxation of the muscle activity.

The filter used is shown in Figure 3-7 with its performance in experimental conditions.

The transfer function of the filter can then be written as:

$$G(p) = - \frac{(1 + R^2c^2p^2)}{(1 + 2Rcp)(1 + 1.2\ Rcp + 1.6\ R^2C^2p^2)}$$

The idealized impulse response and the frequency response of this filter are shown in Figure 3-7(b) and (c) respectively. The cutoff frequency is at $\omega = \frac{1}{RC}$ and its approximate input - output relation is given by:

$$e = \frac{1}{T} \int_{t-T}^{t} e_1(\tau)\ d\tau$$

where $T = 2\pi RC$ represents the time-interval for the moving average. The filter was built by using $R = 300$ kilohms and $C = 0.0265\ \mu f$ in order to have the averaging time interval of approximately $T = 50$ msec. The actual values of R and C in the networks were selected by close approximation to standard components.

It may be pointed out that the impulse response of the third order moving-average filter has some similarity with the characteristic twitch response of a muscle. The twitch represents a quick

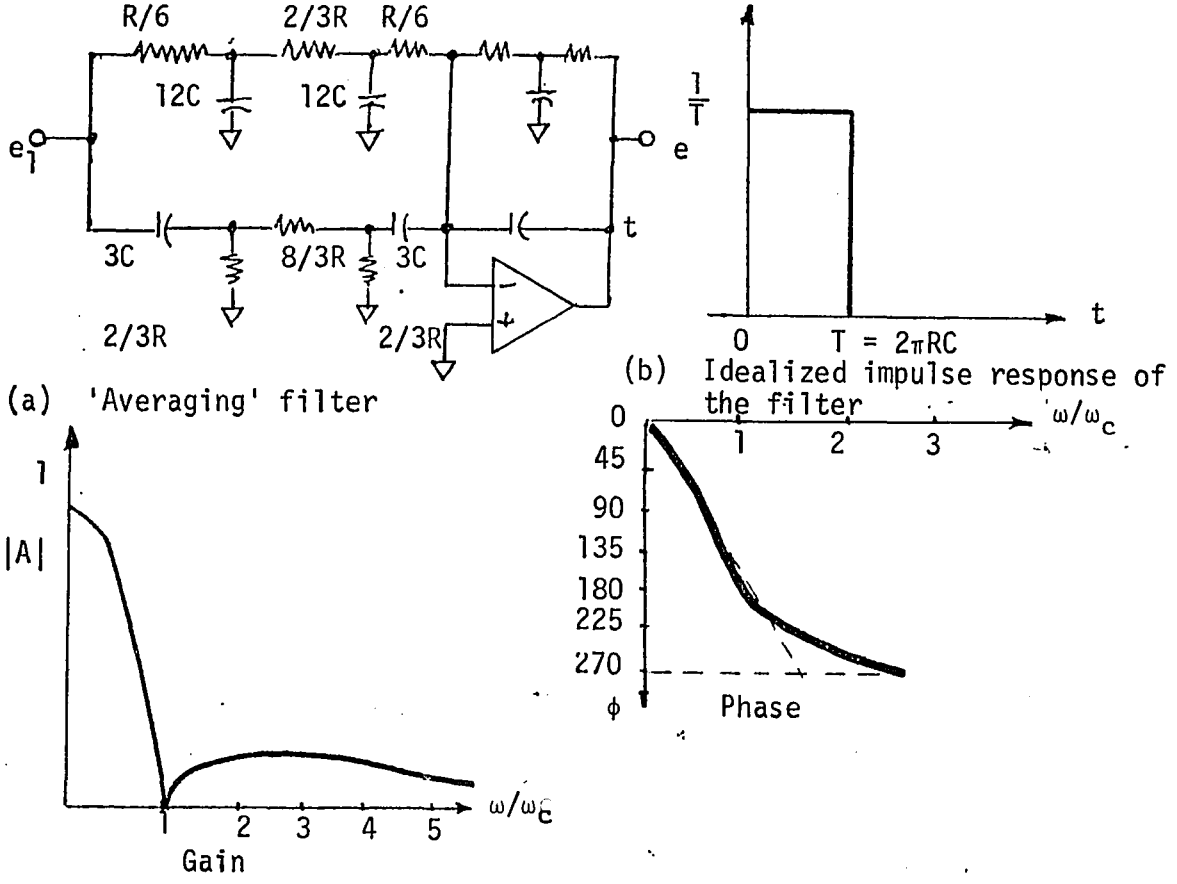


(c) Frequence response of the filter (from [109])

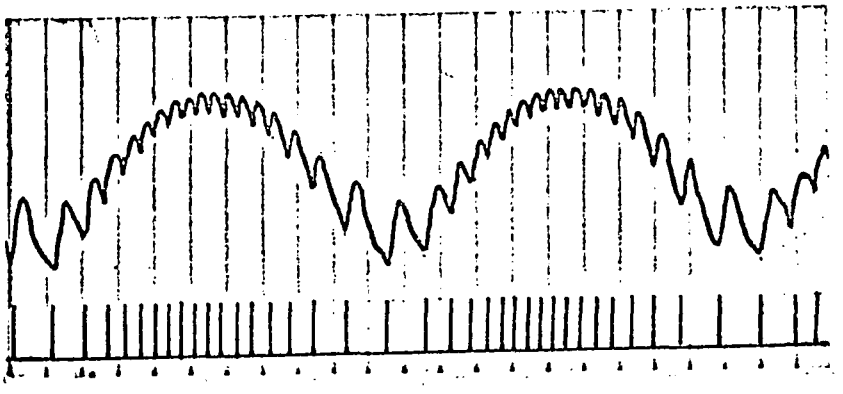

(d) Filter response (top trace) to PFM input (bottom trace) (sinewave modulation at 0.25 HZ; pulse width 5 msec.)

Figure 3-7 Averaging filter used for the EMG.

rise of tension followed by a slower recovery during relaxation. The total time period, in skeletal muscles, may be somewhere between 30 msec to 185 msec. If successive stimuli are applied to the muscle, the tension responses can fuse to produce a tetanus in the muscle. The actual strength of the tetanus or the smoothness in fusion depends on the frequency of pulses used for stimulation.

Figure 3-7(d) shows the response of the filter to a PFM signal. The phenomenon of recruitment and the randomness in firing in the actual muscle response would make it difficult to establish the similarity of the filter response and the muscle response to the same signal. It is reasonable to assume that the recruitment phenomenon in muscle fibers would produce a tension response due to linear superposition of the responses in all fibers. With this assumption, the filtered version of the EMG represents a variable related to the contraction of the muscle. The input to the filter is a rectified EMG as recorded by bipolar electrodes whereas the input to the muscle is a train of action potentials in all active muscle fibers. Furthermore, the transfer function of the filter may not be the same as that of the muscle. Therefore, their response to exactly the same input is not to be expected.

It may be concluded that the moving-average-filter does provide a significant tool with which the EMG-tension relationship in the diaphragm could be explored.

## 4. DYNAMIC RELATIONSHIP BETWEEN NEUROMUSCULAR ACTIVITY AND RESPIRATORY MECHANICS

Several experiments, described in Appendix A, were conducted on anasthetized dogs under various environmental conditions. The following variables were considered:

(i) Phrenic nerve activity and its envelope, obtained by feeding the signal, picked up by bipolar platinum wire electrodes, through a full-wave rectifier and a moving average filter.

(ii) The electromyogram (EMG) from the diaphragm and its envelope, obtained by feeding the signal, picked up by wire electrodes (surgically inserted in the diaphragm), through a full-wave rectifier and a moving average filter.

(iii) Transpulmonary pressure, obtained by a differential pressure transducer from an esophageal balloon and a pressure probe in the mouth. In some cases, transdiaphragmatic pressure was also obtained by a differential pressure transducer, from an esophageal balloon and either an abdominal probe or a gastric pressure probe using appropriate correcting factors.

(iv) Air-flow obtained from a differential pressure transducer with the pneumotachograph attached to the tracheal tube; volume obtained by integrating the air-flow signal.

The following type of tests were performed:

(1) Natural Breathing: The animal was kept in an environment with either room air or with certain known $CO_2$ contents in the inspired air. In all cases, only the steady-state response was studied.

(2) External Stimulation: The phrenic nerve was stimulated, using bipolar platinum electrodes, by either squarewave modulated pulse trains or by sinusoidally pulse-frequency modulated signals.

## 4.1 Mechanics of the Diaphragm

The mammalian skeletal muscle can be regarded as an electro-mechanical transducer. The input to the muscle is the neuroelectrical command signal and its output can be measured as force, change in length (due to contraction), or rate of change of length, i.e., the velocity of contraction. Pioneering work, leading to a mechanical analog of a muscle, was done by A. V. Hill [110]. Hill, in 1922, had proposed that the muscle, as a mechanical system, consists of an elastic element in series with a contractile component. Another elastic element is assumed to function in parallel with the contractile component. Later developments [111], [112] suggest a viscoelastic element in parallel with the contractile element. A recent approach [113], represents the muscle mechanics in terms of a nonlinear elastic element in series with contractile element and both in parallel to another nonlinear elastic element. The parameters depend on muscle length and/or velocity of contraction (or extension). Furthermore, their values depend on the type of muscle and its load and may vary between species. Such a study in the diaphragm is not included in the present investigation.

Since the diaphragm is a skeletal muscle, some characteristic features of such muscle models may be pointed out. The contraction process begins with the arrival of the neural command and the excita-

tion of the contractile component. Due to the excitation the contractile componenet goes into 'active state' and functions as a force generator. Muscle contraction occurs slowly due to greater 'stiffness' of the series elastic component. If the length is kept constant, then the response can be measured as isometric tension generated in the whole muscle. Increase in pulse rate of the command signal increases the tension resulting in a family of curves result as shown in Figure 4-1(a). The velocity of contraction can be studied by reducing the external load (i.e., making it less than maximum tension needed for isometric contraction) resulting in a family of curves as shown in Figure 4-1(b). These curves obey the basic relationship described by Hill's equation $(T + a)(\dot{L} + b) = (T_o + a)b$ where $T$ is the force at zero velocity and $a$ and $b$ are constants with demensions of force and velocity respectively. With the help of physiological data a simple model has been proposed by linearizing the family of curves about an operating point [114].

A significant feature, related to the role of neuromuscular command, shall now be discussed. The increase in contraction is related to increase in pulse rate as well as the recruitment of motor units. Bigland and Lippold [17], while studying the human hand muscles concluded that the gradation of muscular contraction was mainly due to recruitment of motor units. Furthermore, they also established the interdependence between force of contraction, velocity of change in length and the integrated electrical activity in the muscle during activation. Bigland and Lippold have observed

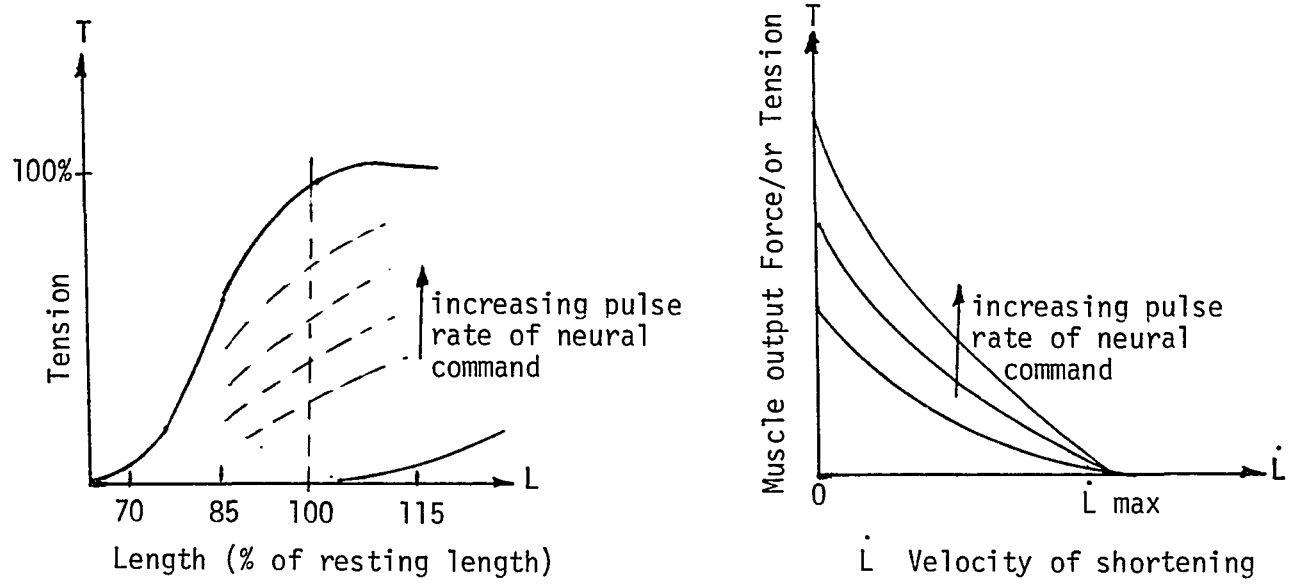


Figure 4-1 Some properties of a skeletal muscle [114].

a linear relationship between the integrated EMG and the muscle force. If the increase in EMG is due to recruitment, then one should expect some nonlinear relationship between averaged rectified EMG and the number of fibers recruited [98]-[100]. The linearity as observed by Bigland and Lippold may then be explained by progressive synchronicity in recruitment [100]. The EMG, then, carries an important information whose functional relationship with the mechanical output of the muscle could be established by getting measurable variable in functioning muscle in human or animal body. Gottlieb and Agarwal have used this approach to model the neuromuscular dynamics of the human solens muscle under voluntary isometric foot torque [115]-[117].

An investigation of the neuromuscular dynamics of the diaphragm considering tension length or curvature changes under stimulation would be desirable. However, these variables are, at present, very difficult to measure. Even if their measurement were possible, their effect on respiratory mechanics would remain unexplored. In order to avoid the complexity of measurements of the above variables relating the contractile mechanism of the diaphragm to the mechanical events in respiration, it was decided that the modeling approach must rest with observable variables in the diaphragm under natural conditions or under artificial stimulation of the phrenic nerve.

The correspondence between the phrenic neurogram (PNG), and the electromyogram (EMG), was first established by recording both of these variables in an anasthetized dog. The neural command was

altered by steady-state response of the animal under various $CO_2$ concentration in the inspired air. A typical result is shown in Figure 4-2 which shows the ramp-like nature of both the neurogram and the electromyogram (both were rectified and filtered by a moving averager). The result clearly indicates a visual similarity between the PNG and the EMG and supports similar results by Lourenço et al. [84] though their own results were obtained by different techniques. Any conclusion regarding the EMG under different $CO_2$ breathing, is not intended from the results shown in Figure 4-2. However, a quantitative relationship between the variables may be possible by using long-time averaging of the signals.

Figure 4-3(a) shows the relation between EMG and esophageal pressure for three different $CO_2$ concentrations. The esophageal pressure was measured by esophageal balloon technique. Actually, the contractile mechanism of the diaphragm is more related to the transdiaphragmatic pressure than to the esophageal pressure. The latter was obtained by connecting the esophageal balloon to one side of a differential pressure transducer the otherside of which was connected to an abdominal probe. The relation between EMG and transdiaphragmatic pressure thus obtained is shown in Figure 4-3(b).

Before a model could be proposed, the linearity of the response should be investigated from both measurements and physiological data. An indirect approach to establish linear relationship between the EMG and the pressure is available from the investigations by

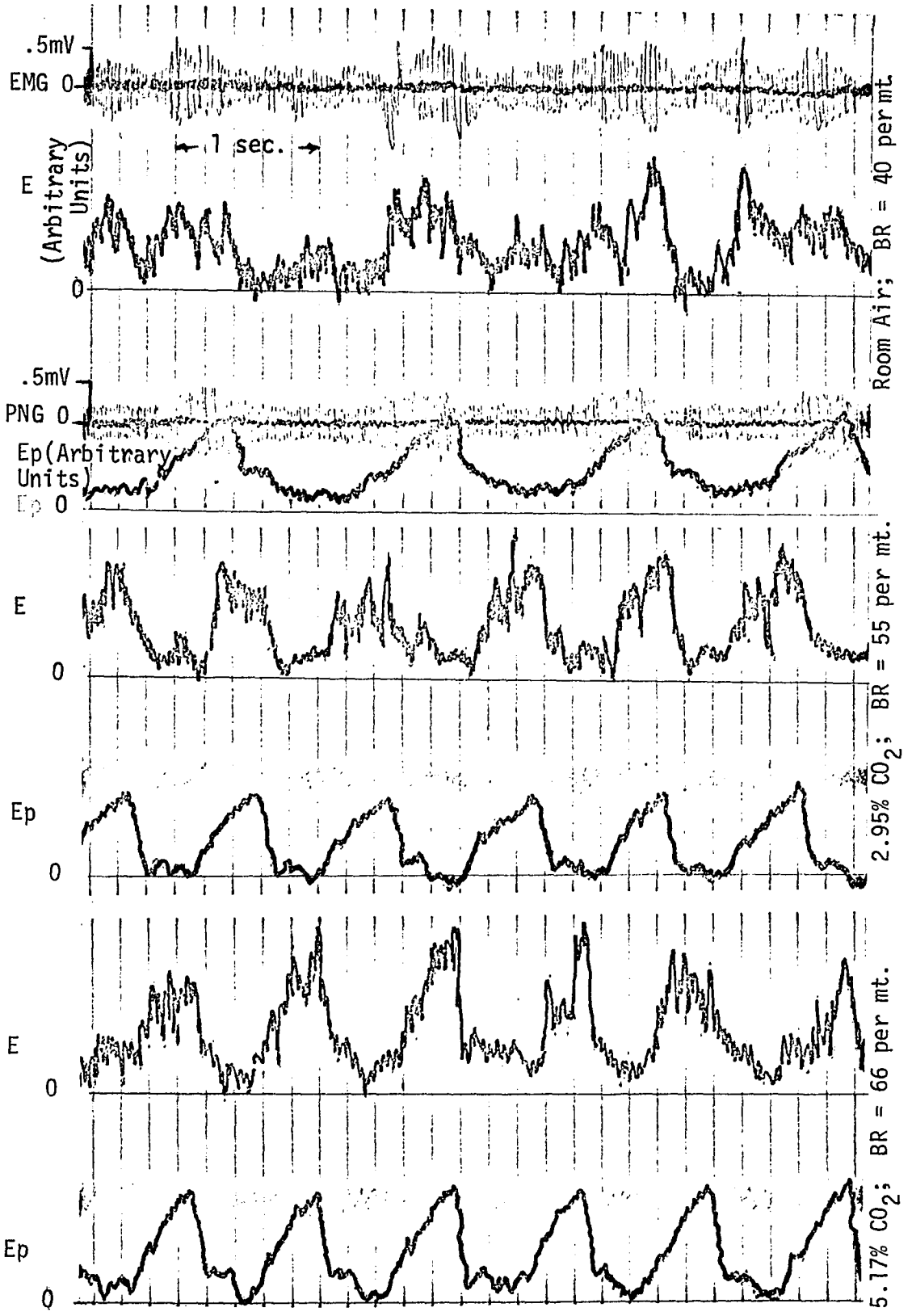


Figure 4-2 EMG, PNG, and their filtered versions (E and Ep) under different $CO_2$ breathing. The amplitudes of E and Ep are in arbitrary units.

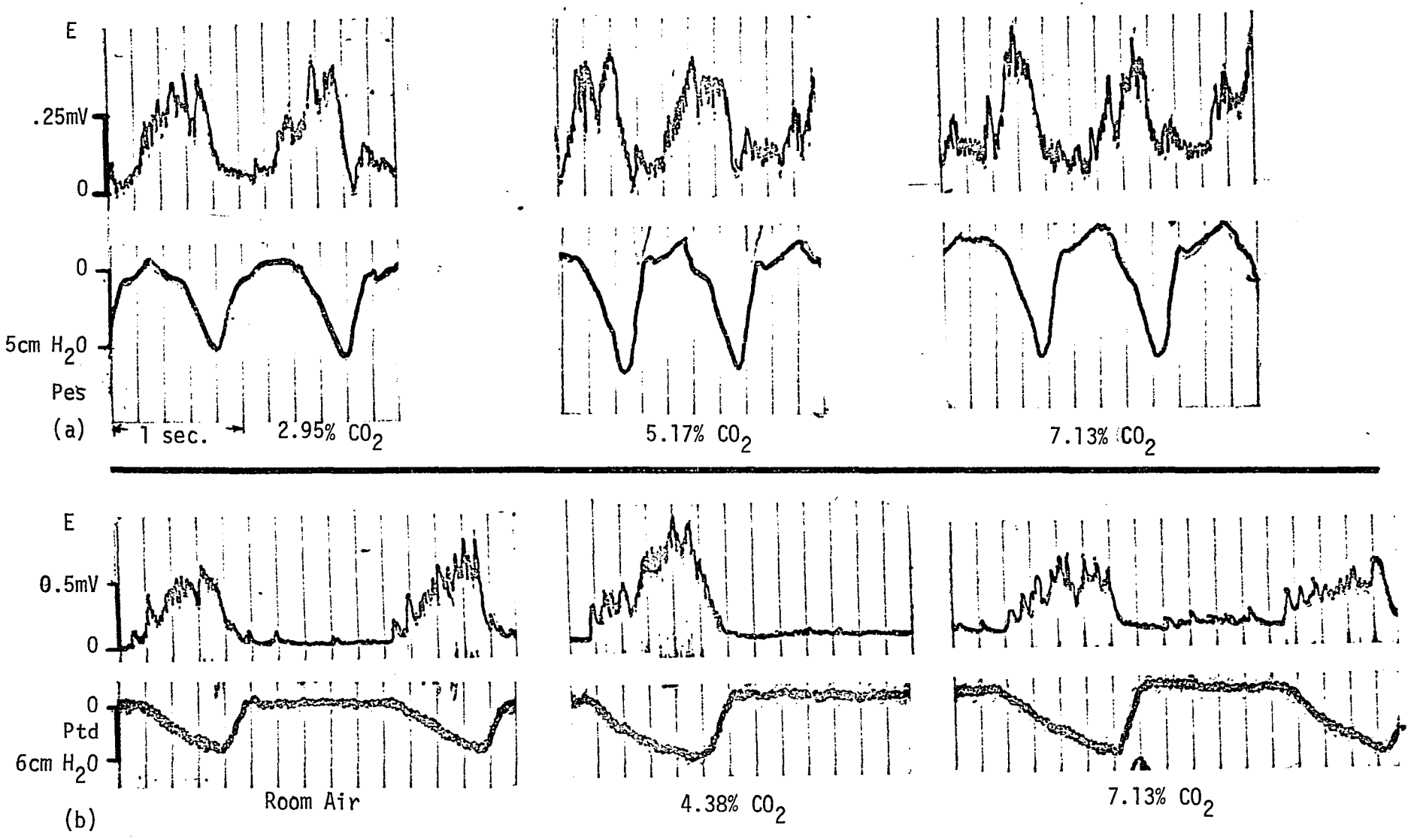


Figure 4-3 Typical records of E and pressures under different $CO_2$ breathing. Top section (a) shows records of esophageal pressure, Pes and the bottom section (b) shows transdiaphragmatic pressure, Ptd.

Lourenco et al. [84], if the pressure changes are linearly related to changes in the tidal volume. This linearity is supported, at least over a certain range around the resting volume in normal breathing, by the findings of Agostoni and Rahn [18]. In skeletal muscles also, a linear relationship between EMG and muscle tension has been reported [82], [116]. If such a linearity exists for the diaphragm, then a linear - first or second order model - may be postulated and verified experimentally by step-response measurements on the muscle from electrophrenic stimulation.

Such experiments were conducted in several dogs by electrophrenic stimulation in the cervical region, using pulse rates of 20 pps and 50 pps. The stimulation being supramaximal eliminates recruitment and probably causes maximum diaphragmatic contraction, thus showing practically no difference in transdiaphragmatic pressure when the stimulation was increased from 20 pps to 50 pps. The results, as shown in Figure 4-4, do suggest a first order linear transfer function between EMG and transdiaphragmatic pressure at least during the initiation of active state.

There are considerable physiological data available for the contractile mechanism of the diaphragm in mammals. Sant'Ambrogio and Saibene [27], using electrophrenic stimulation (100 pps) with closed airways, have recorded intrapulmonary pressure. The condition, resembling an isometric contraction though the deformation of the rib cage, affects the contraction time of the diaphragm. In dogs,

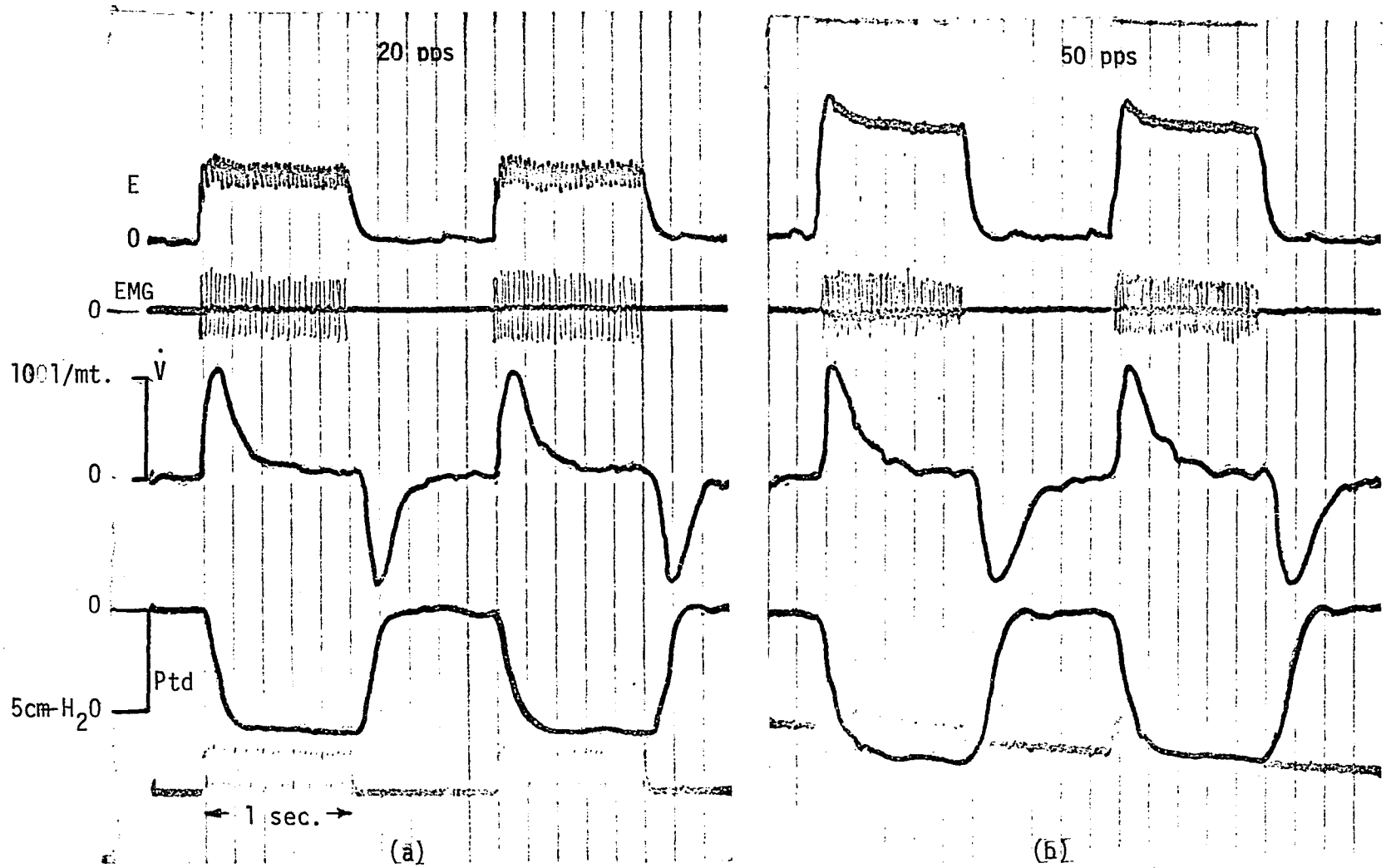


Figure 4-4 Electrophrenic stimulation using square-wave modulated pulse trains. Left section (a) for 20 pps and right section (b) for 50 pps. For flow curve inspiration is upwards; for pressure, it is downwards.

they found the contraction time, to step response, of about 64.7 msec. Earlier (1968), Mognoni et al. [30] reported the half-time of pressure swing in dogs during tetanic stimulation, to about 61.9 msec. They found similar results in human subjects also. They also reported that during maximum and quickest inspiratory and expiratory efforts by man, the esophageal pressure, Pes, and the gastric pressure, Pg, increase exponentially. The transdiaphragmatic pressure, which can be approximately represented as the difference between Pes and Pg, cannot be a single exponential. However, an exponential rise in the transdiaphragmatic pressure is possible only if it is assumed to be similar to the esophageal pressure. This is a reasonable assumption under normal quiet breathing.

These observations lead to a simple first order transfer function, between E and T, of the type $\frac{k}{1 + \tau p}$ where the time constant $\tau$ was estimated to be about 0.1 sec. Here E represents the filtered version of rectified EMG and T represents the muscle tension. Normally such a tension should be measurable in skeletal muscles as a force in Kg/cm. If such a measurement is difficult, as in the case of the diaphragm, some criterion must be established to treat pressure (either transdiaphragmatic or esophageal) as a measure of the tension. This shall be developed in the next section.

The transfer function mentioned above has one more limitation. It is valid during excitation of the diaphragm only. The square wave pressure response, as shown in Figure 4-4, exhibits a quicker relaxa-

tion upon cessation of the electrical activity. This quick recovery, during relaxation, requires a modification in the transfer function. Such a modification represents a nonlinearity. Similar nonlinearities have been reported by Partridge [118] who studied the muscle response to sinusoidally modulated pulse trains. The nature of such a nonlinearity shall be discussed later though a clear physiological explanation does not seem to be possible at present. The significant feature in the respiratory muscle is a sudden cessation of the activity which facilitates the dynamics in two stages seperately. Such a seperation should yield a transfer function during active state of the muscle and the other one during its relaxation. This may still leave the sinusoidal response without a satisfactory explanation. In that case, the closest approximation should relate the reduction of pulse rate to a'partial-relaxation'. Another possibility is to introduce two limiter type of nonlinearities [117].

The lack of physiological 'meaning' of these nonlinearities suggested that the present work should consider a very simple linear model. On the basis of the step response data, as shown in Figure 4-4, the rise of pressure is almost exponential with a time constant of approximately 0.1 second which is somewhat larger than 0.0647 second as reported by Sant'Ambrogio and Saibene [27]. Nevertheless, the results of a computer simulation with this time constant compare very well with the experimental data. It is assumed that this simple model, as shown in Figure 4-5 does not differentiate relaxation time

constant from that of the active state. As pointed out earlier, such a distinction between the relaxation dynamics and the active state dynamics is limited because of the lack of any visco-elastic model of the diaphragm.

If the behavior of the diaphragm is assumed to be representative of the skeletal muscle, then one might assume the relaxation to be much faster than contraction. It may be reasonable to assume the relaxation time constant to be 0.02 second compared with the time constant of 0.1 second for the active state. Seperation of the 'active state' and the 'relaxation state' in a muscle is rather difficult. If the muscle is regarded as an electromechanical transducer, its physiological input is represented by the electromyogram. The onset of this activity may be regarded as the onset of the 'active state' of the muscle. On the other hand, the relaxation may begin either by the cessation or by the reduction of the amplitude of the electromyogram. The use of filtered EMG, therefore, suggests that the rate of change of the filtered EMG, E, may be selected to represent the active state (when such a rate is positive) or the relaxation (when the rate is negative). One may also distinguish between active and relaxation states in terms of the polarity of the rate of change of tension T, using a rate-sensitive control [119]. The basic problem in the application of such a control is the presence of noise in the EMG. An alternate approach is the use of air-flow to represent the active state and the relaxation state

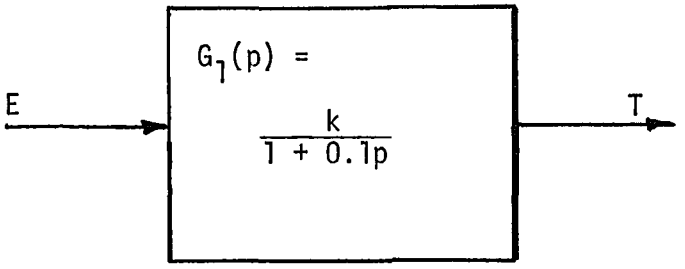


Figure 4-5 Linear model of electromechanical dynamics of the diaphragm. E represents filtered EMG, T tension and constant k is to normalize the input level.

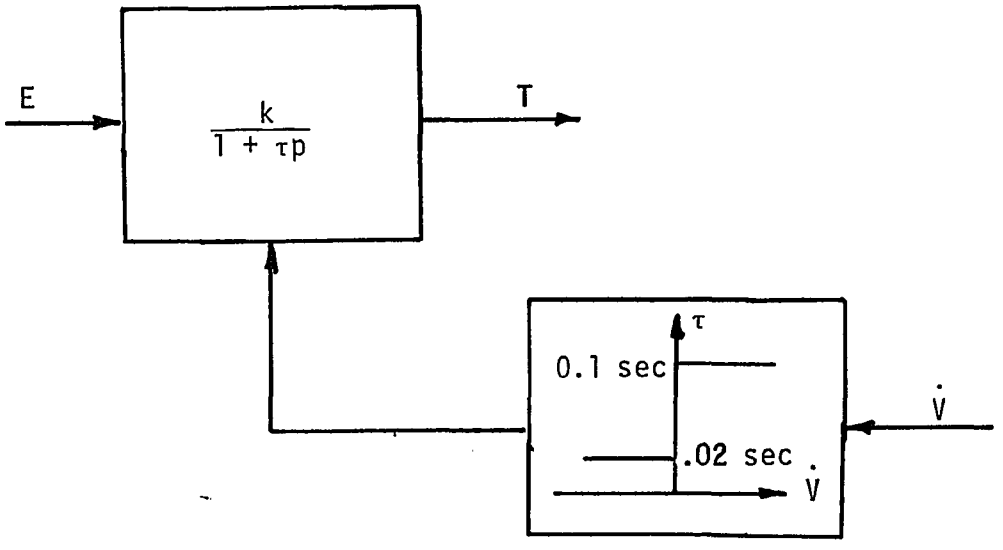


Figure 4-6 Possible nonlinear model for the neuromuscular dynamics. The time constant, $\tau$, is 0.1 sec. representing slow response during excitation, with $\dot{V}>0$, and $\tau = 0.02$ sec. represents relaxation response when $\dot{V}<0$.

of the diaphragm. Here the inspiration, with $\dot{V} > 0$, manifests contraction of the diaphragm and the expiration, with $\dot{V} < 0$ represents the relaxation of the diaphragm. It may then be possible to represent the tension-EMG dynamics of the diaphragm by the following equation:

$$\dot{T} = \frac{1}{\tau} [-T + kE]$$

where

$$\tau = \begin{cases} 0.02 \text{ sec when } \dot{V} < 0 \\ 0.1 \text{ sec when } \dot{V} > 0 \end{cases} \qquad (4.1)$$

The block diagram of such a model is shown in Figure 4-6.

The choice of $\dot{V}$ to represent activation or relaxation of the diaphragm has physiological appeal - especially in the model of a respiratory system. However, the dynamics of the respiratory pump, which relate pressure and air flow, produce a time lag which may create errors. More study on this subject is required. The present investigtion considers a simple first-order linear model representing the EMG tension dynamics of the diaphragm which disregards the change of the time constant .

## 4.2 Laplace's Law Under Dynamic Conditions

Since measurement of tension in the diaphragm has been ruled out, the pressure, either across the diaphragm, or just above it in the thoracic cavity may be considered as an output variable representing the muscle response. An attempt must be made to define the relationship between the tension and the pressure related

to the diaphragm. In 1962, Marshall [32] observed that if by electrophrenic stimulation the diaphragm tension is kept constant, under steady-state, the intrathoracic pressure in the dog becomes less negative while the tidal volume increases. Considering the diaphragm as a segment of a hemispherical dome, Marshall explained this by the pressure-tension relationship of Laplace's Law. This law is usually applicable to a soap bubble. It states that if there is a curved membrane partioning two seperate spaces with fluid contents and the membrane has a tension in it of T, as elastic tension (in gm/cm), then there will be a difference of pressure of P (in $gm/cm^2$), which is obtained as:

$$P = T \left(\frac{1}{r_1} + \frac{1}{r_2}\right)$$

where $r_1$ and $r_2$ are principal radii of curvature of the membrane at any point. In a spherical membrane, where $r = r_1 = r_2$, this equation reduces to $P = 2T/r$. It must be pointed out that this Law refers to 'surface tension' and thus applies to thin membrane surface, such as that of a soap bubble. The similarity of a diaphragm to a thin film membrane may be questionable, however, it possesses the property of an elastic muscle. With this property, all skeletal muscles, when stretched under external force tend to restore its original length by their elastic behavior. A simple relationship between the elastic tension, $T_e$, and muscle length can be expressed as:

$$T_e = k(L - Lo) \qquad (4.2)$$

where $L_0$ represents resting length with zero tension and L is length under stretch (or compression) and k is a constant due to elasticity. Here the elastic tension $T_e$ represents force needed to restore equilibrium length $L_0$ when the driving force is removed. If the muscle receives neural command, the active state represents an additional force generator. A previous section has considered the electrically generated tension, T, as an output of such a generator. The toal muscle tension, $T_m$ then yields $T_m = T_e + T = K(L - L_0) + T$.

It is assumed that the diaphragm represents a segment of a hemispherical dome of radius of curvature, r, as shown in Figure 4-7(a). It is also assumed that under contraction, only the arc length, shown as ACDB in Figure 4-7(a), changes but the section diameter AB, $2r_1$, is unchanged. The tension and pressure relationship can be derived from a small square element, of length 2a, as shown in Figure 4-7(b). Without loss of generality, this section has a side length CD parallel to the horizontal axis. By equating the vertical component of the tension vector and the pressure it can be shown that $P = \frac{2T_m}{r}$, where $T_m$ represents the total muscle tension. Thus,

$$P = \frac{2k(L-L_o)}{r} + \frac{2T}{r} \qquad (4.3)$$

where the first past on the righthand side represents the elastic component due to mechanical forces alone. Pengelly et al. [33] observed that in decerebrate cats (i.e., where supra-segmental control of the medullary respiratory center is interrupted) a pressure difference exists when the diaphragm's contraction results in

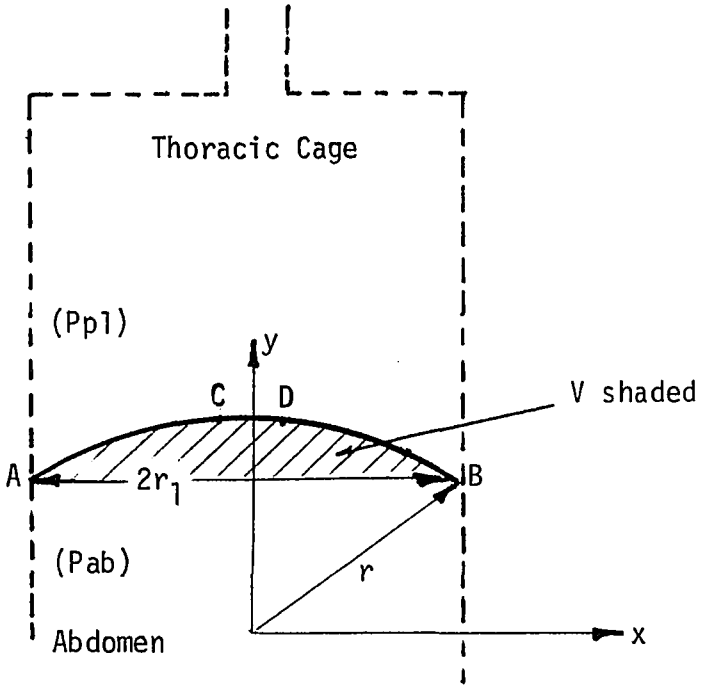


(a) Diaphragm representing segment of a hemispherical dome.

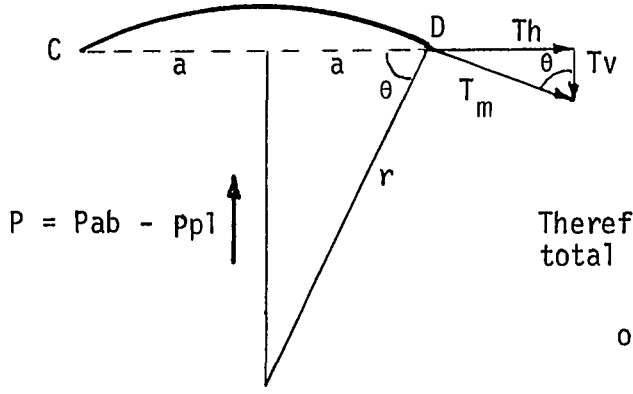


Th = Horizontal Component of $T_m$

Tv = Vertical Component of $T_m$

$= T_m \cos\theta = \frac{T_m a}{r}$

Therefore, total vertical tension $= \frac{8 a^2 T_m}{r}$

opposing pressure $= 4 a^2 P$

Thus $P = 2T_m/r$

(b) Cross-section of a selected square element in the diaphragm.

Figure 4-7 Geometrical representation of the diaphragm as a segment of hemispherical dome.

mechanical alteration of the diaphragm length and in electrophrenic stimulation which adds on to the electromechanical 'active state'. The authors conducted the mechanical alteration, without electrophrenic stimulation but by changing lung volume with relaxed muscles. Their results indicate that with electrophrenic stimulation, the pressure across the diaphragm is much larger compared with the pressure difference contributed by mechanical action alone. The first term on the righthand side of the equation (4.3) confirms this since the arc length L is related to r, i.e.,

$$L = 2r\left[\frac{\pi}{2} - \tan^{-1}\sqrt{\frac{r^2 - r_1^2}{r_1}}\right] \tag{4.4}$$

which shows that length of the diaphragm arc reduces when radius of curvature increases. The actual contribution due to elastic component can be estimated if the elastic constant k is known. The results of Pengelly et al. [33] suggest that the pressure under relaxed state is small compared to that under stimulation. It is, therefore, reasonable to assume that:

$$P \approx \frac{2T}{r} \tag{4.5}$$

where T represents tension generated in the diaphragm due to neural command.

The pressure-tension relationship, (4.5), includes the radius of curvature of the diaphragm. This increases during contraction of the diaphragm (during inspiration) and reduces back to normal resting

value, $r_0$, at the end of expiration. The prediction of pressure, therefore, depends on the temporal nature of the tension T and the radius of curvature, r, which, in turn, is a function of the tidal volume which reflects the volume changes in the thoracic cage.

In Figure 4-7(a), A and B represent the points where the diaphragm is in contact with the chestwall. These points are assumed to be fixed, i.e., the diameter AB = $2r_1$, represents a constant. The contraction of the diaphragm will then reduce the shaded area (Figure 4-7(a)) and increase the volume in the chestcage above the diaphragm.

It can be shown that

$$V(r) = V \text{ shaded} = \pi \left[ \frac{2}{3} r^3 - r^2 (r^2 - r_1^2) + \frac{1}{3} (r^2 - r_1^2)^{3/2} \right] \tag{4.6}$$

where $r_1$ is a constant. Equation (4.6) represents a nonlinear relationship between V shaded and r.

It is assumed that at rest, i.e., with lungs at functional residual capacity (FRC) it is $r = r_0 > r_1$. If r increases from $r_0$ to $r_0 + \Delta r$, due to the contracting muscle, Taylor series expansion of equation (4.6) and with higher power terms ignored, gives

$$V(r) = V(r_0) + V'(r_0)(r - r_0) \tag{4.7}$$

$$\text{where } V(r_0) = \pi \left[ r_0^3 \left( \frac{2}{3} - k + \frac{k^3}{3} \right) \right] = \pi \left[ k_1 r_0^3 \right] \tag{4.8}$$

$$r_0^2 - r_1^2 = k^2 (r_0^2); \quad k^2 < 1 \tag{4.8b}$$

and $$V'(ro) = \pi \left[ r_o^2 (2 - \frac{1}{k} - k) \right] = \pi \left[ k_2 r_o^2 \right] \quad (4.9)$$

Here again, since $k < 1$, $k_2$ in equation (4.9) is always negative thus representing reduction in V shaded due to contraction of the diaphragm. This change is given as:

$$\Delta V \text{ shaded} = \pi \left[ k_2 \, r_o^2 \right] \Delta r \quad (4.10)$$

Thus, reduction in V shaded (Figure 4-7) represents an increase in lung volume due to inspiration, V tidal, designated here as V. Similarly the lung volume at rest (FRC) can be expressed as Vo.

Let $$Vo = k_3 \, V \text{ shaded} = k_3 \left[ \pi k_1 \, r_o^3 \right] = \underset{(FRC)}{k_4 \, r_o^3} \quad (4.11)$$

And $$V = k_3 \, \Delta V \text{ shaded} = k_3 \left[ \pi k_2 \, r_o^2 \right] \Delta r = \underset{(\text{Tidal Volume})}{k_5 \, r_o^2 \, \Delta r} \quad (4.12)$$

where $k_3$, $k_4$ and $k_5$ are constants. Then, equations (4.11) and (4.12) yield:

$$r_o = \left[ \frac{Vo}{k_4} \right]^{1/3} \quad (4.13)$$

and $$\Delta r = \left[ \frac{V}{k_5 \, r_o^2} \right] \quad (4.14)$$

With equations (4.13) and (4.14), the radius of curvature of the diaphragm can be expressed as:

$$r = r_o + \Delta r = \left[ \frac{V_o}{k_4} \right]^{\frac{1}{3}} + \left[ \frac{V}{k_5 \, r_o^2} \right] \quad (4.15)$$

Actual computation of $k_4$ and $k_5$ depends on ratio of radius of curvature of the diaphragm and the radius of circular cross-section of chestwall as well as the proportionally constant relating the

lung volume and the volume of the shaded area below the diaphragm. The resulting system model is shown in Figure 4-8.

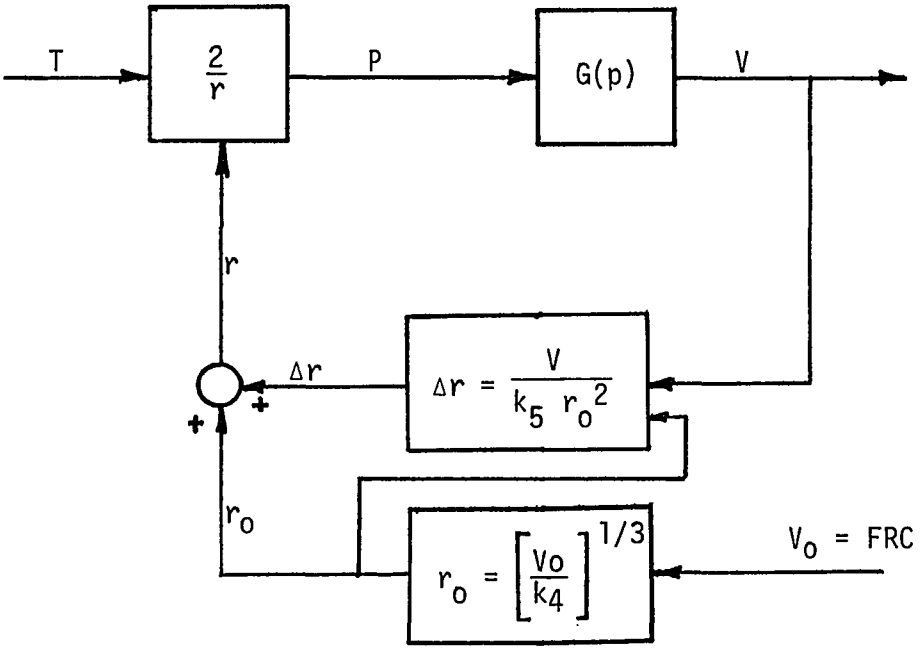


Figure 4-8 Model of electromechanical dynamics of the diaphragm with respiratory mechanics.

## 4.3 Respiratory Mechanics

The mechanical parts of the respiratory system containing lungs, pleural space and surrounding respiratory muscles and rib cage constitute a mechanical pump which results in airflow, in and out of lung, when suitable force input is available. The force which operates the mechanical pump at inflow is generated by the active muscular contraction. This force can be represented in terms of applied force or applied pressure and it is opposed by elastic recoil of lungs and muscles, frictional resistance due to deformation of tissues and the airway resistance. The intertia is also considered for an ideal model. The compliance, resistance, and inertia are distributed parameters, but may be approximated to be lumped. Using these considerations Mead and Milic-Emili [37], have shown the entire respiratory system as an analog of an electrical network. The electrical analog of such a system was illustrated in Figure 2-3.

An excellent summary of the statics and the dynamics of such a system have been provided by Agostoni [120]. There are several techniques with which the lumped parameters shown in Figure 2-3 can be determined. The measurement of which is outside the domain of this dissertation. What is attempted here is to use the available data to construct a model to simulate the respiratory mechanics with transpulmonary pressure as its input.

The respiratory mechanics includes several aspects of pressure which require distinction. For this purpose, the electrical analog

of Figure 2-3 is redrawn in a simpler form, by excluding the R-L-C elements related to mouth and gas compressibility. Figure 4-9 illustrates such a simple model.

In this model the applied pressure, Papp, is represented by Prs, as the pressure input to entire respiratory system. This pressure represents the algebraic sum of all pressure 'drops'. The chest wall, w includes the ribcage and the diaphragm, representing the only section which adds dynamic conditions under muscular contraction. The ribcage and the diaphragm operate in parallel since the total volume displacement in the thoracic cage, $\Delta Vw$,is due to sum of volume displacements of ribcage and diaphragm-abdomen structures, i.e.,

$$\Delta Vw = \Delta Vrc + \Delta V(ab + di) = \Delta Vrs \qquad (4.16)$$

Several pressure relations are clear from Figure 4-9. These are shown in that Figure. If the applied pressure, represented as Prs or Palv is the known input then the volume and flow signals can be found with the R-L-C elements of the entire system known. Jodat et al. [63] simulated such a model by using this approach. They had also included an added factor representing the compliance of the pleural space. They also considered the interaction between abdominal and chestwall pressure during inspiration and expiration.

In the present investigation, the pleural compliance is considered insignificant and the diaphragm is consider the major muscle during

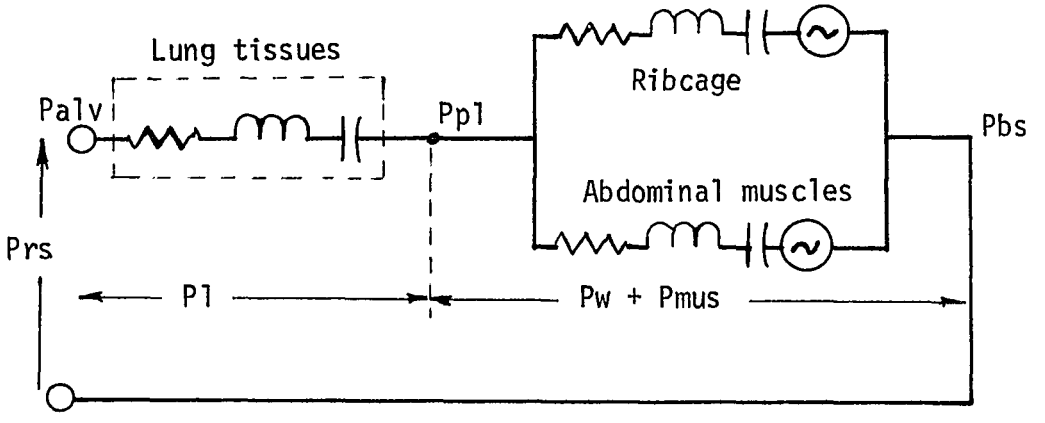


$$P_{app} = P_{rs} = P_{alv} - P_{bs}$$

If Pbs (body pressure at normal atmospheric pressure) is considered to be zero, as a reference, then

$$P_{rs} = P_{alv}$$

$$= P_l + P_w \text{; under static conditions}$$

$$\text{or } P_{rs} = P_l + P_w + P_{mus} \text{; under dynamic conditions}$$

where $P_w + P_{mus} = P_{pl}$, the pleural pressure

Thus, $P_{rs} = P_{alv} = P_l + P_{pl}$

Therefore, $P_l = P_{alv} - P_{pl}$ where $P_{pl}$ includes pressure changes due to contracting muscle structure.

Figure 4-9 Simplified analog of respiratory mechanics with relations between various pressure variables (from [37]).

normal breathing. It is, therefore, possible to simplify the model further and approach the simulation with transpulmonary pressure as the measurable variable. As described in Figure 4-9, the pressure across the lungs, Pl, along with the flow resistance and compliance is sufficient to generate the volume and flow in the entire respiratory system. The alveolar pressure equation shown in Figure 4-9 can be written as:

$$Pl = Palv - Ppl \tag{4-17}$$

If this equation is to be used as a relation between measurable variables, then measurement of Palv and Ppl is necessary. An alternate approach is to consider transpulmonary pressure, i.e., the difference between the mouth pressure and the pleural pressure. Under dynamic conditions, i.e., with muscular contraction under neural command, the muscle pressure, Pmus, is also included in the measurement of Ppl. Transpulmonary pressure, therefore, seems to be a desirable variable in the model, if the parameters of the respiratory pump across which it acts like an input are known.

One factor which needs explanation is whether transpulmonary pressure includes the pressure due to muscle contraction in the diaphragm which was earlier related to the muscle tension. Ideally, the transdiaphragmatic pressure should be considered as the output of the contracting muscle. Experimentally, this can be obtained by esophageal balloon techniques, where one balloon is slightly above the diaphragm and the other one goes to the stomach. The actual pressure on the abdominal side of the diaphragm is assumed to be

Pg - 11 cm H20 (in man) [18]. The pressure on the abdominal side thus obtained does not seem to have significant temporal variation [18], [31] and it is also reasonable to assume that esophageal pressure is a significant representative of the muscle output. These simplifying assumptions lead to transpulmonary pressure, Ptp, as an input to a linear element G(p) representing the dynamics of the respiratory mechanics. Since the intertial factor is insignificant, the transfer function is represented by:

$$G(p) = \frac{C}{1 + RCP} \tag{4.18}$$

where C is the pulmonary compliance in liters/cm $H_2O$ and R is pulmonary resistance in Cm $H_2O$/liters per sec. This transfer function represents the input-output relationship between Ptp and the volume V, i.e.,

$$Ptp = \frac{V}{C} + R\dot{V} \tag{4.19}$$

With R and C known from the data on dogs, the entire subsystem shown in Figure 4-10 has been simulated on an analog computer.

## 4.4 Computer Simulation and Results

The model of Figure 4-10 was simulated on EAI-380 computer. Figure 4-11 represents the analog computer diagram. E represents the filtered EMG as the input to the model, $k_1$ represents the gain factor k in the tension-EMG transfer function. It is also used to normalize the amplitude of the recorded EMG, which was necessary

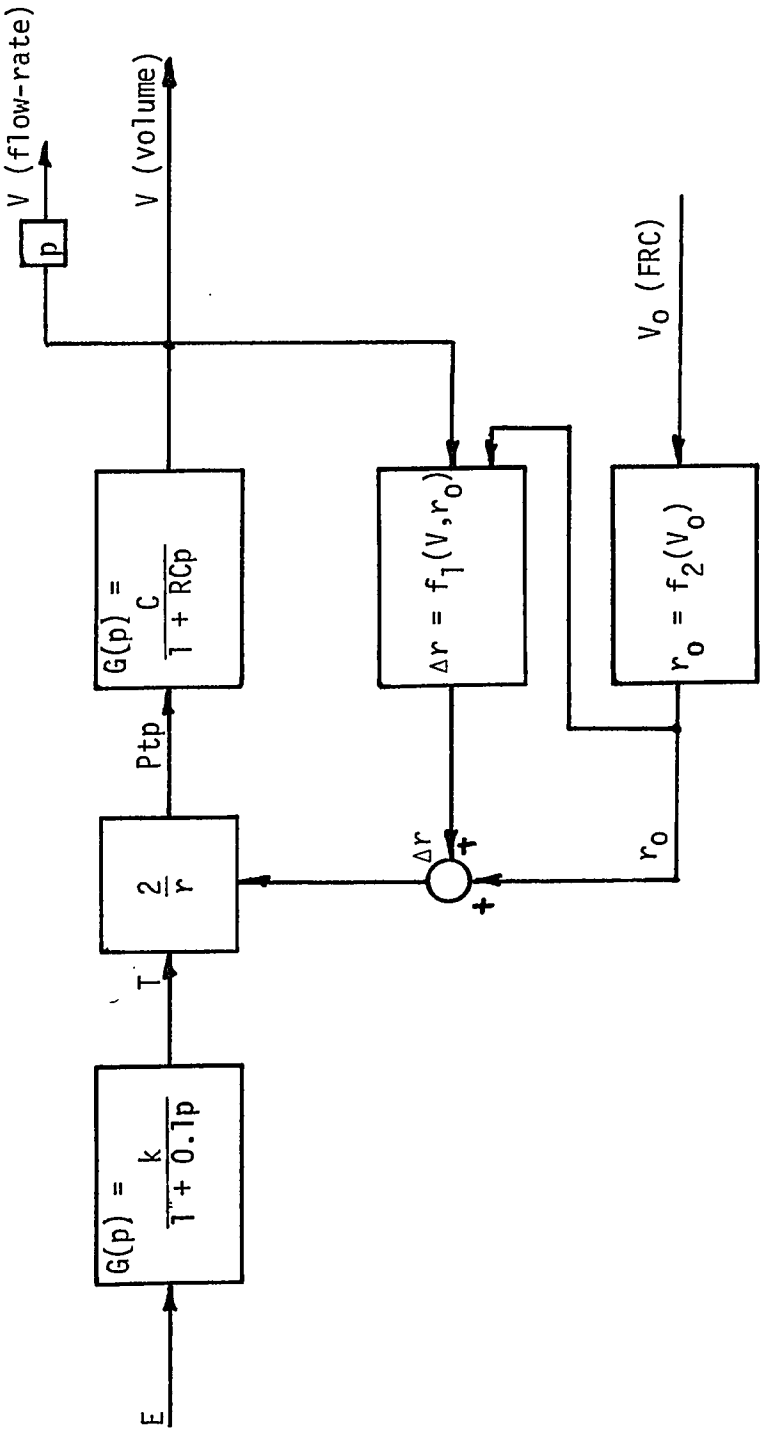


Figure 4-10 Model of the entire electromechanical subsystem of the respiratory controller.

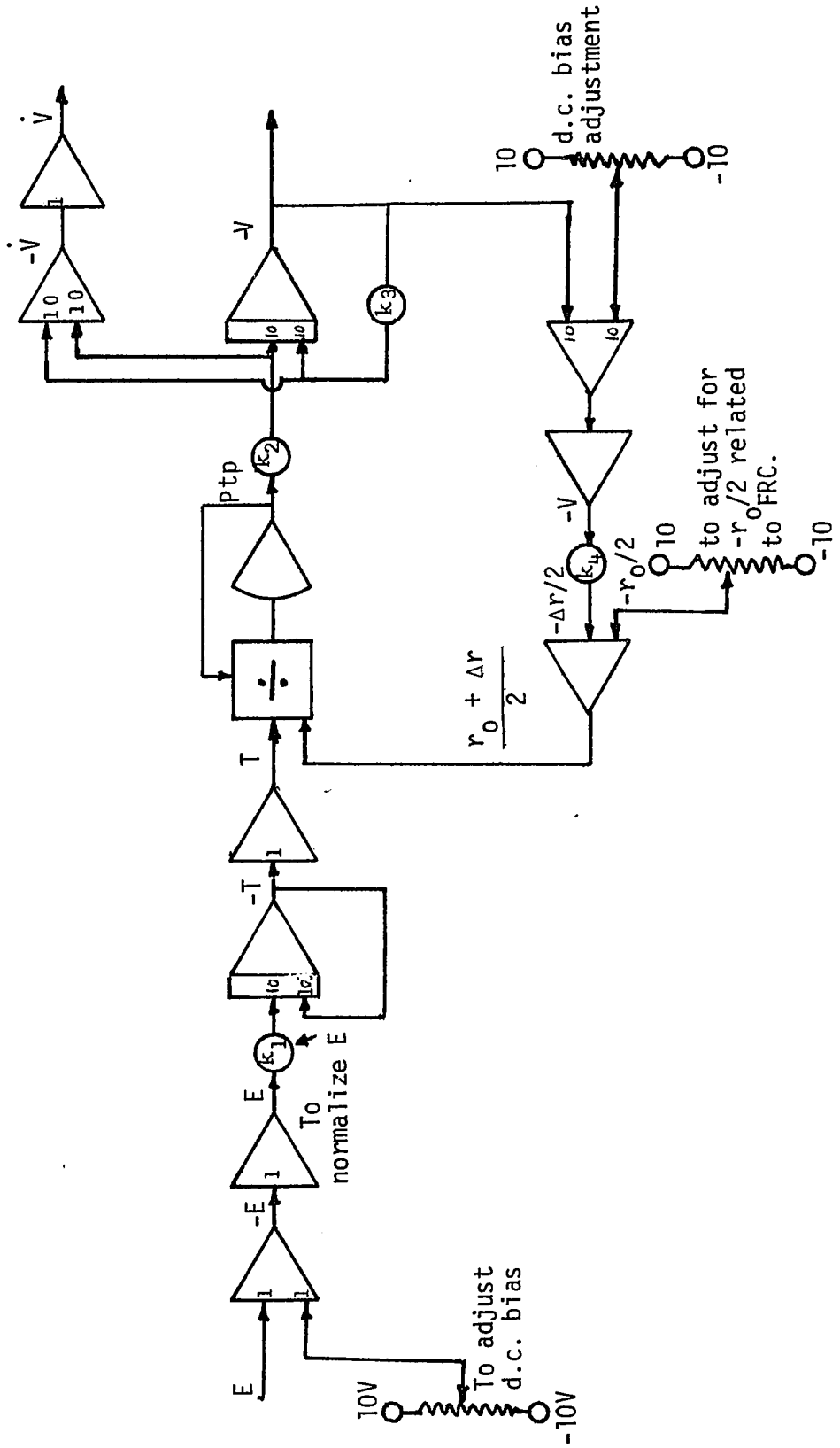


Figure 4-11 Block diagram of EAI-380 computer mechanics to simulate the subsystem model of Figure 4-10.

since all EMG recordings had arbitrary amplitude scaling. The adjustment of $k_2$ and $k_3$ depends on selection of pulmonary resistance R, pulmonary compliance C, and the time constant RC. Data on compliance in dogs is available [37] which varies according to the body size of the dog. For example, C = 0.048 l/cm $H_2O$ for 20 kg dog and about 0.0265 l/cm $H_2O$ for 11.8 kg dog. In this investigation the compliance of about 0.035 l/cm $H_2O$ was found to be a good approximation. Data on the pulmonary resistance in dogs are not available; but an approximate method to calculate RC exists based on volume and flow data [29]. This approach rests on the assumption that during passive relaxation, the applied muscular pressure (represented here as Ptp in equation (4.19) is zero. Therefore, from (4.19) itself it can be shown that $RC = \frac{V}{\dot{V}}$. Available data shows that the tidal volume, $V_t$, in dog varies between 100 to 300 ml and drops to about 70-80% of $V_t$ when the maximum $\dot{V}$, between 200 to 900 ml/sec,occurs in expiration. Thus, the range for RC may be between 1/2 to 1/5 second. Even during a single breath, the variation of R is conceivable since the constriction of airways can alter the resistance. For the present simulation RC = 1/4 second and R = 7cm $H_2O$/liter/sec. was found to be adequate.

The model was simulated with the filtered electromyogram, E, as the input which was obtained FM-tape with experimental records. Figure 4-12 shows the model response and the experimental response obtained from a dog under three different levels of $CO_2$ in the inspired air. The response of the model depends entirely on the recorded signal E. Any noise present in this signal, therefore, is

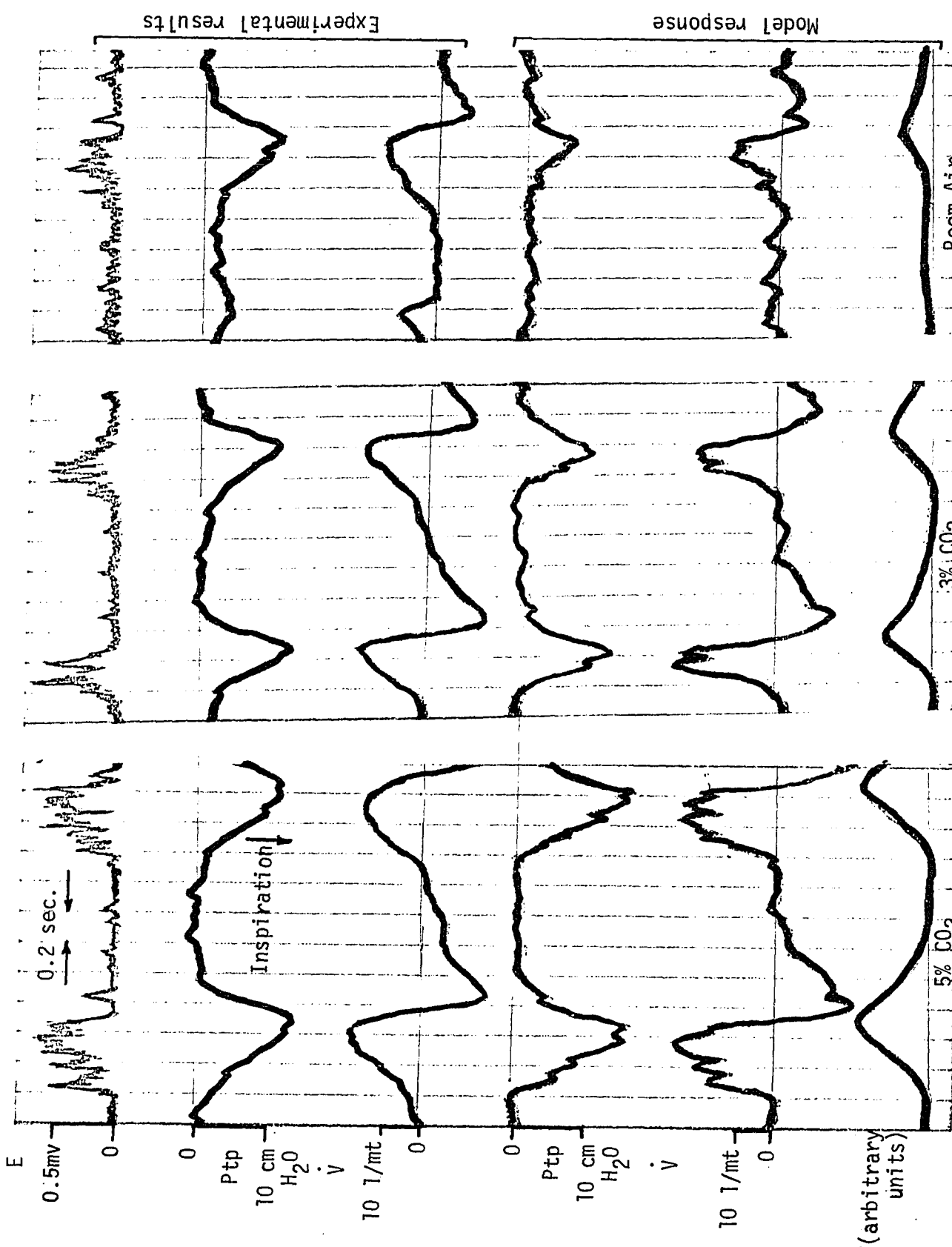


Figure 4-12 Experimental results and model response under three different levels of inspired $CO_2$. Top traces in each column represent experimental results and bottom three traces represent the corresponding model response with E as its input.

reflected in the results. Response data for electrophrenic stimulation were also compared with the simulated response. This is shown in Figure 4-13. The left column compares the responses for a modulating signal of 1.0 Hz and the right column provides similar comparison for a modulating signal of 0.5 Hz.

In conclusion, the simple model provides a reasonable simulation of the dynamics between the variables considered. Its simplicity leaves a few gaps when the phrenic nerves are stimulated by pulse frequency modulated signals. This may perhaps be explained by nonlinearities in the neuromuscular dynamics of the respiratory muscle. Some possible sources of nonlinearities are discussed later.

In addition to the simplicity of the model, it is relevant to point out that the entire investigation uses the electromyogram of the diaphragm and some variables such as transpulmonary pressure, volume and airflow - all of which are measurable in human subjects by noninvasive techniques.

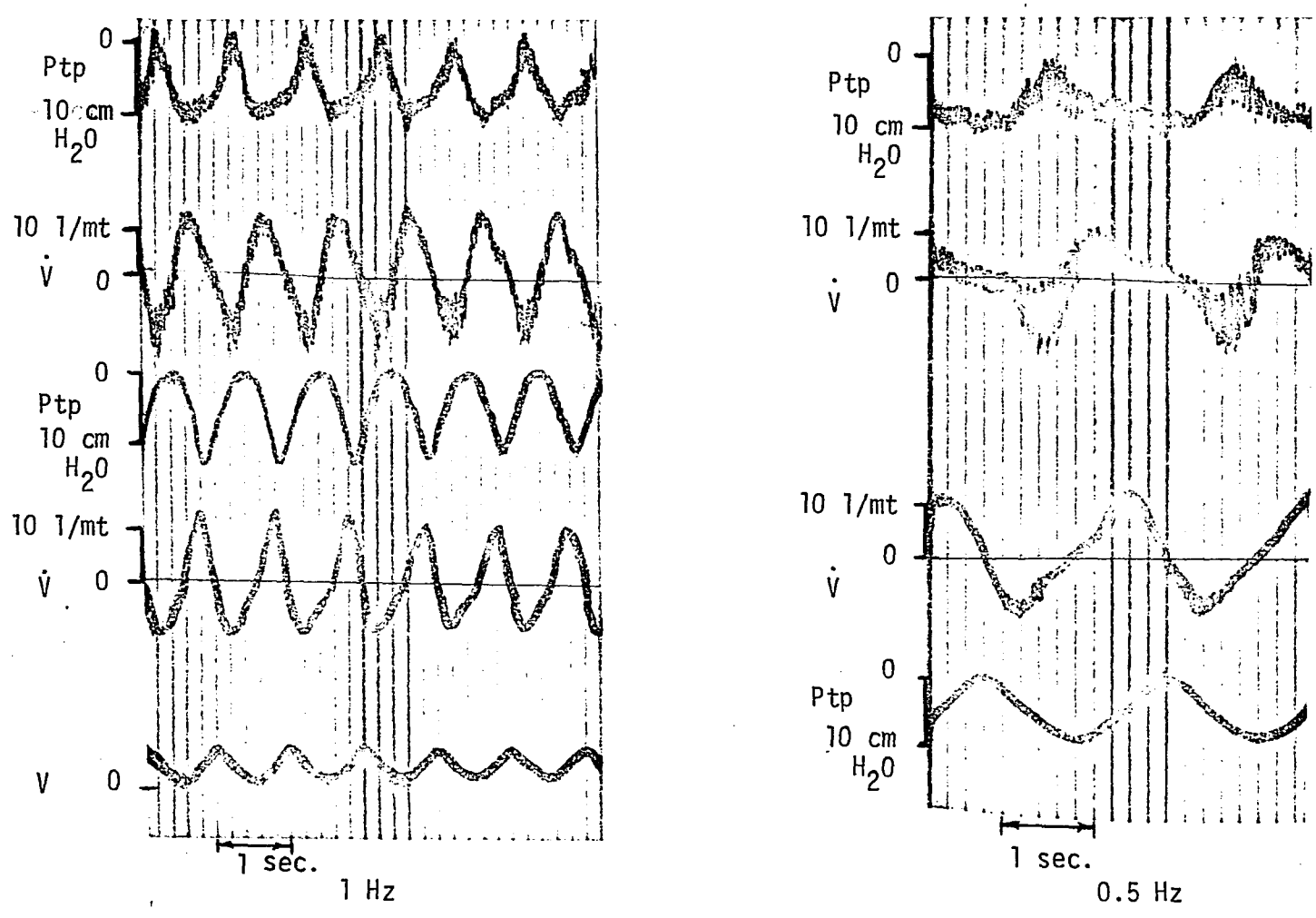


Figure 4-13 Experimental results and model response for electrophrenic stimulation. Pulse rate for stimulation was 10 < pps < 50 in both sinusoidal modulation frequencies. Top two traces, in both columns represent experimental results.

# 5. DISCUSSION

The investigation of neuromuscular command resulting in a model of the neuromuscular subsystem depends on several assumptions which include basic aspects from the physiological point of view.

The first assumption deals with the correspondence between the phrenic neurogram and the electromyogram of the diaphragm. It is recognized that there is a one-to-one correspondence between each action potential in the muscle fiber and the action potential in the axon of the phrenic nerve which acts as the input path to the muscle. This correspondence does not include the transport delay in the phrenic nerve. An additional delay factor occurs at the neuromuscular junction where the release of acetylcholine causes generation of the action potential in the muscle fiber. These two factors alone would cause a 'randomness' in the superposed action potentials due to several muscle fibers even if all of the axons of the phrenic nerve at a given location were firing synchronously with constant interspike interval. Figure 3-1 illustrates the visual dissimilarity between the phrenic neurogram and the electromyogram of the diaphragm. It is conceivable that among the factors which are also responsible for this result are the location of the electrodes in the diaphragm and the spatial distribution of the fibers. The assumption, therefore, excludes these finer details and emphasizes only the quantitative proportionality between a filtered neurogram and a filtered electromyogram as supported by experimental

observation shown in Figure 4-2. Quantitatively, this proportionality is not affected by the filtering technique. Lourenco and his associates [84], by using a simple integrator, came to the same conclusion. By using a moving average filter, the present investigation further supports this observation and provides a better insight into the relationship between the averaged EMG and the number of motor units recruited in the process [98]-[101]. The present investigation did not attempt to support the theoretical prediction that the averaged EMG is proportional to the square root of the number of motor units recruited. Irrespective of the possibility that such a relationship may not exist in the EMG of the diaphragm, the intention is simply to assume that averaged EMG and the averaged PNG will have the same waveform since the number of active motor units is the same as the number of active efferent fibers. The only situation where this may not hold is if the recorded PNG also includes afferent discharge due to proprioceptive feedback. In the present investigation such a possibility has been ignored. There is one more implicit assumption about the use of a linear filter in recording the EMG. Such a filter would have a response similar to linear summation of the polyphasic signals of all excited motor units. It is, therefore, questionable whether a similar linear summation takes place either for the pressure or for the tension due to recruitment of muscle fibers. As of now, no experimental evidence is available in this direction. Without such evidence, the linear relationship between the PNG and the EMG as well as the

treatment of these two signals as of similar waveform may be questionable. In any case, since the investigation treats the EMG as the input to the system model, the model performance is not likely to be affected. Furthermore, the assumption that the EMG represents the information of the neural command has the feature of extending the model to human subjects where the recording of the EMG - and not the PNG - can be obtained by noninvasive technique.

The second assumption is that the diaphragm is the major muscle of respiration. It is recognized that even during normal ventilation, there are two muscle forces involved. They are contributed by the ribcage muscles and the diaphragm. Figure 4-9 includes both these factors in the electrical analog of the respiratory system. The role of ribcage movement and the movement of the diaphragm has been summarized by Agostoni [121]. The actual inspiration thus includes lateral and vertical motion of the ribcage and the downward displacement of the diaphragm due to the contraction of the intercostal muscles and the diaphragm. Several techniques have been used to separate the contribution of the diaphragm and the ribcage to provide total volume change [122]-[124]. Konno and Mead [122] observed that during quiet breathing the volume displacement by abdomen is about 40% of the tidal volume in standing posture and is about 70% of the tidal in supine position. Here the volume displacement by abdomen does not necessarily indicate the contribution by the contracting diaphragm. On the basis of a geometrical ap-

proach to estimate the contribution of the diaphragm, the general agreements seems to accept the diaphragmatic contribution to be about 64% of the tidal volume and 36% provided by the movement of the ribcage [123]-[124]. It may be pointed out that these measurements are under static conditions. The implicit assumption, in the dynamic case, is that the total volume displacement is a linear summation of the volume displacement by the ribcage and the diaphragm. In the computer simulation, the response represents the entire system with the EMG of the diaphragm as the only input. If the above mentioned linearity is assumed then, adjustment of potentiometer $k_1$ and $k_2$ could produce the response due to the contracting diaphragm alone. It is known that flattening of the diaphragm also expands the lower ribcage. Jodat et al. [63] have described this as a coupling effect by assuming that this effect lasts only during the initial phase of inspiration and expiration. In the present study, this factor has not been considered to have any significant effect - especially during normal, quiet breathing.

The third assumption is related to the geometry of the diaphragm. It is assumed that the diaphragm is a segment of a hemispherical dome and the two radii of its curvature are equal. Furthermore, the cross-sectional distance between the two points, where the diaphragm touches the thoracic 'cylinder' is same [see Figure 4-7]. It is true that the lateral and dorso-ventral diameters of the ribcage are not equal [121]. The diaphragm's shape, as a segment of hemispherical dome,

is also questionable. This assumption, therefore, must be considered as an attempt to simplify mathematical complexity related to the actual geometrical shape of the diaphragm. Even if this was attempted, the lack of anatomical data would still be a major hurdle to cross. This simplified assumption, nevertheless, is not new and has been used to interpret pressure-volume dynamics due to contraction of the diaphragm [32], [33].

The fourth assumption considers the transpulmonary pressure as the mechanical response of the diaphragm. With reference to the application of Laplace's Law, to a dome-shaped diaphragm, it would seem appropriate to consider the transdiaphragmatic pressure as the output of the muscle. This can be done by placing an esophageal balloon just above the diaphragm and another one just below in the gastric region [18] or alternately by placing the second balloon not in the gastric region but just below the diaphragm in the abdomen. As shown by Agostoni and Rahn [18], the pressure on the abdominal side, Pab, is about 11cm $H_2O$ less than the gastric pressure, Po, i.e., Pab = Pg -11 cm $H_2O$. The transdiaphragmatic pressure is the pressure difference between Pab and Pes (or between Pg, with the d.c. shift of 11 cm H20 and Pes). (Some physiologists consider this pressure as becoming more positive during inspiration. In the figures of this dissertation, inspiration is shown to make the transpulmonary or transdiaphragmatic pressure more negative with reference to the atmospheric pressure). During static conditions, the difference between esophageal pressure and gastric

pressure remains constant [18], at least in normal respiration, i.e., with volume of more than 20% of vital capacity. Agostoni et al. [31] investigated the pressure difference between Pes and Pg under dynamic condition with special reference to the EMG of the diaphragm representing the input to the contracting diaphragm. Even though their results show considerable changes in the gastric pressure, the calculation of abdominal pressure shows a considerably small percent change during the inspiratory phase. Under these conditions, the measurement of esophageal pressure, just above the diaphragm, seems to be a fairly accurate measure of the transdiaphragmatic pressure. The tension T, generated by neural command (or by electrophrenic stimulation), is dominant over the elastic tension. Its dynamics are represented by the first-order relation $0.1\ \dot{T} + T = KE$ (illustrated by the element $\frac{k}{1 + 0.1\ p}$ in Figure 4-10).

Based on justification of the measurement of esophageal pressure as the neuromuscular response of the respiratory system, the model was completed by inclusion of the dynamics of the pulmonary pump whose input is the transpulmonary pressure and whose outputs are volume and flow. Its parameters are the pulmonary compliance and the pulmonary resistance. Here the compliance refers to elastic recoil of the lungs and the resistance includes airway and tissue resistances (due to motion of lung tissues). The intertial element is negligible and airflow is assumed to be laminar.

The first important aspect of the proposed model is the input-output relationship among the variables involved in the contracting diaphragm. Ideally, the dynamics of the skeletal muscle should include a functional relationship between the active state as the force generator and the resulting length, tension and velocity of contraction as the output of the muscle. Active state, as a force generator, is nonmeasurable. However, the electromyogram as a factor producing the active state is measurable and can be considered to represent the active state. Again, since tension and length or area changes in the contracting diaphragm were not measured, the functional relationship between EMG and tension has been demonstrated on the basis of the measurability of the transpulmonary pressure and its relation to tension and radius of curvature of the diaphragm. This relationship is described by a simple first order linear model and its validity has been tested by simulation. Inspite of the fact that a skeletal muscle is a nonlinear electromechanical transducer [113], a simplified linear model, at least around the operating point, may be justified [82], [114]-[117]. The significant observation in this dissertation is that such a model can be a first-order transfer function. This is supported by the square-wave response study in this investigation as well as by step response studies by Sant'Ambrogio and Saibene [27] and by Mognoni et al. [30]. These investigations reveal an almost exponential rise of pressure under square-wave stimulation with a half time of the response of around 60 msec. A trial and error adjustment of the

time constant to 100 msec. presents good simulation results under natural breathing. Natural breathing implies a ramp-like filtered EMG signal ,E ,during excitation and during sudden cessation at the onset of relaxation.

Sinusoidal response was used to test the linearity by a simple technique. It is here that the limitations of the linear model become visible. Partridge, while investigating the response of tricep surae in cat to sinusoidally modulated pulse trains as stimulus, concluded that the muscle, under isometric conditions [125], and under isotonic conditions with or without inertial load [118], [126], [127], represents an almost linear system. The investigations by Partridge explore two possible sources of nonlinearity. One may be represented in terms of the difference of response to increasing and to decreasing pulse rate in the stimulus. This should give rise to a hysterisis type of response in which the response is almost linear during increasing pulse rate but during decreasing pulse rate the response is quicker after an initial time delay. Under natural breathing, the pulse rate rises to a peak, but drops suddenly at the onset of expiration. It is, therefore, suitably represented by the linear model under natural breathing. The second source is described by Partridge as an intrinsic feedback in the muscle for inertial compensation. In the present investigation, the inertial load of the diaphragm is constant and was left unexplored.

It may be pointed out that in the present investigation, a sinusoidally modulated pulse train was used for supramaximal and synchronous stimulation of all fibers of the phrenic nerve. Both the sinusoidal modulation and the synchronous stimulation thus create an input which is different from the actual input under natural breathing. If the tension of the muscle is the output of the electro-mechanical transducer, it is conceivable that the response of the parallel recruited motor units receiving asynchronous stimulus pulse trains may be different from its response under synchronous and supramaximal stimulation. Unless this phenomenon is investigated by use of physiological evidence, the nature of the nonlinearity in the muscle model cannot be defined explicitly.

One simple approach to include nonlinearity, under natural conditions, is to modify the time constant of the model to exhibit fast recovery during relaxation. Such a possibility was discussed. Ideally, the time-constant should depend on the sign of the rate of the filtered EMG or on that of the tension T. Due to presence of noise in the EMG and its filtered version, such an input to the rate sensitive control has its limitation. The choice of pressure or flow variable as the alternate input also presents a problem due to phase difference between these variables and the EMG.

The second significant feature of this investigation is the nonlinear relationship between the transpulmonary pressure and the tension of the diaphragm. The inclusion of this nonlinearity was

necessary for two reasons. First, the tension was not measured in the present investigation. Therefore, an alternate variable, namely the transpulmonary pressure, was selected to represent the mechanical response of the diaphragm. Second, the functional relationship between the transpulmonary pressure and the tension depends on the radius of curvature of the diaphragm which was assumed to be a segment of the hemispherical dome. By assuming the cross-sectional diameter of such a segment to be constant, the increase in radius of curvature of the contracting diaphragm also exhibits the reduction of the area of the diaphragm.

The inclusion of first-order system representing the pressure-flow-volume dynamics completes the neuromuscular subsection of the respiratory controller. The model (Figure 4-10) includes only the diaphragm as the major muscle. If the activity of the intercostal muscles is also to be included, then one may incorporate a linear summation of pressure changes due these two muscle units.

It is hoped this simple model shall be useful for clinical diagnosis. This possibility exists because of the use of measurable variables which are possible in human subjects by noninvasive techniques. Diagnostic applications are possible even with the chemostat models where emphasis has been placed on modeling of the controlled system. Diagnosis of respiratory abnormalities related to the controlled system, e.g., the factors affecting the function of the lungs as liquid-gas interface, blood transport delays,

changes in the metabolic production of $CO_2$ or consumption of $O_2$ etc. may be possible. Inclusion of the dynamics of the controlled system, as proposed in the present investigation, extend the region where location of the abnormalities could be explored by investigating the response of the respiratory center to known chemical inputs and by examining the mechanical response of the respiratory controller when the output of the respiratory center is known. Without an understanding of these dynamics, the ventilation as a response to $CO_2$ inhalation fails to provide any information about the abnormality of the controlling system. Since the controlling system includes the respiratory center as the source of neuromuscular command as well as the muscles and other mechanical variables, the investigation of their performance was undertaken in this work.

There are at least two significant sources of abnormalities which could be explored by using this model. One represents the failure of the respiratory center to provide sufficient normal neuromuscular command and the other represents normal neuromuscular command going to myopathic muscle structures and/or the failure in the respiratory mechanics such as those found in patients with chronic obstructive lung disease [128], [129]. With the help of the model and measurable variables like EMG, transpulmonary pressure, volume and flow, the problem of diagnosis might be reduced to that of parameter identification.

The model presented in this dissertation is rather simple. The assumptions on which it is based may point out its limitations. Other possible areas related to the neuromuscular dynamics in respiration in which future investigation may be of interest are:

(1) Simulation of the phrenic neurogram and the electromyogram by superposition of waveforms in parallel signal channels. While such an investigation has been done to describe the EMG of a skeletal muscle as a noisy signal pattern [98]-[101], there are several parameters which place the PNG and the EMG in respiration in a different category, especially when these signals are compared to the EMG in skeletal muscles under sustained isometric contraction. The principal parameters are the temporal variation both in the recruitment of fibers and in the pulse rate during a single burst, the possibility of change from asynchronous discharge to synchronous discharge and the basic periodicity of such a discharge as a continuous command signal.

(2) Establishment of the cause of nonlinearity in the model of the diaphragm as a striated muscle. While such a nonlinear model has been described, for a skeletal muscle, by Bayler [113], the mechanics of contraction and the structural relationship between the contractile or viscoelastic components in the diaphragm, may need special attention due to the geometric shape of such a muscle. Furthermore, the measurement of significant parameters like tension, area of the muscle, and the rate of change of area of the contracting diaphragm may be difficult.

(3) Inclusion of intercostal muscles as a factor contributing to the transpulmonary pressure as well as to the mechanics of the lungs, is relevant. This may be more significant in abnormal or forced breathing where the diaphragm ceases to be the major muscle responsible for respiration. Finally,

(4) In order to complete the investigation of the internal dynamics of the respiratory controller, the output of the respiratory center should be studied with feedback due to known chemical and mechanical factors and the basic 'rhythmicity' of the respiratory center.

# 6. APPENDICES

## Appendix A: Experimental Procedures

The experiments were performed on 26 mongrel dogs weighing 10 - 18 kilograms. Each dog was lightly anasthetized by intravenous injection of pentobarbital (nembutal) 0.6 cc/kg body weight. The femoral vein, selected for the introduction of the anasthetic agent was cannulated with a stop valve for further infusion of the drug if necessary. The femoral artery was also cannulated and the cannula was filled with anticoagulant (Heperin) and attached to Statham P23 Transducer for blood pressure records.

Each dog was placed in supine position on the surgical table and intubated with tracheal tube, to the outside end of which a small phneumotechograph (Electronics for Medicine) with Statham differential transducer PM5-0.2-350 was connected. This enabled the air flow, and volume records on the Electronics for Medicine, multichannel data recording system. For airflow Model SGA and for volume records the output of the Model SGA was fed to the integrator (Model IRD) channel of the Electronics for Medicine multichannel recorder. For the measurement of pressure a latex rubber balloon (5 c.c. long, 3.5c.c. circumference) was inserted in the esophagous into the lower 1/3rd of the thorax. Before insertion, the amount of air necessary to maintain the pressure inside the balloon at the atmospheric pressure, is first tested by filling the balloon with air from a syringe and measuring the pressure by using Statham.

differential pressure transducer (PM 131 TC + 2.5 - 350). The syringe is used to empty the balloon before insertion and to refill the balloon after insertion by the volume of air necessary for atmospheric pressure. In most experiments, the needle inserted at the tracheal tube, outside the mouth, provides the reference input to the differential pressure transducer thus yielding transpulmonary pressure. In some experiments, where transdiaphragmatic pressure was recorded, another balloon is inserted in the esophagous into the gastric region and attached to reference input end of the transducer. In either case, resting pressure level was used as zero line and downward shift of the pressure level, representing negative pressure, was selected for the inspiratory phase. Model SGM (Electronics for Medicine) channel was used for pressure recording.

The pressure transducer was calibrated by a water manometer and the pnemotechograph flow transducer was calibrated either with a rotometer or by a spirometer (with different weights on floating bell to produce different flow rates).

The abdomen was opened by about 10 cms incision of the midline just below the sternum. The electrodes were either of teflon coated stainless steel or insulated copper wire, both with exposed tips. Two electrodes were inserted and sewn about 0.5 cm apart along the radial line in the right lumbar region of the diaphragm. The abdominal incision was then closed by stitching. The two electrodes passing through the stitched area, and a third electrode attached to the

leg, provided the input to the amplifier channel. (Model EID, Electronics for Medicine). This amplifier's bandwidth was adjusted in the 40-2000 Hz range. The output of the amplifier was displayed on the oscilloscope for visual observation while adjusting the amplifier gain and the modified Paynter filter was used for envelope detection of the EMG after full-wave rectification.

By a surgical procedure the right phrenic nerve was exposed in the lower part of cervical region. The nerve itself is identified by stimulating it (single or multiple pulse output of Grass Stimulator) and by observing the mechanical response of the diaphragm. Once identified, the phrenic nerve, surrounded by a pool of mineral oil, rested on the semicircular tips of two platinum wire electrodes (approximately 0.5 cm apart). Similar pair of electrodes could be placed distally from the first pair. In such a situation the proximal pair was used for electrophrenic stimulation and the distal pair for detecting phrenic neurogram. The neurogram itself was amplified by the balanced amplifier model EEP (Electronics for Medicine, adjusted bandwidth 40-2000 Hz).

The entire experimental setup is shown in Figure 6-1. All measurable variables are inputs to the multi-channel amplifier and recorder system (Electronics for Medicine, Model DR-12). The channel outputs could be displayed on the oscilloscope or recorded on photographic paper tape or could be recorded on a Hewlett-

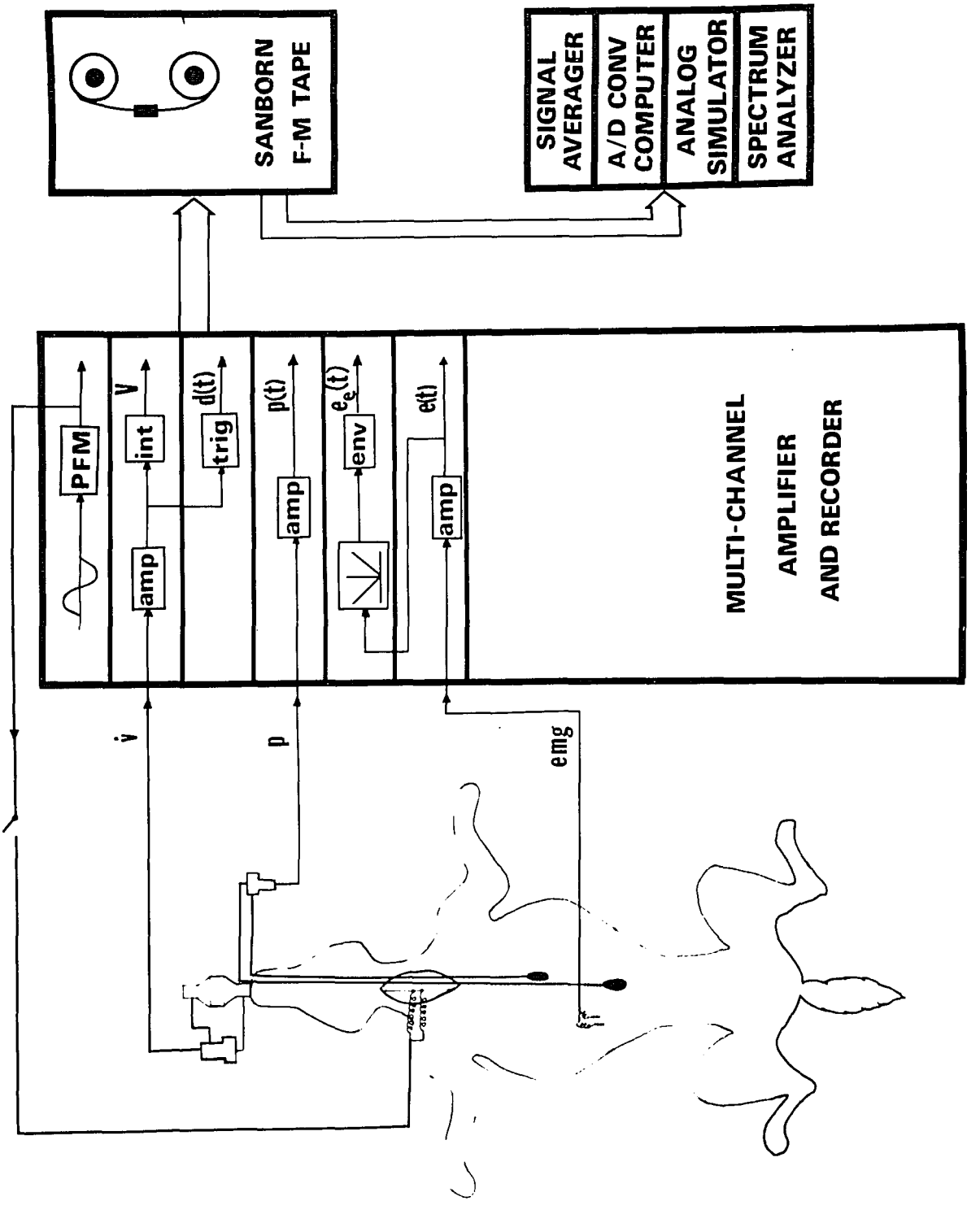


Figure 6-1 Experimental data recording and analysis system.

Packard Sanborn 8-channel FM-tape recorder. For the FM-tape recording the interface between the Model DR-12 and the tape recorder is provided by a matching amplifier Model UMA (Electronics for Medicine).

Data collection and selection was done by replay of the magnetic tape. The use of digital computer (as shown in Figure 6-1) was not attempted since the A/D Converter was not available.

The experimental procedures and results can be summarized as follows:

(a) Experiments were done on 15 dogs with spontaneous breathing under various steady state $CO_2$ response (room air, 2.95% $CO_2$, 4.38% $CO_2$, 6.73% $CO_2$ and in one case 7.13% $CO_2$). Variables recorded were Ep, E, $\dot{V}$, V and Ptd. The basic purpose was to confirm the one-to-one correspondence between the phrenic neurogram and the electromyogram as well as to support the linear relationship between the pressure and the flow (or volume) variables. Except that the neurogram and the electromyogram were filtered, the results are not different from those reported by Lourenço et al. [84] and as summarized by Agostoni et al. [30], [120].

(b) Experiments on 7 dogs were related to the respiratory response to square-wave modulated pulse trains as the stimulus to the right phrenic nerve. Pulse rates were 20, 40 and 80 pps with 1-2 msec. pulse width. In each case the amplitude was increased from 0.1 volt to 1.0 volt. Results were intended to confirm the process

of recruitment until supramaximal stimulation is achieved (with fixed pulse rate but increasing amplitude) and to demonstrate saturation, due to tetanous (with fixed amplitude but increasing pulse rate). It was also possible to suggest a linear first order model to represent E-P relationship by the study of step response. Similar results have been reported, though the use of filtered EMG due to electrophrenic stimulation is not included in those reports [30], [32], [33].

(c) On 7 dogs, response to supramaximal right phrenic stimulation (and in one case bilateral stimulation) by sinusoidally modulated pulse trains was studied. The range of pulse frequency, during one cycle, was from 10 - 50 pps. The modulating frequency was 0.05, 0.1, 0.25, 0.5, 1.0, 2.0, 4.0 and 6.0 Hz. During this range, there was no substantial alteration in the p-p amplitude of E, $\dot{V}$ and Ptp.

(d) Recorded EMG in 8 dogs were used to select sections of the magnetic tape from which closed tape loops were prepared and used for spectrum analysis as described in Appendix B.

Appendix B: Spectral Analysis of the EMG

The replay of tape loop (from a selected section containing the EMG) provided the periodic EMG whose period depends on the length of the loop and the tape speed. These were selected in order to keep the period of the EMG wave within the range of the dogs' breathing period. Spectral analysis was done on Tekronix 3L5 plugged into

Type 564 dual trace autoerase storage oscilloscope with Type 3B3 time base unit. The analyser displays amplitudes of the spectral range from 10 Hz to 1M Hz with a 10 Hz resolution.

The general schematic of the spectral analysis is shown in Figure 6-2. This figure also shows a system which was devised to examine the contribution of any narrow section of the periodic EMG wave. This needs a pre-recorded narrow pulse coinciding with the onset of electrical activity in the tape loop. This narrow pulse, during replay of the loop, triggers a waveform generator to produce a rectangular pulse, the position and width of which are adjustable. Figure 6-2(a), for example, shows that the rectangular pulse is coinciding with the time interval $t_2$ to $t_3$ (corresponding to the entire duration of the EMG.) The rectangular pulse operates an on-off relay which can control the output of a pulse generator. This pulse generator then provides the input to z-axis modulation of the oscilloscope beam. It is possible to intensify the beam only for the duration of the rectangular pulse and to keep it dark otherwise.

Figure 6-2(b) shows the spectral display of the entire period of the EMG which also includes the contribution due to noise and the cardiac spikes.

Figure 6-3(a) shows that annoying contribution by the cardiac spikes could be reduced by improving the EMG/EKG ratio. The exact contribution by the cardiac spike is displaced in Figure 6-3(b) by

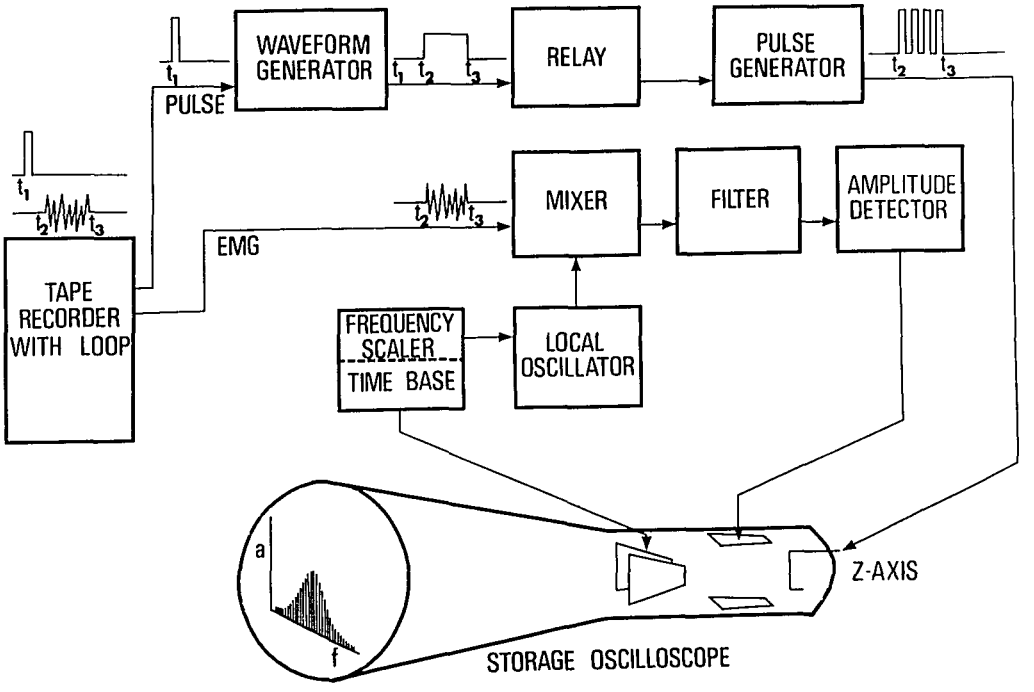


(a)

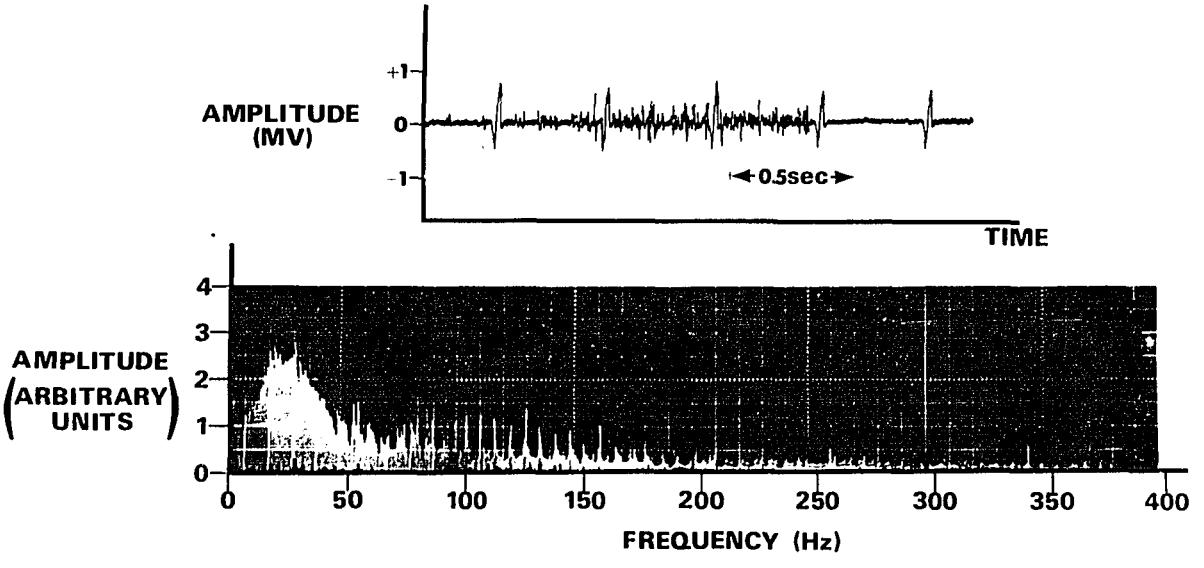


(b)

Figure 6-2 Experimental setup for spectral analysis of the EMG. Top trace (a) shows the procedure for z-axis intensification during the time interval ($t_2$-$t_3$) for spectral display and (b) shows typical spectrum of the EMG if the time interval $t_2$-$t_3$ covers the entire inspiratory phase.

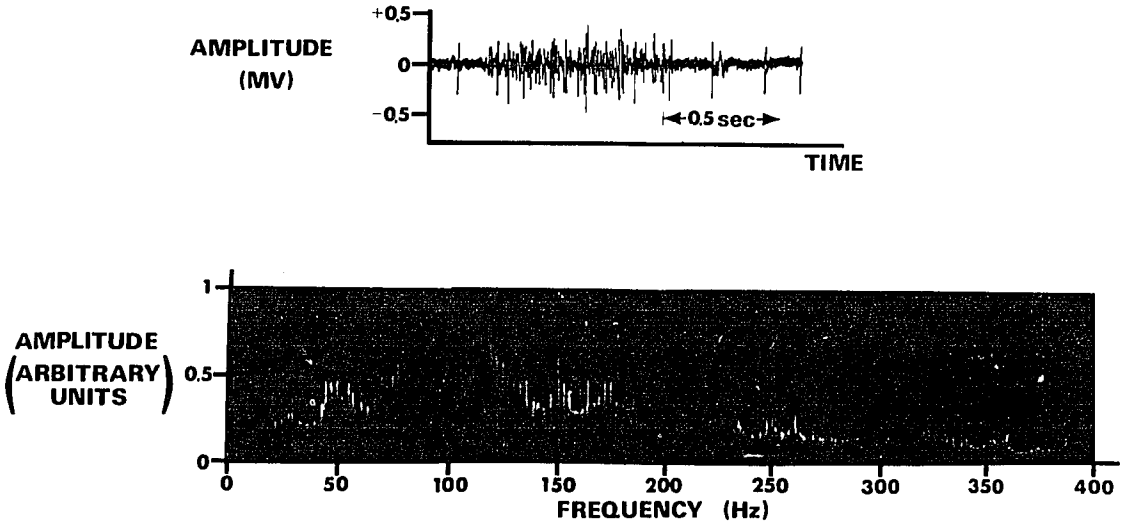


(a) Spectrum of the EMG with improved EMG/EKG ratio.

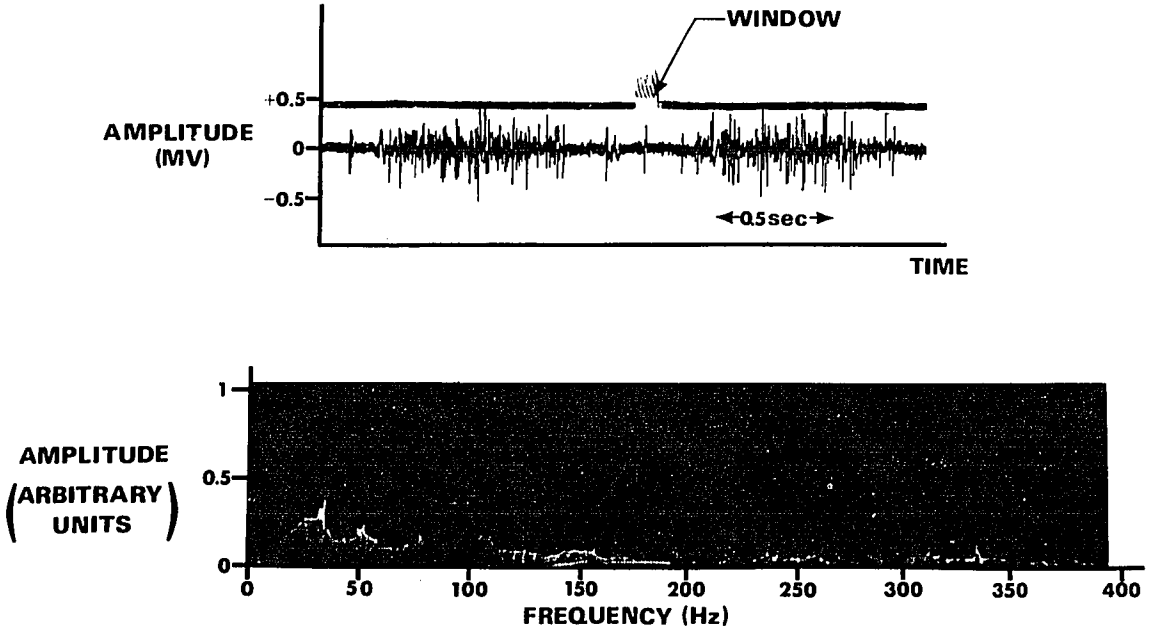


(b) Spectrum of cardiac activity recorded in the diaphragm.

Figure 6-3 Spectral displays showing the contribution of the cardiac activity in the spectrum of the EMG. Top section (a) shows spectrum of EMG with improved EMG/EKG ratio. In bottom trace (b), due to the location of the window , the display represents the spectrum of the EKG spike in the EMG.

placing the z-axis intensification window over a selected cardiac spike. The presence of cardiac spike clearly affects the amplitude of low frequency section of the spectrum of the EMG.

The significance of the z-axis intensification technique in the elimination of cardiac spike, during the spectral analysis of the EMG is illustrated in Figure 6-4. The upper part (A) in Figure 6-4 shows the spectrum of the activity mixed with noise and the portion of activity analyzed is shown by the position of the window. The lower section (B) shows the spectrum if the window is moved over the portion without the EMG and where the only signal present is noise. By comparing these two results, it is possible to conclude that the presence of noise does not alter the amplitudes of the spectral lines of the EMG significantly.

An analytical approach to interpret the spectrum of the pulse frequency modulated signals (sinusoidally modulated) was published by Bayly [107]. To interpret the spectrum of the EMG as obtained in respiratory muscles, entails ramp-like modulating signal and recruitment, as a function of time. This was not attempted in the present investigation.

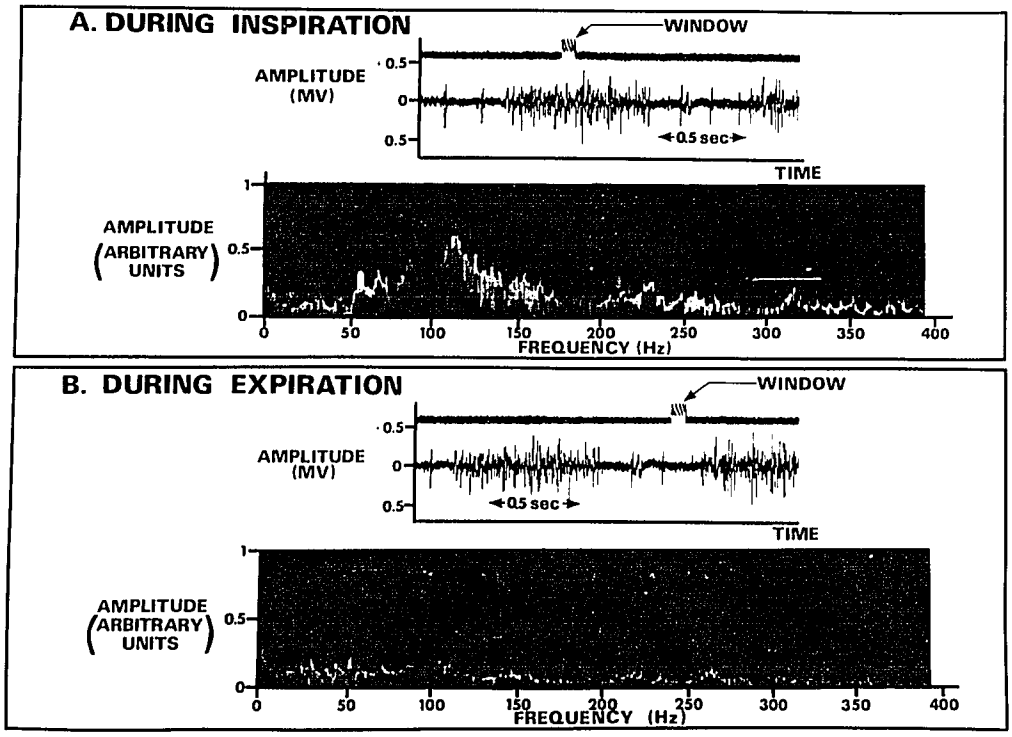


Figure 6-4 Spectrum of the electrical activity of the diaphragm at selected time intervals. Top trace (A) exhibits the spectrum of the EMG during inspiratory phase. Bottom trace (B) shows the spectrum of the 'noisy' section of the activity during expiratory phase.

## 7. REFERENCES


[1] Haldane, J.S., and J.G. Priestley. Respiration, Oxford University Press, pp. 16-42 and pp. 193-194, 1935.

[2] Gray, J.S. The Multiple Factor Theory of Control of Respiratory Ventilation, Science, 103, pp. 739-744, 1946.

[3] Grodins, F.S., J.S. Gray, K.R. Schroeder, A.L. Norins and R.W. Jones. Respiratory Response to $CO_2$ Inhalation. A Theoretical Study of a Nonlinear Biological Regulator, J. Appl. Physiol., 7, pp. 283-308, 1954.

[4] Salmoiraghi, G.C., and B.D. Burns. Notes on Mechanism of Rhythmic Respiration, J. Neurophysiol., 23, pp. 14-26, 1960.

[5] Salmoiraghi, G.C., and R. von Baumgarten. Intracellular Potentials from Respiratory Neurons in Brain-Stem of Cat and Mechanism of Rhythmic Respiration, J. Neurophysiol., 24, pp. 203-218, 1961.

[6] Adrian, E.D., and D.W. Bronk. The Discharge of Impulses in Motor Nerve Fibers, Part I, J. Physiol., 66, pp. 81-101, 1928.

[7] Gesell, R., C.S. Magee, and J.W. Bricker. Activity Patterns of the Respiratory Neurons and Muscles, A.J. Physiol., 128, pp. 615-628, 1940.

[8] Larrabee, M.G., and G.C. Knowlton. Excitation and Inhibition of Phrenic Motoneurons by Inflation of the Lungs, A.J. Physiol., 147, pp. 90-99, 1946.

[9] Gill, P.K., and M. Kuno. Properties of Phrenic Motoneurons, J. Physiol., 168, pp. 258-273, 1963.

[10] Gill, P.K., and M. Kuno, Excitatory and Inhibitory Actions on Phrenic Motoneurons, J. Physiol., 168, pp. 274-289, 1963.

[11] Garcia, A., and N.S. Cherniack. Integrated Phrenic Activity in Hypercapnia and Hypoxia, Anasthesiol., 28, pp. 1029-1035, 1967.

[12] Cohen, M.I. Discharge Pattern of Brain-Stem Respiratory Neurons in Relatin to Carbon Dioxide Tension, J. Neurophysiol., 31, pp. 142-165, 1968.

[13] Szidon, J.S., N.S. Cherniack, and A.P. Fishman. Traube-Hering Waves in the Pulmonary Circulation of the Dog, Science, 164, pp. 75-76, 1969.

[14] Cohen, M.I. Discharge Pattern of Brain-Stem Respiratory Neurons During Hering-Breuer Reflex Evoked by Lung Inflation, J. Neurophysiol., Vol. XXXII, pp. 356-374, 1969.

[15] Cohen, M.I. and P.M. Gootman. Spontaneous and Evoked Oscillations in Respiratory and Sympathetic Discharge, Brain Research, 16, pp. 265-268, 1969.

[16] Cohen, M.I. and P.M. Gootman. Periodicities in the Efferent Discharge on the Splanchnic Nerve of the Cat, Partially in Ph.D. Thesis, P.M. Gootman, Albert Einstein Coll. of Med., 1970.

[17] Bigland, B., and O.C.G. Lippold. The Relation Between Force, Velocity and Integrated Electrical Activity in Human Muscles, J. Physiol., 123, pp. 214-224, 1954.

[18] Agostoni, E., and H. Rahn. Abdominal and Thoracic Pressure at Different Lung Volumes, J. Appl. Physiol., 15, pp. 1087-1092, 1960.

[19] Read, David. Transient $CO_2$ Response, Personal Communication, Feb.-Mar., 1969.

[20] Bachofen, H. Lung Tissue Resistance and Pulmonary Hysterisis, J. Appl. Physiol., 24 (3), 1968.

[21] Saibene, F., and J. Mead. Frequency Dependence of Pulmonary Quasi-Static Hysterisis, J. Appl. Physiol., 26 (6), 1969.

[22] Miranda, J.M. and R.V. Lourenço. Influence of Diaphragm Activity on the Measurement of Total Chest Compliance, J. Appl. Physiol., 24, pp. 741-746, 1968.

[23] Turino, G.M., R.V. Lourenço, and G.H. McCraken. Role of Connective Tissue in Large Pulmonary Airways, J. Appl. Physiol., 25, pp. 645-653, 1968.

[24] Marin, M.G., and P.E. Morrow. Effect of Changing Inspired $O_2$ and $CO_2$ Levels on Tracheal Mucociliary Transport Rate, J. Appl. Physiol., 27, pp. 385-388, 1969.

[25] Wright, D.L., and R.R. Sonnenschein. Muscle Force and Electromyogram with Alterations in Flow and Composition of Blood, A. J. Physiol., 216, pp. 1075-1080, 1969.

[26] Murphy, T.W. Modeling of Lung Gas Exchange - Mathematical Model of the Lung: The Bohr Model, Static and Dynamic Approaches, Math. Biosciences, 5, pp. 427-447, 1969.

[27] Sant' Ambrogio, G., and F. Saibene. Contractile Properties of the Diaphragm in Some Mammals, Resp. Physiol., 10, pp. 349-357, 1970.

[28] Remmers, J.E. Inhibition of Inspiratory Activity by Intercostal Muscle Afferents, Resp. Physiol., 10, pp. 358-383, 1970.

[29] McIllroy, M.B., D.F. Tierney, and J.A. Nadel. A Method for the Measurement of Compliance and Resistance for Lungs and Thorax, J. Appl. Physiol., 18, pp. 424-427, 1963.

[30] Mognoni, P., F. Saibene, G. Sant' Ambrogio, and E. Agostoni. Dynamics of the Maximal Contraction of Respiratory Muscles, Resp. Physiol., 4, pp. 193-202, 1968.

[31] Agostoni, E., G. Sant' Ambrogio, and H. del Portillo Carrasco. Electromyography of the Diaphragm in Man and Transdiaphragmatic Pressure, J. Appl. Physiol., 15, pp. 1093-1097, 1960.

[32] Marshall, R. Relationship Between Stimulus and Work of Breathing at Different Lung Volumes, J. Appl. Physiol., 17, pp. 917-921, 1962.

[33] Pengelly, L.D., A.M. Alderson, and J. Milic-Emili. Mechanics of the Diaphragm, J. Appl. Physiol., 30, pp. 797-805, 1971.

[34] Burns, B.D., and G.C. Salmoiraghi. Repetitive Firing of Respiratory Neurons During Their Burst Activity, J. Neurophysiol., 23, pp. 27-46, 1960.

[35] Abbrecht, P.H. Notes on Chapter on Respiration in Physiological Systems for Engineers, University of Michigan, Ann Arbor, 1969.

[36] Hildebrandt, J., and A.C. Young. Anatomy and Physics of Respiration, Chap. 39, Physiology and Biophysics, edited by Ruch and Patton, W.B. Saunders Co., Philadelphia, p. 748, 1966.

[37] Mead, Jere and J. Milic-Emili. Theory and Methodology in Respiratory Mechanics, Chap. 11, Handbook of Physiology, Sect. 3, Respiration, Vol. 1, Am. Physiological Society, Washington, D.C. 1964.

[38] Gray, J.S. Pulmonary Ventilation and Its Physiological Regulation, Charles C. Thomas, Springfield, Illinois, 1950.

[39] Defares, J.G., H.E. Derksen and J. W. Duyff. Cerebral Blood Flow in the Regulation of Respiration, Acta. Physiol. Pharmacol. Neerlandica., 9, pp. 327-360, 1960.

[40] Yamamoto, W.S. Mathematical Analysis of the Time Course of Alveolar $CO_2$, J. Appl. Physiol., 15(2), pp. 215-219, 1960.

[41] Grodins, F.S., and G. James. Mathematical Models of Respiratory Regulation, Ann. N.Y. Acad. Sci., 109, pp. 852-865, 1963.

[42] Milhorn, Jr., H.T., R. Benton, R. Ross and A.C. Guyton. A Mathematical Model of Respiratory Control System, Biophysical J., 5, pp. 27-46, 1965.

[43] Horgan, J.D., and R.L. Lange. Analog Computer Studies of Periodic Breathing, IRE Trans. BME-9(4), pp. 221-227, 1962.

[44] Horgan, J.D., and R.L. Lange. Digital Computer Simulation of Human Respiratory System, IEEE Internat'l Conv. Rec., part 9, pp. 149-157, 1963.

[45] Horgan, J.D., and R.L. Lange. Digital Computer Simulation of Respiratory Response to Cerebrospinal Fluid $PCO_2$ in the Cat, Biophysical J., 5, pp. 935-945, 1965.

[46] Milhorn Jr., H.T., and A.C. Guyton. An Analog Computer Analysis of Cheyne-Stokes Breathing, J. Appl. Physiol., 29, pp. 328-333, 1965.

[47] Longobardo, G.S., N.S. Cherniack, and A.P. Fishman. Cheyne-Stokes Breathing Produced by a Model of the Human Respiratory System, J. Appl. Physiol., 21(6), pp. 1839-1846, 1966.

[48] Cherniack, N.S. and G.S. Longabardo, O.R. Levine, R. Mellins, and A.P. Fishman. Periodic Breathing in Dogs, J. Appl. Physiol., 21(6), pp. 1847-1854, 1966.

[49] Cherniack, N.S., G.S. Longobardo, I. Staw, and M. Heymann. Dynamics of Carbon Dioxide Stores Changes Following an Alteration in Ventilation, J. Appl. Physiol., 21(3), pp. 785-793, 1966.

[50] Cherniack, N.S., and G.S. Longabardo, F.P. Palermo, and M. Heymann. Dynamics of Oxygen Stores Changes Following an Alteration in Ventilation, J. Appl. Physiol., 24, p. 809, 1968.

[51] Edwards, Jr., M.W., and W.S. Yamamoto. Carbon Dioxide Balance and the Control of Breathing, Physiological Control and Regulation, pp. 158-186, W.B. Saunders Co., Philadelphia, 1965.

[52] Yamamoto, W.S., and W.F. Raub. Models of External Respiration in Mammals, Problems and Promises, Computers & Biomed. Res., 1, pp. 65-104, 1967.

[53] Horgan, J.D., and R.L. Lange. Chemical Control in the Respiratory System, IEEE Trans. BME-15(2), pp. 119-127, 1968.

[54] Grodins, F.S., J. Buell, and A.J. Bart. Mathematical Analysis and Digital Simulation of the Respiratory Control System, J. Appl. Physiol., 22(2), pp. 260-276, 1967.

[55] Goodman, L. Oscillatory Behaviour of Ventilation in Resting Man, IEEE Trans. BME-11(3), pp. 82-93, 1964.

[56] Goodman, L., D.M. Alexander, and D.G. Fleming. Oscillatory Behaviour of Respiratory Gas Exchange in Resting Man, IEEE Trans. BME-13(2), pp. 57-64, 1966.

[57] Rubio, J.E. A Mathematical Model of the Respiratory Center, Bull. Math. Biophys., 29, pp. 719-736, 1967.

[58] Merrill, E.G. Observations on the Activity of the Respiratory Neurones in Cats, Ph.D. Thesis, Mass. Inst. Tech., 1968, Abstract of Dissertation in IEEE-Trans. BME-16, 1969.

[59] Aizerman, M.A., and E.A. Andrejeva. On Some Control Mechanism of Skeletal Muscles, Institute of Automation & Telemechanics, Moscow, 1968.

[60] Zakharova, L.M., and A.I. Litvintsev. Search Activity of Muscle Closed by Artificial Feedback Loop, Automat. Remote Control, 27(11), pp. 1942-1950, 1966.

[61] Tenenbaum, L.A. Laws of Search and Control in Respiration, Automat. Remote Control, 27(11), pp. 1951-1959, 1966.

[62] Tenenbaum, L.A. On Control Process of External Respiratory Parameters, Automatica, Pergamon Press, Vol. 7, pp. 407-416, 1971.

[63] Jodat, R.W., J.D. Horgan, and R.L. Lange. Simulation of Respiratory Mechanics, Biophys. J., 6, pp. 773-785, 1966.

[64] Wald, A.A., T.W. Murphy, and V.D.B. Mazzia. A Theoretical Study of Controlled Ventilation, IEEE Trans. BME-15(4), pp. 237-248, 1968.

[65] Jain, V.K., and S.K. Guha. A Control System for Long-Term Ventilation of the Lungs, IEEE Trans. BME-19, (1), pp. 47-52, 1972.

[66] Stoll, P.J. Respiratory System Analysis Based on Sinusoidal Variations of $CO_2$ in Inspired Air, J. Appl. Physiol., 27(3), pp. 389-399, 1969.

[67] Stoll, P.J., and J.S. Meditch. Least Square Estimation of Respiratory System Parameters, Math. Biosciences, 8, pp. 307-321, 1970.

[68] Feinberg, B.N., E.H. Chester, and J.B. Schoffler. Parameter Estimation: A Diagnostic Aid for Lung Diseases, Instrument Technology, 17(7), pp. 40-46, 1970.

[69] Landau, Barbara R., K. Akert and T.S. Roberts. Studies on the Innervation of the Diaphragm, J. Comp. Neurol., 119, pp. 1-10, 1962.

[70] Ogawa, T. Studies on the Phrenic Nerves and the Diaphragm of the Dog, Amer. J. Surg., 30, pp. 744-748, 1959.

[71] Moore, G.P., D.H. Perkel and J.P. Segundo. Statistical Analysis and Functional Interpretation of Neuronal Spike Data, Annual Review of Physiol., 28, pp. 493-522, 1966.

[72] Jones, R.W., C.C. Li, A.U. Meyer and R.B. Pinter. Pulse Modulation in Physiological Systems, Phenomenological Aspects, IRE Trans. BME-8(1), pp. 59-67, 1961.

[73] Dallos, P.J. and R.W. Jones. A Receptor Analog Having Logarithmic Response, IEEE Trans. BME-10(1), pp. 13-15, 1963.

[74] Brown, B.H. Theoretical and Experimental Waveform Analysis of Human Compound Nerve Action Potentials using Surface Electrodes, Med. and Biol. Engng, 6, pp. 375-386, Pergamon Press, 1968.

[75] Kendell, H.W., A.A. Rodriguez, J.L. Murphy, and H.W. Pavela. Researches in Electromyology, Archives of Phys. Med., pp. 755-763, 1951.

[76] Gatev, V. Method of Quantitative Evaluation of the Results Obtained from Electromyographic Investigations, Dokl. Bolg. Akad. Science, 19, pp. 69-71, 1966.

[77] Dowling, M.H., P. Fitch and R.G. Willison. A Special Purpose Digital Computer (BIOMAC 500) Used in the Analysis of the Human Electromyogram, Electenceph. Clin. Neurophysiol., 25, pp. 570-573, 1968.

[78] Mason, R.R. and R.R. Munro. Relationship Between EMG Potentials and Tension in Abduction of the Little Finger, Electromyography, 9(2), pp. 185-199, 1969.

[79] Lippold, O.C.J. The Relation Between Integrated Action Potentials in a Human Muscle and its Isometric Tension, J. Physiol., 117, pp. 492-499, 1952.

[80] Millman, J. and H. Taub. Pulse and Digital Circuits, pp. 212-216, McGraw-Hill Co. Inc., New York, 1956.

[81] Kuroda, E., V. Klissouras, and J.H. Milsum. Electrical and Metabolic Activities and Fatigue in Human Isometric Contraction. J. Appl. Physiol. 29(3), pp. 358-367, 1970.

[82] Coggshall, J.C. and G.A. Bekey. EMG - Force Dynamics in Human Skeletal Muscle. Med & Biol. Engng. 8, pp. 265-270, 1970.

[83] Fink, B.R., and M.L. Scheiner. The Computation of Muscle Activity from the Integrated Electromyogram, IRE Trans. Med. Elect. 6(3), pp. 119-120, 1959.

[84] Lourenço, R.V., N.S. Cherniack, J.R. Malm, and A.P. Fishman. Nervous Output from the Respiratory Center During Obstructed Breathing. J. Appl. Physiol. 21(2), pp. 527-533, 1966.

[85] Lourenço, R.V. and E.P. Mueller. Quantification of Electrical Activity in the Human Diaphragm. J. Appl. Physiol. 22(3), pp. 598-600, 1967.

[86] Mueller, E.P., and R.V. Lourenço. On-line Subtraction of the Cardiac Activity from the Esophageal Electromyogram of the Diaphragm, IEEE Trans. BME-15(2), pp. 115-118, 1968.

[87] Communications Biophysics Group of Res. Lab of Electronics and W.M. Siebert. Processing Neuroelectric Data, Technical Report 351, M.I.T., 1959.

[88] Barlow, J.S. Autocorrellation and Crosscorrelation Analysis in Electroencephalography, IRE Trans. Med. Elect. 6(3), pp. 179-189, 1959.

[89] Saunders, M.G. Problems in Electroencephalograph Analysis, IRE Trans. Med. Elect. 6(3), pp. 147-148, 1959.

[90] Krendal, E.S. The Analysis of Electroencephalograph by the Use of Cross-Spectrum Analyser, IRE Trans. Med. Elect. 6(3), pp. 149-156, 1959.

[91] Hiltz, F.F., and C.T. Pardoe. A Correlator of Time Intervals Between Pulses, IEEE Trans. Biomed. Elect. 12(2), pp. 113-120, 1965.

[92] Person, R.S., and L.N. Mishin. Auto- and Cross- Correlation Analysis of the Electrical Activity of Muscles. Med. & Biol. Engng. 2, pp. 155-159, 1964.

[93] Person, R.S. and L.P. Kudina. Cross-correlation of Electromyograms Showing Interference Patterns, Electroenceph. Clin. Neurophysiol., 25, pp. 58-68, 1968.

[94] Wierwille, W.W. A Theory and Method for Correlation Analysis of Nonstationary Signals. IEEE Trans. Elect. Computers, 14(6), pp. 909-919, 1965.

[95] Schroeder, M.R., and B.S. Atal. Generalized Short-Time Power Spectra and Autocorrelation Functions, J. Acoust. Soc. Am. 34(11), pp. 1679-1683, 1962.

[96] Bendat, J.S. Mathematical Analysis of Average Response Values for Nonstationary Data, IEEE Trans. Biomed. Elect. 11(3), pp. 72-81, 1964.

[97] Meyer, A.U. Pulse Frequency Modulation and its Effect in Feedback Systems, Ph.D. Dissertation, Northwestern University, Evanston, Illinois, 1961.

[98] Moore, A.D. Synthesized EMG Waves and Their Implications. Am. J. Phys. Med. 46(3), pp. 1302-1316, 1967.

[99] Person, R.S. and M.S. Libkind. Modelling of Interference Bioelectric Activity, Biofizika, 12(1), English Trans., Biophysics, pp. 145-153, 1967.

[100] Libkind, M.S. II. Modelling of Interference Bioelectric Activity, Biofizika, English Trans., Biophysics, pp. 811-821, 1968.

[101] Person, R.S., and M.S. Libkind. Simulation of Electromyogram Showing Interference Patterns. Electroenceph. Clin. Neurophysiol. 28, pp. 625-632, 1970.

[102] Walton, J.N. The Electromyogram in Myopathy: Analysis with the Audio-Frequency Spectrometer, J. Neurol. Neurosurg. Psych. 15, pp. 219-226, 1952.

[103] Johansson, S., L.E. Larsson, and R. Ortengren. An Automated Method for the Frequency Analysis of Myoelectric Signals Evaluated by an Invesiigation of the Spectral Charge Following a Strong Sustained Contractions. Med. & Biol. Engng., 8, pp. 257-264, 1970.

[104] Gersten, J.W., F.S. Cenkovich, and G.D. Jones. Harmonic Analysis of Normal and Abnormal Electromyograms. Am. J. Phys. Med. 44(5), pp. 235-240, 1965.

[105] Kadefors, R., E. Kaiser, and I. Petersen. Dynamic Spectrum Analysis of Myo-potentials and with Special Reference to Muscle Fatigue. Electromyography 8, pp. 39-74, 1968.

[106] Kwatny, E., D.H. Thomas, and H.G. Kwatny. An Application of Signal Processing Techniques to the Study of Myoelectric Signals. IEEE Trans. Bio Med. Engng, 17(4), pp. 303-312, 1970.

[107] Bayly, E.J. Spectral Analysis of Pulse Frequency Modulation in the Nervous Systems. IEEE Trans. BME-15 (4), pp. 257-265, 1968.

[108] Gottlieb, G.L., and G.C. Agarwal. Filtering of Electromyographic Signals. Am. J. Phys. Med. 49(2), pp. 142-146, 1970.

[109] Philbrick/Nexus Research. Application Manual for Operational Amplifiers, Boston, Nimrod Press, 1968.

[110] Hill, A.V. First and Last Experiments in Muscle Mechanics, Cambridge University Press, 1970.

[111] Ritchie, J.M., and D.R. Wilkie. The Effect of Previous Stimulation on the Active State of the Muscle, J. Physiol. 130, pp. 488-496, 1955.

[112] Ritchi, J. M. and D. R. Wilkie. The Dynamics of Muscular Contraction, J. Physiol. 143, pp. 104-113, 1958.

[113] Bahler, A. S. Modeling of Mammalian Skeletal Muscle, IEEE Trans. BME-15, (4), pp. 249-256, 1968.

[114] McRuer, D. T., R. E. Megdaleno, and G. P. Moore. A Neuromuscular Actuation System Model, IEEE Trans. MMS-9, (3), pp. 61-71, 1968.

[115] Gottlieb, G. L. and G. C. Agarwal. A Model of Muscle Activity, 6th Ann. Conf. Manual Control, Wright-Patterson Air Force Base, Ohio, April 1970.

[116] Gottlieb, G. L. and G. C. Agarwal. Dynamic Relationship Between Isometric Muscle Tension and the Electromyogram in Man. J. Appl. Physiol. 30, (3), pp. 345-351, 1971.

[117] Agarwal, G. C. and G. L. Gottlieb. Further Observations on the Relationship of EMG and Muscle Force, 7th Ann. NASA - University Conf. on Manual Control, Univ. of California, June 1971.

[118] Partridge, L. D. Signal-handling Characteristics of Load-Moving Skeletal Muscle, A. J. Physiol. 210, (5), pp. 1178-1191, 1966.

[119] Clynes, M. Respiratory Control of Heast Rate: Laws Derived from Analog Computer Simulation, IRE Trans. ME-7, No. 1, pp. 2-14, 1960.

[120] Agostoni, E. Chapters III and IV in The Respiratory Muscles, Mechanics and Neural Command, Campbell, E.J.M., E. Agostoni and J. Newson Davis, W.B. Saunders Co., Philadelphia, 1970.

[121] Agostoni, E. Chapter II, Kinematics in The Respiratory Muscles, Mechanics and Neural Control [ibid].

[122] Konno, K. and J. Mead. Measurement of the Separate Volume Changes of Ribcage and Abdomen During Breathing, J. Appl. Physiol., 22, pp. 407-422, 1967.

[123] Wade, O. L. Movements of the Thoracic Cage and Diaphragm in Respiration, J. Physiol. (Lond.), 124, pp. 193-212, 1954.

[124] Agostoni, E., P. Mognoni, G. Torri and F. Saracino. Relation Between Changes of Ribcage Circumference and Lung Volume, J. Appl. Physiol., 20, pp. 1179-1186, 1965.

[125] Partridge, L. D. Modifications of Neural Output Signals by Muscles: A Frequency Response Study, J. Appl. Physiol, 20, (1), pp. 150-156, 1965.

[126] Partridge, L. D. Intrinsic Feedback Factors Producing Inertial Compensation in Muscle, Biophys. J. 7(6), pp. 853-863, 1967.

[127] Partridge, L. D. Factors in the Interpretation of the Electromyogram Based on Muscle Response to Dynamic Nerve Signals, A. J. Phys. Med. 46(3), pp. 1276-1289, 1967.

[128] Lourenco, R. V. and J. M. Miranda. Drive and Performance of the Ventilatory Apparatus in Chronic Obstructive Lung Disease, New England J. Med. 279, pp. 53-59, 1968.

[129] Lourenco, R. V. Diaphragm Activity in Obesity. J. Clin. Med. 48(9),'pp. 1609-1614, 1969.

# VITAE

NAME: Nirmal Kumar Mishra

EDUCATION:

1950-54 Government Engineering College, Jabalpur, M.P.; B.E. (Honors) (Telecommunications), University of Saugor, 1955.

1956-59 Government Engineering College, Jabalpur, M.P., M.E. (Telecommunications), University of Jabalpur, 1960.

1961-62 Polytechnic Institute of Brooklyn, M.S. (Electrical Engineering), 1963.

1965-72 Newark College of Engineering, Newark, New Jersey.

HONORS:

1956-58 State Government Scholarship for Graduate Study.

1961-62 Research Fellow, Polytechnic Institute of Brooklyn.

PROFESSIONAL AND TEACHING APPOINTMENTS:

1958-60 Demonstrator, (Telecommunications), Government Engineering College, Jabalpur, M.P., India.

1960 (Summer) Lecturer in Telecommunications, Benaras Hindu University, Varanasi, U.P., India.

1960-61 Student-Trainee, Philips International Institute, Eindhoven, Netherlands.

1963-65 Assistant Professor in Electrical Engineering, Union College, Schenectady, New York.

1965-68 Instructor in Electrical Engineering, Newark College of Engineering, Newark, New Jersey.

1968-71 Research Assistant Professor, Abraham Lincoln School of Medicine, University of Illinois, Chicago, Associate Director (Bioengineering), Respiratory Physiology Laboratory, Hektoen Institute for Medical Research, Chicago, Illinois.

1971-72 Special Lecturer in Mathematics, Newark College of Engineering, Newark, New Jersey.

HONORARY SOCIETY:

Sigma Xi.